MATCH
Communications in Mathematical and in Computer Chemistry

MATCH Commun. Math. Comput. Chem. **87** (2022) 481-525
ISSN: 0340-6253
doi: 10.46793/match.87-3.481F

Standard Mark Table and Standard USCI-CF Table of the Point Group $\boldsymbol{D_{6h}}$. Unification of Candidates Derived from Different $\boldsymbol{D_{6h}}$-Skeletons

Shinsaku Fujita

Shonan Institute of Chemoinformatics and Mathematical Chemistry,
Kaneko 479-7 Ooimachi, Ashigara-Kami-Gun, Kanagawa-Ken, 258-0019 Japan

shinsaku_fujita@nifty.com

(Received November 15, 2021)

Abstract

Combined-permutation representations (CPRs) for characterizing $\boldsymbol{D}_{6h}$-skeletons (a benzene skeleton, a Haworth-projected skeleton, a superphane skeleton, and a coronene skeleton) are constructed by starting from respective sets of generators, where the permutation of each generator is combined with a mirror-permutation of 2-cycle to treat both achiral and chiral substituents under the GAP system. Thereby, the CPR of degree 8 (= 6 + 2) for the benzene skeleton, the CPR of degree 14 (= 12 + 2) for the Haworth-projected skeleton, the CPR of degree 14 (= 12 + 2) for the superphane skeleton, the CPR of degree 14 (= 12 + 2) for the coronene skeleton are generated to give primary mark tables (tables of marks) based on these CPRs. These primary mark tables generated by the GAP system are different in the sequence of subgroups from each other, although they stem from the same point group $\boldsymbol{D}_{6h}$. They are unified into a single standard mark table by means of a newly-devised GAP function `MarkTableforUSCI`. Moreover, another newly-devised GAP function `constructUSCITable` is employed to construct a standard USCI-CF (unit-subduced-cycle-index-with-chirality-fittingness) table concordantly. After a set of PCI-CFs (partial cycle indices with chirality fittingness) is calculated for each skeleton, symmetry-itemized combinatorial enumeration is conducted by means of the PCI method of Fujita's USCI approach (S. Fujita, *Symmetry and Combinatorial Enumeration in Chemistry*, Springer-Verlag, Berlin-Heidelberg, 1991).

1 Introduction

Conventional approaches for symmetry-itemized enumeration of isomers have been based on *Burnside's tables of marks* [1], while conventional approaches for gross enumeration of isomers (without symmetry-itemization) have been based on *Pólya's enumeration method* [2, 3]. Both of the conventional approaches regard isomers as graphs with no chiral substituents, so that they are incapable of enumerating 3D structures with chiral substituents.

The monographs [4, 5] published by the author (Fujita) have discussed the shortcomings of the conventional approaches and have clarified that they lack the concept of *sphericity* of orbits or cycles. On the basis of the concept of *chirality fittingness* stemming from the *sphericity* concept, the author (Fujita) has proposed versatile methods for enumerating 3D structures with chiral substituents, as briefly described below:

- **Fujita's USCI approach for symmetry-itemized enumeration of stereoisomers as 3D-objects (as well as graphs)** [4]. The concept of *sphericity of an orbit* [6] is the basis of *Fujita's USCI (unit-subduced-cycle-index) approach*, which is generally discussed in one monograph published by the author [4]. Fujita's USCI approach has provided us with systematic utilities for discussing symmetry-itemized combinatorial enumeration of (stereo)isomers.

  Thus, the concepts of *unit subduced cycle indices (USCIs)* [7] and *subductions of coset representations* (SCR) [6] were introduced by the author (Fujita) as a substantial extension of *Burnside's tables of marks* [1]. The concept of USCIs is further extended by introducing the concept of *chirality fittingness* (CF) via the concept of *sphericity for an orbit* [8, 9], so as to develop *unit subduced cycle indices with chirality fittingness* (USCI-CFs). The resulting USCI-CFs enable us to accomplish symmetry-itemized combinatorial enumeration of (stereo)isomers as 3D objects.

  Moreover, the concept of USCI-CFs has been recognized to play an important role in *symmetry-itemized enumerations* of 3D objects under respective point groups [4,10–12]. The resulting utilities are useful to combinatorial enumerations of stereoisomers, so as to be referred collectively under the name of *Fujita's USCI approach.*

- **Fujita's proligand method for gross enumeration of isomers as 3D-objects (as well as graphs)** [5]. On the other hand, the concept of *sphericity of a cycle* [13] is the basis of *Fujita's proligand method*, which is generally discussed in another monograph published by the author [5]. Fujita's proligand method has provided us with systematic utilities for discussing gross enumeration of (stereo)isomers without symmetry-itemization.

Thereby, Pólya's enumeration method concerning graphs [2, 3], which is originally incapable of treating chiral proligands, has been extended to develop *the proligand method* [13–15], which is capable of treating chiral as well as achiral proligands for covering enumerations of 3D structures as well as graphs [5].

- **Fujita's stereoisogram approach by considering chirality/achirality and *RS*-stereogenicity/*RS*-astereogenicity as two-kinds of handedness** [11,12]. Recently, I have proposed the concept of stereoisograms controlled by newly-defined *RS*-stereoisomeric groups [16, 17]. The vertical directions of a stereoisogram indicates chirality as the first kind of handedness, while the horizontal directions of a stereoisogram indicates *RS*-stereogenicity as the second kind of handedness. Chirality for supporting Le Bel's way and *RS*-stereogenicity for supporting van't Hoff's way are discussed from a viewpoint of two kinds of handedness [11, 12]. After sclerality is added as the third aspect along the diagonal directions, the two kinds of handedness are integrated into *RS*-stereoisomerism [18].

Tables of marks (mark tables) and USCI-CF tables are essential tools during the enumeration processes of Fujita's USCI approach (cf. Appendices of Ref. [4]). They have been originally prepared in terms of the FORTRAN77 language (cf. note 24 of Ref. [6] and note 17 of Ref. [19]). However, the procedures based on the FORTRAN77 language have been rather tedious, even if the subsequent calculation processes of enumeration can rely on more convenient computer algebraic systems such as the Maple system, the Mathematica system, and the REDUCE system.

Recently, the GAP (Groups, Algorithms, Programming) system [20] (the current version is GAP 4.11.1 released on 02 March 2021) is widely accepted as a system for computational discrete algebra, with particular emphasis on Computational Group Theory. In particular, useful functions concerning tables of marks (mark tables) are now available, e.g., the GAP function `TableOfMarks`.

On the other hand, USCI-CF tables for pursuing Fujita's USCI approach should meet the concepts of *sphericity for an orbit* and *chirality fittingness* (CF). Hence, the author

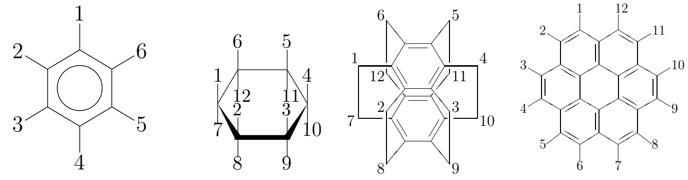

1 **2** **3** **4**

Figure 1. Representative $\boldsymbol{D}_{6h}$-skeletons: a benzene skeleton (**1**), a Haworth-projected skeleton (**2**), a superphane skeleton (**3**), and a coronene skeleton (**4**)

(Fujita) has extended permutation groups by previously-defined *combined-permutation representations* (CPRs) [21–23]. The feasibility of CPRs has been examined by treating $\boldsymbol{T}_d$-skeletons [24], $\boldsymbol{O}_h$-skeletons [25], and $\boldsymbol{D}_{3h}$-skeletons [26] under the GAP system, where concordant generations of "standard" mark tables and "standard" USCI-CF tables are necessary to absorb the differences due to the variety of $\boldsymbol{T}_d$-, $\boldsymbol{O}_h$-, or $\boldsymbol{D}_{3h}$-skeletons.

In the present article, various skeletons of $\boldsymbol{D}_{6h}$-symmetry are testified to unify mark tables and USCI-CF tables into the respective "standard" formats for the purpose of pursuing more efficient procedures of symmetry-itemized enumeration under the point group $\boldsymbol{D}_{6h}$.

2 D$_{6h}$-skeletons to be testified

2.1 Previous studies on D$_{6h}$-skeletons

Figure 1 shows representative $\boldsymbol{D}_{6h}$-skeletons: a benzene skeleton (**1**), a Haworth-projected skeleton (**2**), a superphane skeleton (**3**), and a coronene skeleton (**4**).

Symmetry-itemized enumeration and symmetry characterization of isomers derived from a benzene skeleton **1** as well as from a coronene skeleton **4** have been discussed [27] as an important section for developing the USCI approach. A $\boldsymbol{D}_{6h}$-skeleton **2** of Haworth-type projection has been traditionally used to discuss the stereoisomers of inositols on the analogy of sugar chemistry. In this treatment, a cyclohexane ring is considered to be to be planar and to have upward (β) and downward (α) faces in a dihedral fashion, where the twelve positions (six upward (1 to 6) and six downward positions (7 to 12)) are considered as substitution positions. This Haworth-projected skeleton **2** has been used to α, β-itemized enumeration of inositol derivatives by extending Fujita's proligand method [28]. Strictly speaking, such a Haworth-projected skeleton should be replaced by two-chair forms of a cyclopropane skeleton. The interconversion between the two-chair forms has been discussed by proposing *a pseudo-point group* $\widehat{\boldsymbol{D}}_{6h}$ [29–31]. The twelve bridge positions of a superphane ($[2_6](1,2,3,4,5,6)$cyclophane) skeleton (**3**) can be replaced by divalent units, where resulting isomers are counted by the PCI (partial-cycle-index) method of the USCI approach [32].

2.2 Basic properties of the point group $\boldsymbol{D_{6h}}$

The skeletons depicted in Figure 1 belong to the same point group $\boldsymbol{D}_{6h}$ (order 24), which is algebraically defined by a multiplication table containing 24 symmetry operations. To conduct combinatorial enumeration, the skeletons are differentiated by their coset representations (CRs, $(\boldsymbol{G}_i\backslash)\boldsymbol{D}_{6h})$, which are permutation representations defined by the respective subgroups, $\boldsymbol{G}_i$ ($\subset \boldsymbol{D}_{6h}$).

Each skeleton is specified by set(s) of fixed (stabilized) entities (e.g., points, vertices, and edges), each of which is fixed (stabilized) under a subgroup $\boldsymbol{G}_i$ ($\subset \boldsymbol{D}_{6h}$). For example, the benzene skeleton (**1**) has six vertices, each of which is regarded as a fixed point under the subgroup $\boldsymbol{C}'_{2v}$. The subgroup $\boldsymbol{C}'_{2v}$ is contained as a subgroup listed in a *non-redundant set of subgroups (SSG)* for $\boldsymbol{D}_{6h}$, which is a list of subgroups $\boldsymbol{G}_i$ ($\subset \boldsymbol{D}_{6h}$) collected in an ascending order of sizes (orders), *i.e.*,

$$\begin{aligned}\mathrm{SSG}_{\boldsymbol{D}_{6h}} = \{ & \underbrace{\boldsymbol{C}_1}_{1}, \underbrace{\boldsymbol{C}_2}_{2}, \underbrace{\boldsymbol{C}'_2}_{3}, \underbrace{\boldsymbol{C}''_2}_{4}, \underbrace{\boldsymbol{C}_s}_{5}, \underbrace{\boldsymbol{C}'_s}_{6}, \underbrace{\boldsymbol{C}''_s}_{7}, \underbrace{\boldsymbol{C}_i}_{8}, \underbrace{\boldsymbol{C}_3}_{9}, \underbrace{\boldsymbol{D}_2}_{10}, \\ & \underbrace{\boldsymbol{C}_{2v}}_{11}, \underbrace{\boldsymbol{C}'_{2v}}_{12}, \underbrace{\boldsymbol{C}''_{2v}}_{13}, \underbrace{\boldsymbol{C}_{2h}}_{14}, \underbrace{\boldsymbol{C}'_{2h}}_{15}, \underbrace{\boldsymbol{C}''_{2h}}_{16}, \underbrace{\boldsymbol{C}_6}_{17}, \underbrace{\boldsymbol{D}_3}_{18}, \underbrace{\boldsymbol{D}'_3}_{19}, \underbrace{\boldsymbol{C}_{3v}}_{20}, \\ & \underbrace{\boldsymbol{C}'_{3v}}_{21}, \underbrace{\boldsymbol{C}_{3h}}_{22}, \underbrace{\boldsymbol{C}_{3i}}_{23}, \underbrace{\boldsymbol{D}_{2h}}_{24}, \underbrace{\boldsymbol{D}_6}_{25}, \underbrace{\boldsymbol{C}_{6v}}_{26}, \underbrace{\boldsymbol{C}_{6h}}_{27}, \underbrace{\boldsymbol{D}_{3h}}_{28}, \underbrace{\boldsymbol{D}'_{3h}}_{29}, \underbrace{\boldsymbol{D}_{3d}}_{30}, \underbrace{\boldsymbol{D}'_{3d}}_{31}, \underbrace{\boldsymbol{D}_{6h}}_{32}\}. \end{aligned} \quad (1)$$

The word "non-redundant" means that an appropriate subgroup is selected as a representative, if there exist two or more conjugate subgroups. In the present article, the alignment of subgroups shown in Eq. 1 is adopted as a standard alignment, as indicated by a sequential number under a brace below each subgroup. Note that the subgroup $\boldsymbol{C}'_{2v}$ for a benzene skeleton appears as the 12th subgroup of $\mathrm{SSG}_{\boldsymbol{D}_{6h}}$ (Eq. 1).

According to a coset decomposition by each subgroup of the SSG, we have a *set of* *coset representations (SCR)* as follows:

$$\begin{aligned}\mathrm{SCR}_{\boldsymbol{D}_{6h}} = \{&(\boldsymbol{C}_1\backslash)\boldsymbol{D}_{6h}, (\boldsymbol{C}_2\backslash)\boldsymbol{D}_{6h}, (\boldsymbol{C}'_2\backslash)\boldsymbol{D}_{6h}, (\boldsymbol{C}''_2\backslash)\boldsymbol{D}_{6h}, (\boldsymbol{C}_s\backslash)\boldsymbol{D}_{6h},\\ &(\boldsymbol{C}'_s\backslash)\boldsymbol{D}_{6h}, (\boldsymbol{C}''_s\backslash)\boldsymbol{D}_{6h}, (\boldsymbol{C}_i\backslash)\boldsymbol{D}_{6h}, (\boldsymbol{C}_3\backslash)\boldsymbol{D}_{6h}, (\boldsymbol{D}_2\backslash)\boldsymbol{D}_{6h}, (\boldsymbol{C}_{2v}\backslash)\boldsymbol{D}_{6h},\\ &(\boldsymbol{C}'_{2v}\backslash)\boldsymbol{D}_{6h}, (\boldsymbol{C}''_{2v}\backslash)\boldsymbol{D}_{6h}, (\boldsymbol{C}_{2h}\backslash)\boldsymbol{D}_{6h}, (\boldsymbol{C}'_{2h}\backslash)\boldsymbol{D}_{6h}, (\boldsymbol{C}''_{2h}\backslash)\boldsymbol{D}_{6h}, (\boldsymbol{C}_6\backslash)\boldsymbol{D}_{6h},\\ &(\boldsymbol{D}_3\backslash)\boldsymbol{D}_{6h}, (\boldsymbol{D}'_3\backslash)\boldsymbol{D}_{6h}, (\boldsymbol{C}_{3v}\backslash)\boldsymbol{D}_{6h}, (\boldsymbol{C}'_{3v}\backslash)\boldsymbol{D}_{6h}, (\boldsymbol{C}_{3h}\backslash)\boldsymbol{D}_{6h}, (\boldsymbol{C}_{3i}\backslash)\boldsymbol{D}_{6h},\\ &(\boldsymbol{D}_{2h}\backslash)\boldsymbol{D}_{6h}, (\boldsymbol{D}_6\backslash)\boldsymbol{D}_{6h}, (\boldsymbol{C}_{6v}\backslash)\boldsymbol{D}_{6h}, (\boldsymbol{C}_{6h}\backslash)\boldsymbol{D}_{6h}, (\boldsymbol{D}_{3h}\backslash)\boldsymbol{D}_{6h},\\ &(\boldsymbol{D}'_{3h}\backslash)\boldsymbol{D}_{6h}, (\boldsymbol{D}_{3d}\backslash)\boldsymbol{D}_{6h}, (\boldsymbol{D}'_{3d}\backslash)\boldsymbol{D}_{6h}, (\boldsymbol{D}_{6h}\backslash)\boldsymbol{D}_{6h}\}\end{aligned} \quad (2)$$

Such $\boldsymbol{D}_{6h}$-skeletons as collected in Figure 1 are differentiated by means of respective CRs. For example, the six vertices of the benzene skeleton (**1** in Figure 1) are governed by the CR $(\boldsymbol{C}'_{2v}\backslash)\boldsymbol{D}_{6h}$, the degree of which is calculated to be $|\boldsymbol{D}_{6h}|/|\boldsymbol{C}'_{2v}| = 24/4 = 6$; the twelve vertices of the $\boldsymbol{D}_{6h}$-skeleton **2** of Haworth-type projection (Figure 1) are governed by the CR $(\boldsymbol{C}_s\backslash)\boldsymbol{D}_{6h}$, the degree of which is calculated to be $|\boldsymbol{D}_{6h}|/|\boldsymbol{C}_s| = 24/2 = 12$; the twelve bridge positions of a superphane ($[2_6]$(1,2,3,4,5,6)cyclophane) skeleton (**3**) are governed by the CR $(\boldsymbol{C}_s\backslash)\boldsymbol{D}_{6h}$, the degree of which is calculated to be $|\boldsymbol{D}_{6h}|/|\boldsymbol{C}_s| = 24/2 = 12$; and the twelve vertices of the coronene skeleton **4** (Figure 1) are governed by the CR $(\boldsymbol{C}''_s\backslash)\boldsymbol{D}_{6h}$, the degree of which is calculated to be $|\boldsymbol{D}_{6h}|/|\boldsymbol{C}''_s| = 24/2 = 12$.

The modes of such differentiation are explained by means of a mark table (a table of marks introduced by Burnside [1]). The mark table of $\boldsymbol{D}_{6h}$ is shown in Figure 2. The standard mark table (Figure 2) is illustrated in the form of a matrix form of the GAP system, where each row in an inner pair of square brackets shows a row vector corresponding to the CR $(\boldsymbol{G}_i\backslash)\boldsymbol{D}_{6h}$. Note that the standard mark table (Figure 2) is found to be a lower-triangular matrix, i.e., all values are zero in the upper-right triangular part. Such a set of a standard mark table and its inverse has been calculated originally by a FORTRAN77 program [27] under the research environment of the author. The standard mark table shown here (Figure 2) is calculated by starting from the inverse mark table reported in Ref. [27].

3 Permutation groups corresponding to the point group $\boldsymbol{D}_{6h}$

The GAP system stresses permutation groups, where a permutation group (PG) is derived from each of the $\boldsymbol{D}_{6h}$-skeletons (e.g., Figure 1) by using the corresponding set of generators.

```
1: [ [ 24,0,0,0,0,0,0,0,0,0,0,0,0,0,0,0,0,0,0,0,0,0,0,0,0,0,0,0,0,0,0,0 ],
2:     [ 12,12,0,0,0,0,0,0,0,0,0,0,0,0,0,0,0,0,0,0,0,0,0,0,0,0,0,0,0,0,0,0 ],
3:     [ 12,0,4,0,0,0,0,0,0,0,0,0,0,0,0,0,0,0,0,0,0,0,0,0,0,0,0,0,0,0,0,0 ],
4:     [ 12,0,0,4,0,0,0,0,0,0,0,0,0,0,0,0,0,0,0,0,0,0,0,0,0,0,0,0,0,0,0,0 ],
5:     [ 12,0,0,0,4,0,0,0,0,0,0,0,0,0,0,0,0,0,0,0,0,0,0,0,0,0,0,0,0,0,0,0 ],
6:     [ 12,0,0,0,0,4,0,0,0,0,0,0,0,0,0,0,0,0,0,0,0,0,0,0,0,0,0,0,0,0,0,0 ],
7:     [ 12,0,0,0,0,0,12,0,0,0,0,0,0,0,0,0,0,0,0,0,0,0,0,0,0,0,0,0,0,0,0,0 ],
8:     [ 12,0,0,0,0,0,0,12,0,0,0,0,0,0,0,0,0,0,0,0,0,0,0,0,0,0,0,0,0,0,0,0 ],
9:     [ 8,0,0,0,0,0,0,0,8,0,0,0,0,0,0,0,0,0,0,0,0,0,0,0,0,0,0,0,0,0,0,0 ],
10:    [ 6,6,2,2,0,0,0,0,0,2,0,0,0,0,0,0,0,0,0,0,0,0,0,0,0,0,0,0,0,0,0,0 ],
11:    [ 6,6,0,0,2,2,0,0,0,0,2,0,0,0,0,0,0,0,0,0,0,0,0,0,0,0,0,0,0,0,0,0 ],
12:    [ 6,0,2,0,2,0,6,0,0,0,0,2,0,0,0,0,0,0,0,0,0,0,0,0,0,0,0,0,0,0,0,0 ],
13:    [ 6,0,0,2,0,2,6,0,0,0,0,0,2,0,0,0,0,0,0,0,0,0,0,0,0,0,0,0,0,0,0,0 ],
14:    [ 6,6,0,0,0,0,6,6,0,0,0,0,0,6,0,0,0,0,0,0,0,0,0,0,0,0,0,0,0,0,0,0 ],
15:    [ 6,0,2,0,0,2,0,6,0,0,0,0,0,0,2,0,0,0,0,0,0,0,0,0,0,0,0,0,0,0,0,0 ],
16:    [ 6,0,0,2,2,0,0,6,0,0,0,0,0,0,0,2,0,0,0,0,0,0,0,0,0,0,0,0,0,0,0,0 ],
17:    [ 4,4,0,0,0,0,0,0,4,0,0,0,0,0,0,0,4,0,0,0,0,0,0,0,0,0,0,0,0,0,0,0 ],
18:    [ 4,0,4,0,0,0,0,0,4,0,0,0,0,0,0,0,0,4,0,0,0,0,0,0,0,0,0,0,0,0,0,0 ],
19:    [ 4,0,0,4,0,0,0,0,4,0,0,0,0,0,0,0,0,0,4,0,0,0,0,0,0,0,0,0,0,0,0,0 ],
20:    [ 4,0,0,0,4,0,0,0,4,0,0,0,0,0,0,0,0,0,0,4,0,0,0,0,0,0,0,0,0,0,0,0 ],
21:    [ 4,0,0,0,0,4,0,0,4,0,0,0,0,0,0,0,0,0,0,0,4,0,0,0,0,0,0,0,0,0,0,0 ],
22:    [ 4,0,0,0,0,0,4,0,4,0,0,0,0,0,0,0,0,0,0,0,0,4,0,0,0,0,0,0,0,0,0,0 ],
23:    [ 4,0,0,0,0,0,0,4,4,0,0,0,0,0,0,0,0,0,0,0,0,0,4,0,0,0,0,0,0,0,0,0 ],
24:    [ 3,3,1,1,1,1,3,3,0,1,1,1,1,3,1,1,0,0,0,0,0,0,1,0,0,0,0,0,0,0,0,0 ],
25:    [ 2,2,2,2,0,0,0,0,2,2,0,0,0,0,0,0,2,2,2,0,0,0,0,0,2,0,0,0,0,0,0,0 ],
26:    [ 2,2,0,0,2,2,0,0,2,0,2,0,0,0,0,0,2,0,0,2,2,0,0,0,0,2,0,0,0,0,0,0 ],
27:    [ 2,2,0,0,0,0,2,2,2,0,0,0,0,2,0,0,2,0,0,0,0,2,2,0,0,0,2,0,0,0,0,0 ],
28:    [ 2,0,2,0,2,0,2,0,2,0,0,2,0,0,0,0,0,2,0,2,0,2,0,0,0,0,0,2,0,0,0,0 ],
29:    [ 2,0,0,2,0,2,2,0,2,0,0,0,2,0,0,0,0,0,2,0,2,2,0,0,0,0,0,0,2,0,0,0 ],
30:    [ 2,0,2,0,0,2,0,2,2,0,0,0,0,0,2,0,0,2,0,0,2,0,2,0,0,0,0,0,0,2,0,0 ],
31:    [ 2,0,0,2,2,0,0,2,2,0,0,0,0,0,0,2,0,0,2,2,0,0,2,0,0,0,0,0,0,0,2,0 ],
32:    [ 1,1,1,1,1,1,1,1,1,1,1,1,1,1,1,1,1,1,1,1,1,1,1,1,1,1,1,1,1,1,1,1 ] ]
```

Figure 2. Standard mark table of the point group $\boldsymbol{D}_{6h}$ (GAP matrix expression). For the sake of convenience, the sequential number with a colon is added at the left-most column to show each CR (Eq. 2) in accord with the sequential number shown in Eq. 1.

As a result, the mark table (table of marks) of a PG based on one set of generators is different from a standard mark table (Figure 2), when it is produced by the GAP system.

3.1 CPR for a benzene skeleton (1) and the corresponding mark table

A set of generators gen_benz for characterizing the six positions of the benzene skeleton (**1** in Figure 1) produces a permutation group D6h_benz of order 24, which is isomorphic to the point group $\boldsymbol{D}_{6h}$ of order 24.

```
gap> #generators for D6h_benz
gap> gen_benz := [(1,2,3,4,5,6), (1,4)(2,3)(5,6), (7,8)];;
gap> D6h_benz := Group(gen_benz); #benzene skeleton
Group([ (1,2,3,4,5,6), (1,4)(2,3)(5,6), (7,8) ])
gap> Display(Size(D6h_benz));
24
```

```
 1:  24
 2:  12 4
 3:  12 . 12
 4:  12 .   . 12
 5:  12 .   .   . 4
 6:  12 .   .   . . 4
 7:  12 .   .   . . . 12
 8:  12 .   .   . . .   . 4
 9:   8 .   .   . . .   . . 8
10:   6 .   6   6 . .   6 . . 6
11:   6 2   .   6 . 2   . . . . 2
12:   6 2   6   . 2 .   . . . . . 2
13:   6 .   .   6 2 .   . 2 . . . . 2
14:   6 .   6   . . 2   . 2 . . . . . 2
15:   6 2   .   . . .   6 2 . . . . . . 2
16:   6 .   .   . 2 2   6 . . . . . . . . 2
17:   4 .   4   . . .   . . 4 . . . . . . . 4
18:   4 4   .   . . .   . . 4 . . . . . . . . 4
19:   4 .   .   . 4 .   . . 4 . . . . . . . . . 4
20:   4 .   .   4 . .   . . 4 . . . . . . . . . . 4
21:   4 .   .   . . .   4 . 4 . . . . . . . . . . . 4
22:   4 .   .   . . 4   . . 4 . . . . . . . . . . . . 4
23:   4 .   .   . . .   . 4 4 . . . . . . . . . . . . . 4
24:   3 1   3   3 1 1   3 1 . 3 1 1 1 1 1 1 . . . . . . . 1
25:   2 .   2   2 . .   2 . 2 2 . . . . . . 2 . . 2 2 . . . 2
26:   2 2   .   2 . 2   . . 2 . 2 . . . . . . 2 . 2 . 2 . . . 2
27:   2 2   2   . 2 .   . . 2 . . 2 . . . . 2 2 2 . . . . . . . 2
28:   2 .   .   2 2 .   . 2 2 . . . 2 . . . . . 2 2 . . 2 . . . . 2
29:   2 .   2   . . 2   . 2 2 . . . . 2 . . 2 . . . . 2 2 . . . . . 2
30:   2 2   .   . . .   2 2 2 . . . . . 2 . . 2 . . 2 . 2 . . . . . . 2
31:   2 .   .   . 2 2   2 . 2 . . . . . . 2 . . 2 . 2 2 . . . . . . . . 2
32:   1 1   1   1 1 1   1 1 1 1 1 1 1 1 1 1 1 1 1 1 1 1 1 1 1 1 1 1 1 1 1 1
```

Figure 3. Mark table (GAP expression, tom_D6h_benz) of the point group $\boldsymbol{D}_{6h}$ by starting from the the set of generators gen_benz for characterizing the six positions of the benzene skeleton (**1** in Figure 1).

Note that the set of generators gen_benz is adopted as a combined-permutation representation (CPR) which stabilizes the six vertices (1, 2, …, 6) of the benzene skeleton and contains a 2-cycle (7,8) due to a mirror-permutation. Thus, the CPR of degree 8 (= 6 + 2) for the benzene skeleton is used to treat a reflection.

The GAP function TableOfMarks based on a permutation group (D6h_benz) generates the corresponding mark table named tom_D6h_benz, as follows:

```
gap> tom_D6h_benz := TableOfMarks(D6h_benz);;
gap> Display(tom_D6h_benz);
```

This code generates the mark table (GAP expression, tom_D6h_benz) shown in Figure 3, in which each dot (.) shows a zero value; and a upper-triangular blank space indicates the lower-triangular characteristics of the mark table.

The mark table (Figure 3) is different from the standard mark table (Figure 2) described above, even if its GAP expression is transformed into a GAP matrix expression.

Each row of the mark table (numbered sequentially from 1 to 32) corresponds to a subgroup, the generator of which (named sequentially from gen[1] to gen[32]) is calculated by using the GAP command RepresentativeTom as follows:

```
gap> gen := [];;
gap> for i in [1..Size(OrdersTom(tom_D6h_benz))] do
> r_tom := RepresentativeTom(tom_D6h_benz,i);
> gen[i] := GeneratorsOfGroup (r_tom);
> Print("gen[", i, "]␣:=␣", gen[i], "\n");
> od;
gen[1] := [ ]
gen[2] := [ (2,6)(3,5) ]
gen[3] := [ (7,8) ]
gen[4] := [ (1,4)(2,5)(3,6) ]
gen[5] := [ (2,6)(3,5)(7,8) ]
gen[6] := [ (1,2)(3,6)(4,5) ]
gen[7] := [ (1,4)(2,5)(3,6)(7,8) ]
gen[8] := [ (1,2)(3,6)(4,5)(7,8) ]
gen[9] := [ (1,3,5)(2,4,6) ]
gen[10] := [ (7,8), (1,4)(2,5)(3,6) ]
gen[11] := [ (2,6)(3,5), (1,4)(2,5)(3,6) ]
gen[12] := [ (7,8), (2,6)(3,5) ]
gen[13] := [ (2,6)(3,5)(7,8), (1,4)(2,5)(3,6) ]
gen[14] := [ (7,8), (1,2)(3,6)(4,5) ]
gen[15] := [ (1,4)(2,5)(3,6)(7,8), (2,6)(3,5) ]
gen[16] := [ (1,3)(4,6)(7,8), (1,6)(2,5)(3,4) ]
gen[17] := [ (1,3,5)(2,4,6), (7,8) ]
gen[18] := [ (1,3,5)(2,4,6), (2,6)(3,5) ]
gen[19] := [ (1,3,5)(2,4,6), (2,6)(3,5)(7,8) ]
gen[20] := [ (1,3,5)(2,4,6), (1,2,3,4,5,6) ]
gen[21] := [ (1,3,5)(2,4,6), (1,2,3,4,5,6)(7,8) ]
gen[22] := [ (1,3,5)(2,4,6), (1,2)(3,6)(4,5) ]
gen[23] := [ (1,3,5)(2,4,6), (1,2)(3,6)(4,5)(7,8)]
gen[24] := [ (7,8), (2,6)(3,5), (1,4)(2,5)(3,6) ]
gen[25] := [ (1,3,5)(2,4,6), (7,8), (1,2,3,4,5,6)]
gen[26] := [ (1,3,5)(2,4,6), (2,6)(3,5), (1,2,3,4,5,6) ]
gen[27] := [ (1,3,5)(2,4,6), (7,8), (2,6)(3,5) ]
gen[28] := [ (1,3,5)(2,4,6), (2,6)(3,5)(7,8), (1,2,3,4,5,6) ]
gen[29] := [ (1,3,5)(2,4,6), (7,8), (1,2)(3,6)(4,5) ]
gen[30] := [ (1,3,5)(2,4,6), (2,6)(3,5), (1,2,3,4,5,6)(7,8) ]
gen[31] := [ (1,3,5)(2,4,6), (2,6)(3,5)(7,8), (1,2,3,4,5,6)(7,8) ]
gen[32] := [ (1,2,3,4,5,6),(1,4)(2,3)(5,6), (7,8)]
gap>
```

Each set of generators (gen[i], $i = 1$ to 32) generates a non-redundant set of subgroups, although its alignment is different from Eq. 1. For example, the subgroup generated from gen[4] is found to correspond to the point group $\boldsymbol{C}_2$, which is the second subgroup appearing in $\mathrm{SSG}_{\boldsymbol{D}_{6h}}$ (Eq. 1). This correspondence is represented by the symbol $\overbrace{\underbrace{\boldsymbol{C}_2}_{2}}^{4}$, where the upper number 4 is concerned with the SSG for the mark table tom_D6h_benz (named $\mathrm{SSG}^{benz}_{\boldsymbol{D}_{6h}}$), while the lower number 2 is concerned with $\mathrm{SSG}_{\boldsymbol{D}_{6h}}$ (Eq. 1). The remaining mode of correspondence is similarly obtained, so as to give $\mathrm{SSG}^{benz}_{\boldsymbol{D}_{6h}}$ for the mark table tom_D6h_benz as follows:

$$\begin{aligned}
\mathrm{SSG}^{benz}_{\boldsymbol{D}_{6h}} = \{ & \overbrace{\underbrace{\boldsymbol{C}_1}_{1}}^{1}, \overbrace{\underbrace{\boldsymbol{C}'_2}_{3}}^{2}, \overbrace{\underbrace{\boldsymbol{C}''_s}_{7}}^{3}, \overbrace{\underbrace{\boldsymbol{C}_2}_{2}}^{4}, \overbrace{\underbrace{\boldsymbol{C}_s}_{5}}^{5}, \overbrace{\underbrace{\boldsymbol{C}''_2}_{4}}^{6}, \overbrace{\underbrace{\boldsymbol{C}_i}_{8}}^{7}, \overbrace{\underbrace{\boldsymbol{C}'_s}_{6}}^{8}, \overbrace{\underbrace{\boldsymbol{C}_3}_{9}}^{9}, \overbrace{\underbrace{\boldsymbol{C}_{2h}}_{14}}^{10}, \\
& \overbrace{\underbrace{\boldsymbol{D}_2}_{10}}^{11}, \overbrace{\underbrace{\boldsymbol{C}'_{2v}}_{12}}^{12}, \overbrace{\underbrace{\boldsymbol{C}_{2v}}_{11}}^{13}, \overbrace{\underbrace{\boldsymbol{C}''_{2v}}_{13}}^{14}, \overbrace{\underbrace{\boldsymbol{C}'_{2h}}_{15}}^{15}, \overbrace{\underbrace{\boldsymbol{C}''_{2h}}_{16}}^{16}, \overbrace{\underbrace{\boldsymbol{C}_{3h}}_{22}}^{17}, \overbrace{\underbrace{\boldsymbol{D}_3}_{18}}^{18}, \overbrace{\underbrace{\boldsymbol{C}_{3v}}_{20}}^{19}, \overbrace{\underbrace{\boldsymbol{C}_6}_{17}}^{20}, \\
& \overbrace{\underbrace{\boldsymbol{C}_{3i}}_{23}}^{21}, \overbrace{\underbrace{\boldsymbol{D}'_3}_{19}}^{22}, \overbrace{\underbrace{\boldsymbol{C}'_{3v}}_{21}}^{23}, \overbrace{\underbrace{\boldsymbol{D}_{2h}}_{24}}^{24}, \overbrace{\underbrace{\boldsymbol{C}_{6h}}_{27}}^{25}, \overbrace{\underbrace{\boldsymbol{D}_6}_{25}}^{26}, \overbrace{\underbrace{\boldsymbol{D}_{3h}}_{28}}^{27}, \overbrace{\underbrace{\boldsymbol{C}_{6v}}_{26}}^{28}, \overbrace{\underbrace{\boldsymbol{D}'_{3h}}_{29}}^{29}, \overbrace{\underbrace{\boldsymbol{D}_{3d}}_{30}}^{30}, \overbrace{\underbrace{\boldsymbol{D}'_{3d}}_{31}}^{31}, \overbrace{\underbrace{\boldsymbol{D}_{6h}}_{32}}^{32} \}.
\end{aligned} \tag{3}$$

where the upper numbers are taken from the leftmost column of the calculated mark table `tom_D6h_benz` (Figure 3), while the lower numbers are taken from $\mathrm{SSG}_{\boldsymbol{D}_{6h}}$ (Eq. 1), which corresponds to the standard mark table (Figure 2). The mark table `tom_D6h_benz` (Figure 3) due to $\mathrm{SSG}^{benz}_{\boldsymbol{D}_{6h}}$ (Eq. 3) can be converted into the mark table `test_sort` due to $\mathrm{SSG}_{\boldsymbol{D}_{6h}}$ (Eq. 1) by using the GAP function `SortedTom` as follows:

```
gap> perm_benz :=
> PermList([1,3,7,2,5,4,8,6,9,14,10,12,11,13,15,16,22,18,20,17,
> 23,19,21,24,27,25,28,26,29,30,31,32]);
(2,3,7,8,6,4)(10,14,13,11)(17,22,19,20)(21,23)(25,27,28,26)
gap> test_sort := SortedTom(tom_D6h_benz,perm_benz);;
gap> Display(test_sort);
 1: 24
 2: 12 12
 3: 12 . 4
 4: 12 . . 4
 5: 12 . . . 4
 6: 12 . . . . 4
 7: 12 . . . . . 12
 8: 12 . . . . . . 12
 9: 8 . . . . . . . 8
10: 6 6 2 2 . . . . . 2
(omitted)
```

where the permutation `perm_benz` is calculated by applying the GAP function `PermList` to a list derived from the lower numbering in Eq. 3. The resulting sorted mark table `test_sort`, if the former is transformed into the GAP matrix format, is identical with the standard mark table shown in Figure 2.

3.2 CPR for a Haworth-projected skeleton (2) and the corresponding mark table

The twelve positions of a Haworth-projected skeleton (**2**) shown in Figure 1 is characterized by a permutation group `D6h_haworth` of order 24, which is generated by applying the GAP function `Group` to a set of generators `gen_haworth`. The resulting group

```
 1:  24
 2:  12 4
 3:  12 . 4
 4:  12 . . 12
 5:  12 . .  . 12
 6:  12 . .  .  . 4
 7:  12 . .  .  . . 4
 8:  12 . .  .  . . . 12
 9:   8 . .  .  . . .  . 8
10:   6 . 2  6  . . 2  . . 2
11:   6 2 .  6  . 2 .  . . . 2
12:   6 2 2  .  6 . .  . . . . 2
13:   6 . .  6  6 . .  6 . . . . 6
14:   6 . 2  .  . 2 .  6 . . . . . 2
15:   6 2 .  .  . . 2  6 . . . . . . 2
16:   6 . .  .  6 2 2  . . . . . . . . 2
17:   4 . 4  .  . . .  . 4 . . . . . . . 4
18:   4 4 .  .  . . .  . 4 . . . . . . . . 4
19:   4 . .  .  4 . .  . 4 . . . . . . . . . 4
20:   4 . .  4  . . .  . 4 . . . . . . . . . . 4
21:   4 . .  .  . . 4  . 4 . . . . . . . . . . . 4
22:   4 . .  .  . 4 .  . 4 . . . . . . . . . . . . 4
23:   4 . .  .  . . .  4 4 . . . . . . . . . . . . . 4
24:   3 1 1  3  3 1 1  3 . 1 1 1 3 1 1 1 . . . . . . . 1
25:   2 . 2  2  . . 2  . 2 2 . . . . . . 2 . . 2 2 . . . 2
26:   2 2 .  2  . 2 .  . 2 . 2 . . . . . . 2 . 2 . 2 . . . 2
27:   2 2 2  .  2 . .  . 2 . . 2 . . . . 2 2 2 . . . . . . . 2
28:   2 . .  2  2 . .  2 2 . . . 2 . . . . . 2 2 . . 2 . . . . 2
29:   2 . 2  .  . 2 .  2 2 . . . . 2 . . 2 . . . . 2 2 . . . . . 2
30:   2 2 .  .  . . 2  2 2 . . . . . 2 . . 2 . . 2 . 2 . . . . . . 2
31:   2 . .  .  2 2 2  . 2 . . . . . . 2 . . 2 . 2 2 . . . . . . . . 2
32:   1 1 1  1  1 1 1  1 1 1 1 1 1 1 1 1 1 1 1 1 1 1 1 1 1 1 1 1 1 1 1 1
```

Figure 4. Mark table (GAP expression, `tom_D6h_haworth`) of the point group $\boldsymbol{D}_{6h}$ by starting from the the set of generators `gen_haworth` for characterizing the twelve positions of the Haworth-projected skeleton (**2**) shown in Figure 1.

`D6h_haworth` is isomorphic to the point group $\boldsymbol{D}_{6h}$ of order 24.

```
gap> gen_haworth := [(1,2,3,4,5,6)(7,8,9,10,11,12), (1,10)(2,9)(3,8)(4,7)(5,12)(6,11),
> (1,7)(2,8)(3,9)(4,10)(5,11)(6,12)(13,14)];;
gap> D6h_haworth := Group(gen_haworth); #[6]haworth skeleton
Group([ (1,2,3,4,5,6)(7,8,9,10,11,12), (1,10)(2,9)(3,8)(4,7)(5,12)(6,11),
(1,7)(2,8)(3,9)(4,10)(5,11)(6,12)(13,14) ])
gap> Display(Size(D6h_haworth));
24
```

Note that the set of generators `gen_haworth` is adopted as a combined-permutation representation (CPR) which stabilizes the twelve vertices of the Haworth-projected skeleton (**2**) shown in Figure 1 and contains a 2-cycle `(13,14)` due to a mirror-permutation. Thus, the CPR of degree 14 (= 12 + 2) for a Haworth-projected skeleton is used to treat a reflection.

The corresponding mark table `tom_D6h_haworth` can be obtained by inputting the command `TableOfMarks(D6h_haworth)`.

```
gap> tom_D6h_haworth := TableOfMarks(D6h_haworth);;
gap> Display(tom_D6h_haworth);
```

The resulting mark table `tom_D6h_haworth` (Figure 4) is different from the standard mark table (Figure 2) and, at the same time, is different from the mark table `tom_D6h_benz` (Figure 3) described above.

The comparison between the mark table tom_D6h_haworth (Figure 4) and the standard mark table (Figure 2) results in the following $\mathrm{SSG}_{\boldsymbol{D}_{6h}}^{haworth}$ (Eq. 4).

$$\begin{aligned}
\mathrm{SSG}_{\boldsymbol{D}_{6h}}^{haworth} = \{ & \overbrace{\underbrace{\boldsymbol{C}_1}_{1}}^{1}, \overbrace{\underbrace{\boldsymbol{C}_2''}_{4}}^{2}, \overbrace{\underbrace{\boldsymbol{C}_s}_{5}}^{3}, \overbrace{\underbrace{\boldsymbol{C}_2}_{2}}^{4}, \overbrace{\underbrace{\boldsymbol{C}_i}_{8}}^{5}, \overbrace{\underbrace{\boldsymbol{C}_2'}_{3}}^{6}, \overbrace{\underbrace{\boldsymbol{C}_s'}_{6}}^{7}, \overbrace{\underbrace{\boldsymbol{C}_s''}_{7}}^{8}, \overbrace{\underbrace{\boldsymbol{C}_3}_{9}}^{9}, \overbrace{\underbrace{\boldsymbol{C}_{2v}}_{11}}^{10}, \\
& \overbrace{\underbrace{\boldsymbol{D}_2}_{10}}^{11}, \overbrace{\underbrace{\boldsymbol{C}_{2h}''}_{16}}^{12}, \overbrace{\underbrace{\boldsymbol{C}_{2h}}_{14}}^{13}, \overbrace{\underbrace{\boldsymbol{C}_{2v}'}_{12}}^{14}, \overbrace{\underbrace{\boldsymbol{C}_{2v}''}_{13}}^{15}, \overbrace{\underbrace{\boldsymbol{C}_{2h}'}_{15}}^{16}, \overbrace{\underbrace{\boldsymbol{C}_{3v}}_{20}}^{17}, \overbrace{\underbrace{\boldsymbol{D}_3'}_{19}}^{18}, \overbrace{\underbrace{\boldsymbol{C}_{3i}}_{23}}^{19}, \overbrace{\underbrace{\boldsymbol{C}_6}_{17}}^{20}, \\
& \overbrace{\underbrace{\boldsymbol{C}_{3v}'}_{21}}^{21}, \overbrace{\underbrace{\boldsymbol{D}_3}_{18}}^{22}, \overbrace{\underbrace{\boldsymbol{C}_{3h}}_{22}}^{23}, \overbrace{\underbrace{\boldsymbol{D}_{2h}}_{24}}^{24}, \overbrace{\underbrace{\boldsymbol{C}_{6v}}_{26}}^{25}, \overbrace{\underbrace{\boldsymbol{D}_6}_{25}}^{26}, \overbrace{\underbrace{\boldsymbol{D}_{3d}'}_{31}}^{27}, \overbrace{\underbrace{\boldsymbol{C}_{6h}}_{27}}^{28}, \overbrace{\underbrace{\boldsymbol{D}_{3h}}_{28}}^{29}, \overbrace{\underbrace{\boldsymbol{D}_{3h}'}_{29}}^{30}, \overbrace{\underbrace{\boldsymbol{D}_{3d}}_{30}}^{31}, \overbrace{\underbrace{\boldsymbol{D}_{6h}}_{32}}^{32} \}. \qquad (4)
\end{aligned}$$

where the upper numbers are taken from the leftmost column of the calculated mark table tom_D6h_haworth, while the lower numbers are taken from $\mathrm{SSG}_{\boldsymbol{D}_{6h}}$ (Eq. 1). The lower numbers in Eq. 4 result in the appearance of perm_haworth by using the GAP function PermList. Thereby, the mark table tom_D6h_haworth (Figure 4) due to $\mathrm{SSG}_{\boldsymbol{D}_{6h}}^{haworth}$ (Eq. 4) can be converted into the mark table test2_sort due to $\mathrm{SSG}_{\boldsymbol{D}_{6h}}$ (Eq. 1) by using the GAP function SortedTom as follows:

```
gap> perm_haworth := PermList([1,4,5,2,8,3,6,7,9,11,10,16,14,12,13,15,20,19,23,17,
> 21,18,22,24,26,25,31,27,28,29,30,32]);
(2,4)(3,5,8,7,6)(10,11)(12,16,15,13,14)(17,20)(18,19,23,22)(25,26)(27,31,30,29,28)
gap> tom_D6h_haworth := TableOfMarks(D6h_haworth);;
gap> test2_sort := SortedTom(tom_D6h_haworth,perm_haworth);;
gap> Display(test2_sort);
 1: 24
 2: 12 12
 3: 12 . 4
 4: 12 . . 4
 5: 12 . . . 4
 6: 12 . . . . 4
 7: 12 . . . . . 12
 8: 12 . . . . . . 12
 9: 8 . . . . . . . 8
10: 6 6 2 2 . . . . . 2
(omitted)
```

The resulting sorted mark table test2_sort is identical with the sorted mark table test_sort. Then, if the mark table test2_sort is transformed into the GAP matrix format, it is identical with the standard mark table shown in Figure 2.

3.3 CPR for a superphane skeleton (3) and the corresponding mark table

The twelve chain positions of a superphane skeleton (**3**) (Figure 1) are characterized by a permutation group D6h_phane of order 24, which is generated by applying the GAP function Group to a set of generators gen_phane.

The set of generators gen_phane for characterizing the superphane skeleton (**3**) is identical with the set of generators gen_haworth for characterizing the Haworth-projected skeleton (**2**) (Figure 1). As a result, the resulting group D6h_phane (as well as D6h_haworth) is isomorphic to the point group $\boldsymbol{D}_{6h}$ of order 24.

```
gap> gen_phane := [(1,2,3,4,5,6)(7,8,9,10,11,12), (1,10)(2,9)(3,8)(4,7)(5,12)(6,11),
> (1,7)(2,8)(3,9)(4,10)(5,11)(6,12)(13,14)];;
gap> D6h_phane := Group(gen_haworth); #superphane skeleton
Group([ (1,2,3,4,5,6)(7,8,9,10,11,12), (1,10)(2,9)(3,8)(4,7)(5,12)(6,11),
(1,7)(2,8)(3,9)(4,10)(5,11)(6,12)(13,14) ])
gap> Display(Size(D6h_phane));
24
```

The SSG for the superphane **3** ($\mathrm{SSG}_{\boldsymbol{D}_{6h}}^{phane}$) is identical with $\mathrm{SSG}_{\boldsymbol{D}_{6h}}^{haworth}$ (Eq. 4) for the Haworth-projected skeleton **2** (Figure 1), as shown in Eq. 5.

$$
\begin{aligned}
&\mathrm{SSG}_{\boldsymbol{D}_{6h}}^{phane} = \mathrm{SSG}_{\boldsymbol{D}_{6h}}^{haworth}\\
&= \{\overbrace{\underbrace{\boldsymbol{C}_1}_{1}}^{1}, \overbrace{\underbrace{\boldsymbol{C}_2''}_{4}}^{2}, \overbrace{\underbrace{\boldsymbol{C}_s}_{5}}^{3}, \overbrace{\underbrace{\boldsymbol{C}_2}_{2}}^{4}, \overbrace{\underbrace{\boldsymbol{C}_i}_{8}}^{5}, \overbrace{\underbrace{\boldsymbol{C}_2'}_{3}}^{6}, \overbrace{\underbrace{\boldsymbol{C}_s'}_{6}}^{7}, \overbrace{\underbrace{\boldsymbol{C}_s''}_{7}}^{8}, \overbrace{\underbrace{\boldsymbol{C}_3}_{9}}^{9}, \overbrace{\underbrace{\boldsymbol{C}_{2v}}_{11}}^{10},\\
&\quad \overbrace{\underbrace{\boldsymbol{D}_2}_{10}}^{11}, \overbrace{\underbrace{\boldsymbol{C}_{2h}''}_{16}}^{12}, \overbrace{\underbrace{\boldsymbol{C}_{2h}}_{14}}^{13}, \overbrace{\underbrace{\boldsymbol{C}_{2v}'}_{12}}^{14}, \overbrace{\underbrace{\boldsymbol{C}_{2v}''}_{13}}^{15}, \overbrace{\underbrace{\boldsymbol{C}_{2h}'}_{15}}^{16}, \overbrace{\underbrace{\boldsymbol{C}_{3v}}_{20}}^{17}, \overbrace{\underbrace{\boldsymbol{D}_3'}_{19}}^{18}, \overbrace{\underbrace{\boldsymbol{C}_{3i}}_{23}}^{19}, \overbrace{\underbrace{\boldsymbol{C}_6}_{17}}^{20},\\
&\quad \overbrace{\underbrace{\boldsymbol{C}_{3v}'}_{21}}^{21}, \overbrace{\underbrace{\boldsymbol{D}_3}_{18}}^{22}, \overbrace{\underbrace{\boldsymbol{C}_{3h}}_{22}}^{23}, \overbrace{\underbrace{\boldsymbol{D}_{2h}}_{24}}^{24}, \overbrace{\underbrace{\boldsymbol{C}_{6v}}_{26}}^{25}, \overbrace{\underbrace{\boldsymbol{D}_6}_{25}}^{26}, \overbrace{\underbrace{\boldsymbol{D}_{3d}'}_{31}}^{27}, \overbrace{\underbrace{\boldsymbol{C}_{6h}}_{27}}^{28}, \overbrace{\underbrace{\boldsymbol{D}_{3h}}_{28}}^{29}, \overbrace{\underbrace{\boldsymbol{D}_{3h}'}_{29}}^{30}, \overbrace{\underbrace{\boldsymbol{D}_{3d}}_{30}}^{31}, \overbrace{\underbrace{\boldsymbol{D}_{6h}}_{32}}^{32}\}. \qquad (5)
\end{aligned}
$$

Because the group D6h_phane is identical with the group D6h_haworth, the mark table tom_D6h_phane is identical with tom_D6h_haworth (Figure 4), the sorted mark table due to tom_D6h_phane and Eq. 5 is identical with the sorted mark table test_sort, which is calculated by means of tom_D6h_haworth and Eq. 4.

3.4 CPR for a coronene skeleton (4) and the

The twelve vertices of the coronene skeleton **4** (Figure 1) are characterized by a permutation group D6h_coronene of order 24, which is generated by applying the GAP function Group to a set of generators gen_coronene.

```
gap> gen_coronene := [(1,3,5,7,9,11)(2,4,6,8,10,12), (1,6)(2,5)(3,4)(7,12)(8,11)(9,10), (13,14)];;
gap> D6h_coronene := Group(gen_coronene); #coronene skeleton
Group([ (1,3,5,7,9,11)(2,4,6,8,10,12), (1,6)(2,5)(3,4)(7,12)(8,11)(9,10), (13,14) ])
gap> Display(Size(D6h_coronene));
24
```

Note that the set of generators gen_coronene is adopted as a combined-permutation representation (CPR) which stabilizes the twelve vertices of the coronene skeleton (**4**)

```
 1:  24
 2:  12 4
 3:  12 . 12
 4:  12 .  . 12
 5:  12 .  .  . 4
 6:  12 .  .  . . 4
 7:  12 .  .  . . . 12
 8:  12 .  .  . . .  . 4
 9:   8 .  .  . . .  . . 8
10:   6 .  6  6 . .  6 . . 6
11:   6 2  .  6 . 2  . . . . 2
12:   6 2  6  . 2 .  . . . . . 2
13:   6 .  .  6 2 .  . 2 . . . . 2
14:   6 .  6  . . 2  . 2 . . . . . 2
15:   6 2  .  . . .  6 2 . . . . . . 2
16:   6 .  .  . 2 2  6 . . . . . . . . 2
17:   4 .  4  . . .  . . 4 . . . . . . . 4
18:   4 4  .  . . .  . . 4 . . . . . . . . 4
19:   4 .  .  . 4 .  . . 4 . . . . . . . . . 4
20:   4 .  .  4 . .  . . 4 . . . . . . . . . . 4
21:   4 .  .  . . .  4 . 4 . . . . . . . . . . . 4
22:   4 .  .  . . 4  . . 4 . . . . . . . . . . . . 4
23:   4 .  .  . . .  . 4 4 . . . . . . . . . . . . . 4
24:   3 1  3  3 1 1  3 1 . 3 1 1 1 1 1 1 . . . . . . . 1
25:   2 .  2  2 . .  2 . 2 2 . . . . . . 2 . . 2 2 . . . 2
26:   2 2  .  2 . 2  . . 2 . 2 . . . . . . 2 . 2 . 2 . . . 2
27:   2 2  2  . 2 .  . . 2 . . 2 . . . . 2 2 2 . . . . . . . 2
28:   2 .  .  2 2 .  . 2 2 . . . 2 . . . . . 2 2 . . 2 . . . . 2
29:   2 .  2  . . 2  . 2 2 . . . . 2 . . 2 . . . . 2 2 . . . . . 2
30:   2 2  .  . . .  2 2 2 . . . . . 2 . . 2 . . 2 . 2 . . . . . . 2
31:   2 .  .  . 2 2  2 . 2 . . . . . . 2 . . 2 . 2 2 . . . . . . . . 2
32:   1 1  1  1 1 1  1 1 1 1 1 1 1 1 1 1 1 1 1 1 1 1 1 1 1 1 1 1 1 1 1 1
```

Figure 5. Mark table (GAP expression, `tom_D6h_coronene`) of the point group $\boldsymbol{D}_{6h}$ by starting from the the set of generators `gen_coronene` for characterizing the twelve positions of the coronene skeleton (**4**) shown in Figure 1.

and contains a 2-cycle `(13,14)` due to a mirror-permutation. Thus, the CPR of degree 14 (= 12 + 2) for a coronene skeleton is used to treat a reflection. The mark table `tom_D6h_coronene` is obtained by using the GAP function `TableOfMarks` as follows:

```
gap> tom_D6h_coronene := TableOfMarks(D6h_coronene);;
gap> Display(tom_D6h_coronene);
```

The resulting mark table `tom_D6h_coronene` (Figure 5) is different in the sequence of subgroups from the standard mark table (Figure 2) and, at the same time, is different from the mark table `tom_D6h_benz` (Figure 3) described above.

The comparison between the mark table `tom_D6h_coronene` (Figure 5) and the standard mark table (Figure 2) results in the following $\mathrm{SSG}^{coronene}_{\boldsymbol{D}_{6h}}$ (Eq. 6).

$$
\begin{aligned}
\mathrm{SSG}^{coronene}_{\boldsymbol{D}_{6h}} = \{ & \overbrace{\underbrace{\boldsymbol{C}_1}_{1}}^{1}, \overbrace{\underbrace{\boldsymbol{C}''_2}_{4}}^{2}, \overbrace{\underbrace{\boldsymbol{C}''_s}_{7}}^{3}, \overbrace{\underbrace{\boldsymbol{C}_2}_{2}}^{4}, \overbrace{\underbrace{\boldsymbol{C}'_s}_{6}}^{5}, \overbrace{\underbrace{\boldsymbol{C}'_2}_{3}}^{6}, \overbrace{\underbrace{\boldsymbol{C}_i}_{8}}^{7}, \overbrace{\underbrace{\boldsymbol{C}_s}_{5}}^{8}, \overbrace{\underbrace{\boldsymbol{C}_3}_{9}}^{9}, \overbrace{\underbrace{\boldsymbol{C}_{2h}}_{14}}^{10}, \\
& \overbrace{\underbrace{\boldsymbol{D}_2}_{10}}^{11}, \overbrace{\underbrace{\boldsymbol{C}''_{2v}}_{13}}^{12}, \overbrace{\underbrace{\boldsymbol{C}_{2v}}_{11}}^{13}, \overbrace{\underbrace{\boldsymbol{C}'_{2v}}_{12}}^{14}, \overbrace{\underbrace{\boldsymbol{C}''_{2h}}_{16}}^{15}, \overbrace{\underbrace{\boldsymbol{C}'_{2h}}_{15}}^{16}, \overbrace{\underbrace{\boldsymbol{C}_{3h}}_{22}}^{17}, \overbrace{\underbrace{\boldsymbol{D}'_3}_{19}}^{18}, \overbrace{\underbrace{\boldsymbol{C}'_{3v}}_{21}}^{19}, \overbrace{\underbrace{\boldsymbol{C}_6}_{17}}^{20}, \\
& \overbrace{\underbrace{\boldsymbol{C}_{3i}}_{23}}^{21}, \overbrace{\underbrace{\boldsymbol{D}_3}_{18}}^{22}, \overbrace{\underbrace{\boldsymbol{C}_{3v}}_{20}}^{23}, \overbrace{\underbrace{\boldsymbol{D}_{2h}}_{24}}^{24}, \overbrace{\underbrace{\boldsymbol{C}_{6h}}_{27}}^{25}, \overbrace{\underbrace{\boldsymbol{D}_6}_{25}}^{26}, \overbrace{\underbrace{\boldsymbol{D}'_{3h}}_{29}}^{27}, \overbrace{\underbrace{\boldsymbol{C}_{6v}}_{26}}^{28}, \overbrace{\underbrace{\boldsymbol{D}_{3h}}_{28}}^{29}, \overbrace{\underbrace{\boldsymbol{D}'_{3d}}_{31}}^{30}, \overbrace{\underbrace{\boldsymbol{D}_{3d}}_{30}}^{31}, \overbrace{\underbrace{\boldsymbol{D}_{6h}}_{32}}^{32} \}. \quad (6)
\end{aligned}
$$

where the upper numbers are taken from the leftmost column of the calculated mark table `tom_D6h_coronene` (Figure 5), while the lower numbers are taken from $\mathrm{SSG}_{\boldsymbol{D}_{6h}}$ (Eq. 1), which corresponds to the standard mark table (Figure 2). The mark table `tom_D6h_coronene` (Figure 5) due to $\mathrm{SSG}_{\boldsymbol{D}_{6h}}^{coronene}$ (Eq. 6) can be converted into the mark table `test3_sort` due to $\mathrm{SSG}_{\boldsymbol{D}_{6h}}$ (Eq. 1) by using the GAP function `SortedTom` as follows:

```
gap> perm_coronene := PermList([1,4,7,2,6,3,8,5,9,14,10,13,11,12,16,15,22,19,21,17,
> 23,18,20,24,27,25,29,26,28,31, 30,32]);
(2,4)(3,7,8,5,6)(10,14,12,13,11)(15,16)(17,22,18,19,21,23,20)(25,27,29,28,26)(30,31)
gap> tom_D6h_coronene := TableOfMarks(D6h_coronene);;
gap> test3_sort := SortedTom(tom_D6h_coronene,perm_coronene);;
gap> Display(test3_sort);
 1: 24
 2: 12 12
 3: 12 . 4
 4: 12 . . 4
 5: 12 . . . 4
 6: 12 . . . . 4
 7: 12 . . . . . 12
 8: 12 . . . . . . 12
 9: 8 . . . . . . . 8
10: 6 6 2 2 . . . . . 2
(omitted)
```

The resulting sorted mark table `test3_sort` is identical with the sorted mark table `test_sort`. Then, if the mark table `test3_sort` is transformed into the GAP matrix format, it is identical with the standard mark table shown in Figure 2.

4 Concordant construction of a standard mark table and a standard USCI-CF table for $\boldsymbol{D}_{6h}$

As shown in the preceding section, the mark tables stemmed from the various skeletons of $\boldsymbol{D}_{6h}$ (**1**–**4** in Figure 1) are different in their sequences of subgroups, where they obey the respective SSGs, i.e., $\mathrm{SSG}_{\boldsymbol{D}_{6h}}^{benz}$ (Eq. 3) for the benzene skeleton **1**, $\mathrm{SSG}_{\boldsymbol{D}_{6h}}^{haworth}$ (Eq. 4) for the Haworth-projected skeleton **2**, $\mathrm{SSG}_{\boldsymbol{D}_{6h}}^{phane}$ (Eq. 5 for the superphane skeleton **3**, and $\mathrm{SSG}_{\boldsymbol{D}_{6h}}^{coronene}$ (Eq. 6) for the coronene skeleton **4**. As described above, these mark tables with different appearances can be converted into a single format (called *a standard mark table*, Figure 2) based on $\mathrm{SSG}_{\boldsymbol{D}_{6h}}$ (Eq. 1), even if the corresponding different sets of generators are used. This is because the mark table and the USCI-CF table reported in a previous article [33] are based on $\mathrm{SSG}_{\boldsymbol{D}_{6h}}$ (Eq. 1).

The author (Fujita) has developed GAP functions for concordant generation of mark tables and USCI-CF tables, i.e., `MarkTableforUSCI` and `constructUSCITable` (contained in the file `USCICF.genfunc`; cf. Appendix A in [24]). They are here examined to be capable of concordant construction of a mark table and a USCI-CF table by starting from a CPR based on any of $\boldsymbol{D}_{6h}$-skeletons (**1**–**4**). To assure the concordance, a list of subgroups derived from each SSG (Eq. 3–Eq. 6) is given as a list of sets of generators `gen[1]`–`gen[32]`.

As shown in the Source Code 1 named `SubDh6h6-X.gap` (Appendix A), for example, the CPR `D6h_benz` based on the benzene skeleton **1** is characterized by the sets of generators `gen[1]`–`gen[32]`, which are shown as the list derived from $\mathrm{SSG}^{benz}_{\boldsymbol{D}_{6h}}$ (Eq. 3). The set of generators (`gen_benz`) for generating the CPR `D6h_benz` and the corresponding set of generators (`gen_benzx`) for specifying the point group $\boldsymbol{D}_6$ are written as an argument in the GAP function `Group`.

The Source Code 1 (`SubDh6h6-X.gap`, Appendix A) is stored in an appropriate directory, in which the file `USCICF.gapfunc` containing the newly-devised GAP functions `MarkTableforUSCI` and `constructUSCITable` are also stored. To execute the Source Code 1 (`SubDh6h6-X.gap`, Appendix A), the `Read` command shown in the top line is copied and pasted after the command prompt `gap>`. The calculation result is output into the log file named `SubD6h6Xlog.txt`.

The devised GAP function `MarkTableforUSCI` generates the standard mark table (Figure 2), which corresponds to $\mathrm{SSG}_{\boldsymbol{D}_{6h}}$ (Eq. 1) and so identical with `test_sort` calculated by using the GAP function `SortedTom`.

Such a standard mark table as Figure 2 is linked with a USCI-CF table (`USCITableD6h`, Figure 6), which is generated by the other devised GAP function `constructUSCITable` appearing in the above Source Code 1 (`SubDh6h6-X.gap`).

The USCI-CF table (`USCITableD6h`) shown in Figure 6 follows the convention of the GAP system for printing a matrix format, where a nested list of the GAP system is used. Each list in an inner pair of square brackets is a row vector of the matrix, which corresponds to a coset representation (CR) $(\boldsymbol{G}_i\backslash)\boldsymbol{D}_{6h}$. For the sake of convenience, the sequence numbers (1) to (32) are added to show the correspondence to $(\boldsymbol{G}_i\backslash)\boldsymbol{D}_{6h}$ ($i = 1 \cdots 32$) in accord with Eq. 1 and Eq. 2. Each term at the intersection between the $(\boldsymbol{G}_i\backslash)\boldsymbol{D}_{6h}$-row and the $\boldsymbol{G}_j$-column is calculated by means of SCR (subduction of the CR) $(\boldsymbol{G}_i\backslash)\boldsymbol{D}_{6h} \downarrow \boldsymbol{G}_j$. An outer pair of square brackets contains the thirty-two of such row vectors to indicate the whole format of the matrix.

```
##USCI-CF table (USCITableD6h) :
[(1) [ b_1^24, b_2^12, b_2^12, b_2^12, c_2^12, c_2^12, c_2^12, c_2^12, b_3^8, b_4^6, c_4^6, c_4^6, c_4^6, c_4^6,
    c_4^6, c_4^6, b_6^4, b_6^4, b_6^4, c_6^4, c_6^4, c_6^4, c_6^4, c_8^3, b_12^2, c_12^2, c_12^2, c_12^2,
    c_12^2, c_12^2, c_12^2, c_24 ],
 (2) [ b_1^12, b_1^12, b_2^6, b_2^6, c_2^6, c_2^6, c_2^6, c_2^6, b_3^4, b_2^6, c_2^6, c_4^3,
    c_4^3, c_2^6, c_4^3, c_4^3, b_3^4, b_6^2, b_6^2, c_6^2, c_6^2, c_6^2, c_6^2, c_4^3,
    b_6^2, c_6^2, c_6^2, c_12, c_12, c_12, c_12, c_12 ],
 (3) [ b_1^12, b_2^6, b_1^4*b_2^4, b_2^6, c_2^6, c_2^6, c_2^6, c_2^6, b_3^4, b_2^2*b_4^2, c_4^3,
    c_2^2*c_4^2, c_4^3, c_4^3, c_2^2*c_4^2, c_4^3, b_6^2, b_3^4, b_6^2, c_6^2, c_6^2, c_6^2,
    c_6^2, c_4*c_8, b_6^2, c_12, c_12, c_6^2, c_12, c_6^2, c_12, c_12 ],
 (4) [ b_1^12, b_2^6, b_2^6, b_1^4*b_2^4, c_2^6, c_2^6, c_2^6, c_2^6, b_3^4, b_2^2*b_4^2, c_4^3,
    c_4^3, c_2^2*c_4^2, c_4^3, c_4^3, c_2^2*c_4^2, b_6^2, b_6^2, b_3^4, c_6^2, c_6^2, c_6^2,
     c_6^2, c_4*c_8, b_6^2, c_12, c_12, c_12, c_6^2, c_12, c_6^2, c_12 ],
 (5) [ b_1^12, b_2^6, b_2^6, b_2^6, c_2^4*a_1^4, c_2^6, c_2^6, c_2^6, b_3^4, b_4^3, c_4^2*a_2^2,
     c_4^2*a_2^2, c_4^3, c_4^3, c_4^3, c_4^2*a_2^2, b_6^2, b_6^2, b_6^2, a_3^4, c_6^2,
     c_6^2, c_6^2, c_8*a_4, b_12, a_6^2, c_12, a_6^2, c_12, c_12, a_6^2, a_12 ],
 (6) [ b_1^12, b_2^6, b_2^6, b_2^6, c_2^6, c_2^4*a_1^4, c_2^6, c_2^6, b_3^4, b_4^3, c_4^2*a_2^2,
    c_4^3, c_4^2*a_2^2, c_4^3, c_4^2*a_2^2, c_4^3, b_6^2, b_6^2, b_6^2, c_6^2, a_3^4, c_6^2,
    c_6^2, c_8*a_4, b_12, a_6^2, c_12, c_12, a_6^2, a_6^2, c_12, a_12 ],
 (7) [ b_1^12, b_2^6, b_2^6, b_2^6, c_2^6, c_2^6, a_1^12, c_2^6, b_3^4, b_4^3, c_4^3, a_2^6,
    a_2^6, a_2^6, c_4^3, c_4^3, b_6^2, b_6^2, b_6^2, c_6^2, c_6^2, a_3^4, c_6^2, a_4^3,
     b_12, c_12, a_6^2, a_6^2, a_6^2, c_12, c_12, a_12 ],
 (8) [ b_1^12, b_2^6, b_2^6, b_2^6, c_2^6, c_2^6, c_2^6, a_1^12, b_3^4, b_4^3, c_4^3, c_4^3,
    c_4^3, a_2^6, a_2^6, a_2^6, b_6^2, b_6^2, b_6^2, c_6^2, c_6^2, c_6^2, a_3^4, a_4^3,
     b_12, c_12, a_6^2, c_12, c_12, a_6^2, a_6^2, a_12 ],
 (9) [ b_1^8, b_2^4, b_2^4, b_2^4, c_2^4, c_2^4, c_2^4, c_2^4, b_1^8, b_4^2, c_4^2, c_4^2,
     c_4^2, c_4^2, c_4^2, c_4^2, b_2^4, b_2^4, b_2^4, c_2^4, c_2^4, c_2^4, c_2^4,c_8,
     b_4^2, c_4^2, c_4^2, c_4^2, c_4^2, c_4^2, c_4^2,c_8 ],
(10) [ b_1^6, b_1^6, b_1^2*b_2^2, b_1^2*b_2^2, c_2^3, c_2^3, c_2^3, c_2^3, b_3^2, b_1^2*b_2^2,
     c_2^3, c_2*c_4, c_2*c_4, c_2^3, c_2*c_4, c_2*c_4, b_3^2, b_3^2, b_3^2,c_6,c_6,c_6,c_6, c_2*c_4,
     b_3^2, c_6,c_6,c_6,c_6,c_6,c_6,c_6 ],
(11) [ b_1^6, b_1^6, b_2^3, b_2^3, c_2^2*a_1^2, c_2^2*a_1^2, c_2^3, c_2^3, b_3^2, b_2^3,
     c_2^2*a_1^2, c_4*a_2, c_4*a_2, c_2^3, c_4*a_2, c_4*a_2, b_3^2,b_6,b_6, a_3^2, a_3^2,c_6,c_6,
     c_4*a_2,b_6, a_3^2,c_6,a_6,a_6,a_6,a_6,a_6 ],
(12) [ b_1^6, b_2^3, b_1^2*b_2^2, b_2^3, c_2^2*a_1^2, c_2^3, a_1^6, c_2^3, b_3^2, b_2*b_4,
     c_4*a_2, a_1^2*a_2^2, a_2^3, a_2^3, c_2*c_4, c_4*a_2, b_6, b_3^2,b_6, a_3^2,c_6,
     a_3^2,c_6, a_2*a_4,b_6, a_6,a_6, a_3^2,a_6,c_6,a_6,a_6 ],
(13) [ b_1^6, b_2^3, b_2^3, b_1^2*b_2^2, c_2^3, c_2^2*a_1^2, a_1^6, c_2^3, b_3^2, b_2*b_4,
     c_4*a_2, a_2^3, a_1^2*a_2^2, a_2^3, c_4*a_2, c_2*c_4, b_6,b_6, b_3^2,c_6, a_3^2, a_3^2,c_6,
     a_2*a_4,b_6, a_6,a_6,a_6, a_3^2,a_6,c_6,a_6 ],
(14) [ b_1^6, b_1^6, b_2^3, b_2^3, c_2^3, c_2^3, a_1^6, a_1^6, b_3^2, b_2^3, c_2^3,
     a_2^3, a_2^3, a_1^6, a_2^3, a_2^3, b_3^2,b_6,b_6,c_6,c_6, a_3^2, a_3^2, a_2^3,b_6, c_6,
     a_3^2,a_6,a_6,a_6,a_6,a_6 ],
(15) [ b_1^6, b_2^3, b_1^2*b_2^2, b_2^3, c_2^3, c_2^2*a_1^2, c_2^3, a_1^6, b_3^2, b_2*b_4, c_4*a_2,
     c_2*c_4, c_4*a_2, a_2^3, a_1^2*a_2^2, a_2^3, b_6, b_3^2,b_6,c_6, a_3^2,c_6, a_3^2,
     a_2*a_4,b_6, a_6,a_6,c_6,a_6, a_3^2,a_6,a_6 ],
(16) [ b_1^6, b_2^3, b_2^3, b_1^2*b_2^2, c_2^2*a_1^2, c_2^3, c_2^3, a_1^6, b_3^2, b_2*b_4,
     c_4*a_2, c_4*a_2, c_2*c_4, a_2^3, a_2^3, a_1^2*a_2^2, b_6,b_6, b_3^2, a_3^2,c_6,c_6, a_3^2,
     a_2*a_4,b_6, a_6,a_6,a_6,c_6,a_6, a_3^2,a_6 ],
(17) [ b_1^4, b_1^4, b_2^2, b_2^2, c_2^2, c_2^2, c_2^2, c_2^2,b_1^4, b_2^2, c_2^2,c_4,c_4, c_2^2,c_4,
     c_4, b_1^4, b_2^2, b_2^2, c_2^2, c_2^2, c_2^2, c_2^2,c_4, b_2^2, c_2^2, c_2^2,c_4,c_4,c_4,c_4,c_4 ],
(18) [ b_1^4, b_2^2, b_1^4, b_2^2, c_2^2, c_2^2, c_2^2, c_2^2, b_1^4, b_2^2,c_4, c_2^2,c_4,c_4, c_2^2,
     c_4, b_2^2, b_1^4, b_2^2, c_2^2, c_2^2, c_2^2, c_2^2,c_4, b_2^2, c_4,c_4, c_2^2,c_4, c_2^2,c_4,c_4 ],
(19) [ b_1^4, b_2^2, b_2^2, b_1^4, c_2^2, c_2^2, c_2^2, c_2^2, b_1^4, b_2^2,c_4,c_4, c_2^2,c_4,c_4,
     c_2^2, b_2^2, b_2^2, b_1^4, c_2^2, c_2^2, c_2^2, c_2^2,c_4, b_2^2, c_4,c_4,c_4, c_2^2,c_4, c_2^2,c_4 ],
(20) [ b_1^4, b_2^2, b_2^2, b_2^2, a_1^4, c_2^2, c_2^2, c_2^2, b_1^4,b_4, a_2^2, a_2^2,c_4,c_4,c_4,
     a_2^2, b_2^2, b_2^2, b_2^2, a_1^4, c_2^2, c_2^2, c_2^2,a_4,b_4, a_2^2,c_4, a_2^2,c_4,c_4, a_2^2,a_4 ],
(21) [ b_1^4, b_2^2, b_2^2, b_2^2, c_2^2, a_1^4, c_2^2, c_2^2, b_1^4,b_4, a_2^2,c_4, a_2^2,c_4, a_2^2,
     c_4, b_2^2, b_2^2, b_2^2, c_2^2, a_1^4, c_2^2, c_2^2,a_4,b_4, a_2^2,c_4,c_4, a_2^2, a_2^2,c_4,a_4 ],
(22) [ b_1^4, b_2^2, b_2^2, b_2^2, c_2^2, c_2^2, a_1^4, c_2^2, b_1^4,b_4,c_4, a_2^2, a_2^2, a_2^2,c_4,
     c_4, b_2^2, b_2^2, b_2^2, c_2^2, c_2^2, a_1^4, c_2^2,a_4,b_4, c_4, a_2^2, a_2^2, a_2^2,c_4,c_4,a_4 ],
(23) [ b_1^4, b_2^2, b_2^2, b_2^2, c_2^2, c_2^2, c_2^2, a_1^4, b_1^4,b_4,c_4,c_4,c_4, a_2^2, a_2^2,
     a_2^2, b_2^2, b_2^2, b_2^2, c_2^2, c_2^2, c_2^2, a_1^4,a_4,b_4, c_4, a_2^2,c_4,c_4, a_2^2, a_2^2,a_4 ],
(24) [ b_1^3, b_1^3, b_1*b_2, b_1*b_2, c_2*a_1, c_2*a_1, a_1^3, a_1^3, b_3, b_1*b_2, c_2*a_1, a_1*a_2, a_1*a_2,
     a_1^3, a_1*a_2, a_1*a_2, b_3,b_3,b_3,a_3,a_3,a_3,a_3, a_1*a_2,b_3, a_3,a_3,a_3,a_3,a_3,a_3,a_3 ],
(25) [ b_1^2, b_1^2, b_1^2, b_1^2,c_2,c_2,c_2,c_2, b_1^2, b_1^2,c_2,c_2,c_2,c_2,c_2,
     c_2, b_1^2, b_1^2, b_1^2,c_2,c_2,c_2,c_2,c_2, b_1^2, c_2,c_2,c_2,c_2,c_2,c_2,c_2 ],
(26) [ b_1^2, b_1^2,b_2,b_2, a_1^2, a_1^2,c_2,c_2, b_1^2,b_2, a_1^2,a_2,a_2,c_2,a_2,
     a_2, b_1^2,b_2,b_2, a_1^2, a_1^2,c_2,c_2,a_2,b_2, a_1^2,c_2,a_2,a_2,a_2,a_2,a_2 ],
(27) [ b_1^2, b_1^2,b_2,b_2,c_2,c_2, a_1^2, a_1^2, b_1^2,b_2,c_2,a_2,a_2, a_1^2,a_2,
     a_2, b_1^2,b_2,b_2,c_2,c_2, a_1^2, a_1^2,a_2,b_2, c_2, a_1^2,a_2,a_2,a_2,a_2,a_2 ],
(28) [ b_1^2,b_2, b_1^2,b_2, a_1^2,c_2, a_1^2,c_2, b_1^2,b_2,a_2, a_1^2,a_2,a_2,c_2,
     a_2, b_2, b_1^2,b_2, a_1^2,c_2, a_1^2,c_2,a_2,b_2, a_2,a_2, a_1^2,a_2,c_2,a_2,a_2 ],
(29) [ b_1^2,b_2,b_2, b_1^2,c_2, a_1^2, a_1^2,c_2, b_1^2,b_2,a_2,a_2, a_1^2,a_2,a_2,
     c_2, b_2,b_2, b_1^2,c_2, a_1^2, a_1^2,c_2,a_2,b_2, a_2,a_2,a_2, a_1^2,a_2,c_2,a_2 ],
(30) [ b_1^2,b_2, b_1^2,b_2,c_2, a_1^2,c_2, a_1^2, b_1^2,b_2,a_2,c_2,a_2,a_2, a_1^2,
     a_2, b_2, b_1^2,b_2,c_2, a_1^2,c_2, a_1^2,a_2,b_2, a_2,a_2,c_2,a_2, a_1^2,a_2,a_2 ],
(31) [ b_1^2,b_2,b_2, b_1^2, a_1^2,c_2,c_2, a_1^2, b_1^2,b_2,a_2,a_2,c_2,a_2,a_2,
     a_1^2, b_2,b_2, b_1^2, a_1^2,c_2,c_2, a_1^2,a_2,b_2, a_2,a_2,a_2,c_2,a_2, a_1^2,a_2 ],
(32) [ b_1,b_1,b_1,b_1,a_1,a_1,a_1,a_1, b_1,b_1,a_1,a_1,a_1,a_1,a_1,
     a_1, b_1,b_1,b_1,a_1,a_1,a_1,a_1,a_1,b_1, a_1,a_1,a_1,a_1,a_1,a_1,a_1 ] ]
```

Figure 6. Standard USCI-CF Table of $\boldsymbol{D}_{6h}$ (`USCITableD6h`). Each row with an inner pair of brackets corresponds to the coset representation (CR) $(\boldsymbol{G}_i\backslash)\boldsymbol{D}_{6h}$ and contains 32 USCI-CFs (unit subduced cycle indices with chirality fittingness) assigned to the respective subgroups $\boldsymbol{G}_j$. Each USCI-CF at the intersection between the $(\boldsymbol{G}_i\backslash)\boldsymbol{D}_{6h}$-row and the $\boldsymbol{G}_j$-column is calculated by means of SCR (subduction of the CR) $(\boldsymbol{G}_i\backslash)\boldsymbol{D}_{6h} \downarrow \boldsymbol{G}_j$.

5 Generation of SCI-CFs

In general, a given skeleton has one or more orbits, where each orbit is governed by a coset representation (CR). In the preceding section, each of the $\boldsymbol{D}_{6h}$-skeletons collected in Figure 1 has been examined by emphasizing one orbit.

As calculated in Source Code 1 (`SubDh6h6-X.gap`, Appendix A) for the benzene skeleton **1**, for example, the fixed-point vector (`FPVbenz`) is calculated by using the newly-devised GAP function `calculateFPvector`; and the list of SCI-CFs (`l_SCICF_benz`) is calculated by using the newly-devised GAP function `constructSCICF`. The corresponding outputs in the log file `SubDh6h6-Xlog.txt` are as follows:

```
#Fixed point vector for benzene #FPVbenz
[ 6, 0, 2, 0, 2, 0, 6, 0, 0, 0, 0, 2, 0, 0, 0, 0, 0, 0, 0, 0,
  0, 0, 0, 0, 0, 0, 0, 0, 0, 0, 0, 0 ]
#Orbits for benzene #Orbit_benz
[ 0, 0, 0, 0, 0, 0, 0, 0, 0, 0, 0, 1, 0, 0, 0, 0, 0, 0, 0, 0,
  0, 0, 0, 0, 0, 0, 0, 0, 0, 0, 0, 0 ]
#SCI-CF for benzene #l_SCICF_benz
[ b_1^6, b_2^3, b_1^2*b_2^2, b_2^3, c_2^2*a_1^2, c_2^3, a_1^6, c_2^3, b_3^2, b_2*b_4,
  c_4*a_2, a_1^2*a_2^2, a_2^3, a_2^3, c_2*c_4, c_4*a_2, b_6, b_3^2, b_6, a_3^2,
  c_6, a_3^2, c_6, a_2*a_4, b_6, a_6, a_6, a_3^2, a_6, c_6, a_6, a_6 ]
```

Thus, the fixed-point vector (`FPVbenz`) is identical with the 12th row of the standard mark table (its matrix format (Figure 2) or `test_sort`). This is confirmed by the output of `Orbit_benz`, in which the 12th value 1 indicates the appearance of the subgroup $\boldsymbol{C}'_{2v}$. Hence, the six vertices of the benzene skeleton **1** belong to one orbit governed by the coset representation $(\boldsymbol{C}'_{2v}\backslash)\boldsymbol{D}_{6h}$ (size: $|\boldsymbol{D}_{6h}|/|\boldsymbol{C}'_{2v}| = 24/4 = 6$).

The SCI-CF for benzene (`l_SCICF_benz`) calculated by the newly-devised GAP function `constructSCICF` is identical with the 12th row of the standard USCI-CF table of $\boldsymbol{D}_{6h}$ (`USCITableD6h`) shown in Figure 6 because of the presence of one orbit.

In similar ways as Source Code 1 (`SubDh6h6-X.gap`, Appendix A), FPVs, CRs, and SCI-CFs of the skeletons **1**–**4** (Figure 1) are calculated as collected in Table 1, where the respective SSGs are taken into consideration, i.e., $\mathrm{SSG}_{\boldsymbol{D}_{6h}}^{benz}$ (Eq. 3) for the benzene skeleton **1**, $\mathrm{SSG}_{\boldsymbol{D}_{6h}}^{haworth}$ (Eq. 4) for the Haworth-projected skeleton **2**, $\mathrm{SSG}_{\boldsymbol{D}_{6h}}^{phane}$ (Eq. 5) for the superphane skeleton **3**, and $\mathrm{SSG}_{\boldsymbol{D}_{6h}}^{coronene}$ (Eq. 6) for the coronene skeleton **4**.

It should be noted that the present article deals with cases in which each skeleton is considered to contain one orbit corresponding to a single CR, i.e., $(\boldsymbol{G}_i\backslash)\boldsymbol{D}_{6h}$. However, a general case would contain one or more orbits corresponding to a summed CR, i.e., $\sum_i(\boldsymbol{G}_i\backslash)\boldsymbol{D}_{6h}$. The subduction process operated onto a single CR expressed by a symbol $(\boldsymbol{G}_i\backslash)\boldsymbol{D}_{6h} \downarrow \boldsymbol{G}_j$, where each term at the intersection between i-th row and

Table 1. FPV, CR, and SCI-CF for Each $\boldsymbol{D}_{6h}$-Skeleton **1**—**4**

	FPV	CR	list of SCI-CFs
1	[6, 0, 2, 0, 2, 0, 6, 0, 0, 0, 0, 2, 0, 0, 0, 0, 0, 0, 0, 0, 0, 0, 0, 0, 0, 0, 0, 0, 0, 0, 0, 0] (the 12th row of Figure 2)	$(\boldsymbol{C}'_{2v}\backslash)\boldsymbol{D}_{6h}$	$[b_1^6, b_2^3, b_1^2 * b_2^2, b_2^3, c_2^2 * a_1^2,$ $c_2^3, a_1^6, c_2^3, b_3^2, b_2 * b_4,$ $c_4 * a_2, a_1^2 * a_2^2, a_2^3, a_2^3, c_2 * c_4,$ $c_4 * a_2, b_6, b_3^2, b_6, a_3^2,$ $c_6, a_3^2, c_6, a_2 * a_4, b_6,$ $a_6, a_6, a_3^2, a_6, c_6, a_6, a_6]$ (the 12th row of Figure 6)
2	[12, 0, 0, 0, 4, 0, 0, 0, 0, 0, 0, 0, 0, 0, 0, 0, 0, 0, 0, 0, 0, 0, 0, 0, 0, 0, 0, 0, 0, 0, 0, 0] (the 5th row of Figure 2)	$(\boldsymbol{C}_s\backslash)\boldsymbol{D}_{6h}$	$[b_1^12, b_2^6, b_2^6, b_2^6, c_2^4 * a_1^4,$ $c_2^6, c_2^6, c_2^6, b_3^4, b_4^3,$ $c_4^2 * a_2^2, c_4^2 * a_2^2, c_4^3, c_4^3, c_4^3,$ $c_4^2 * a_2^2, b_6^2, b_6^2, b_6^2, a_3^4,$ $c_6^2, c_6^2, c_6^2, c_8 * a_4, b_12,$ $a_6^2, c_12, a_6^2, c_12, c_12, a_6^2, a_12]$ (the 5th row of Figure 6)
3	[12, 0, 0, 0, 4, 0, 0, 0, 0, 0, 0, 0, 0, 0, 0, 0, 0, 0, 0, 0, 0, 0, 0, 0, 0, 0, 0, 0, 0, 0, 0, 0] (the 5th row of Figure 2)	$(\boldsymbol{C}_s\backslash)\boldsymbol{D}_{6h}$	$[b_1^12, b_2^6, b_2^6, b_2^6, c_2^4 * a_1^4,$ $c_2^6, c_2^6, c_2^6, b_3^4, b_4^3,$ $c_4^2 * a_2^2, c_4^2 * a_2^2, c_4^3, c_4^3, c_4^3,$ $c_4^2 * a_2^2, b_6^2, b_6^2, b_6^2, a_3^4,$ $c_6^2, c_6^2, c_6^2, c_8 * a_4, b_12,$ $a_6^2, c_12, a_6^2, c_12, c_12, a_6^2, a_12]$ (the 5th row of Figure 6)
4	[12, 0, 0, 0, 0, 0, 12, 0, 0, 0, 0, 0, 0, 0, 0, 0, 0, 0, 0, 0, 0, 0, 0, 0, 0, 0, 0, 0, 0, 0, 0, 0] (the 7th row of Figure 2)	$(\boldsymbol{C}''_s\backslash)\boldsymbol{D}_{6h}$	$[b_1^12, b_2^6, b_2^6, b_2^6, c_2^6,$ $c_2^6, a_1^12, c_2^6, b_3^4, b_4^3,$ $c_4^3, a_2^6, a_2^6, a_2^6, c_4^3,$ $c_4^3, b_6^2, b_6^2, b_6^2, c_6^2,$ $c_6^2, a_3^4, c_6^2, a_4^3, b_12,$ $c_12, a_6^2, a_6^2, a_6^2, c_12, c_12, a_12]$ (the 7th row of Figure 6)

j-the column is represented by USCI-CF$_{ij}$. The subduction process operated onto a summed CR expressed by a symbol $\sum_i(\boldsymbol{G}_i\backslash)\boldsymbol{D}_{6h} \downarrow \boldsymbol{G}_j$, which corresponds to SCI-CF$_j$ ($= \prod_i \mathrm{USCI} - \mathrm{CF}_{ij}$). When one orbit relates to the $(\boldsymbol{G}_i\backslash)\boldsymbol{D}_{6h}$-row (the i-th row), SCI-CF$_j$ is equal to USCI-CF$_{ij}$, e.g., as found in the 12th row of Figure 6 for the benzene skeleton.

Although the respective combined-permutation representations (CPRs) are different, the standard mark table (its matrix format (Figure 2) or `test_sort`) and the standard USCI-CF table (`USCITableD6h` shown in Figure 6) are commonly obtained, so as to characterize the point group $\boldsymbol{D}_{6h}$ algebraically. Thus, the FPVs, CRs, and SCI-CFs collected in Table 1 are commonly based on the standard mark table (Figure 2) and the standard USCI-CF table (Figure 6) for the point group $\boldsymbol{D}_{6h}$.

6 Generation of PCI-CFs

Fujita's USCI approach [4, 10] supports four methods of combinatorial enumeration, i.e., (1) the FPM (fixed-point matrix) method, which is based on generating functions derived from subduced cycle indices (SCIs) and mark tables [7–9]; (2) the PCI (partial-cycle-index) method, which is based on generating functions derived from partial cycle indices (PCIs) [34, 35]; (3) the elementary superposition method [36]; and (4) the partial superposition method [34,36]. Among them, the partial-cycle-index (PCI) method [34,35] will be applied here to $\boldsymbol{D}_{6h}$-skeletons (Figure 1).

6.1 PCI-CFs for the benzene skeleton 1

As shown in the last part of Source Code 1 (`SubDh6h6-X.gap`, Appendix A), the list of PCI-CFs (`l_PCICF_benz`) for the benzene skeleton **1** has been obtained from the list of SCI-CFs (`l_SCICF_benz`, i.e., the first row at the list of SCI-CFs-column of Table 1), which is multiplied by the inverse of the mark table `Inverse(Matrix_tomD6hbenz)`, as follows.

```
Display("#list␣of␣PCI-CFs␣for␣benzene");
l_PCICF_benz := l_SCICF_benz * Inverse(Matrix_tomD6h_benz);
Display(l_PCICF_benz);
```

The output in the corresponding log file is a matrix format with a single row, which contains a list of 32 PCI-CFs for the respective subgroups:

```
#list of PCI-CFs for benzene
[ 1/24*b_1^6-1/24*a_1^6-1/8*b_1^2*b_2^2-1/8*c_2^2*a_1^2+1/4*a_1^2*a_2^2 -1/6*b_2^3-1/6*c_2^3+1/3*a_2^3
  +1/4*b_2*b_4+1/4*c_2*c_4+1/12*b_3^2+1/2*c_4*a_2-a_2*a_4-1/12*a_3^2-1/12*c_6-1/12*b_6+1/6*a_6,
  1/12*b_2^3-1/12*a_2^3-1/4*b_2*b_4-1/4*c_4*a_2+1/2*a_2*a_4+1/6*b_6-1/6*a_6,
(omitted)
a_6 ]
```

This list is transformed into the respective PCI-CF for each subgroup, i.e., `PCICF[1]`–`PCICF[32]`:

```
#PCI-CFs for subgroups
PCI-CF[1] := 1/24*b_1^6-1/24*a_1^6-1/8*b_1^2*b_2^2-1/8*c_2^2*a_1^2+1/4*a_1^2*a_2^2-1/6*b_2^3-1/6*c_2^3
+1/3*a_2^3+1/4*b_2*b_4+1/4*c_2*c_4+1/12*b_3^2+1/2*c_4*a_2-a_2*a_4-1/12*a_3^2-1/12*c_6-1/12*b_6+1/6*a_6
PCI-CF[2] := 1/12*b_2^3-1/12*a_2^3-1/4*b_2*b_4-1/4*c_4*a_2+1/2*a_2*a_4+1/6*b_6-1/6*a_6
PCI-CF[3] := 1/4*b_1^2*b_2^2-1/4*a_1^2*a_2^2-1/4*b_2*b_4-1/4*c_2*c_4-1/4*b_3^2+1/2*a_2*a_4+1/4*a_3^2
+1/4*c_6+1/4*b_6-1/2*a_6
PCI-CF[4] := 1/4*b_2^3-1/4*a_2^3-1/4*b_2*b_4-1/4*c_4*a_2+1/2*a_2*a_4
PCI-CF[5] := 1/4*c_2^2*a_1^2-1/4*a_1^2*a_2^2-1/2*c_4*a_2+1/2*a_2*a_4
PCI-CF[6] := 1/4*c_2^3-1/4*a_2^3-1/4*c_2*c_4-1/4*c_4*a_2+1/2*a_2*a_4
PCI-CF[7] := 1/12*a_1^6-1/4*a_1^2*a_2^2-1/3*a_2^3+1/2*a_2*a_4+1/6*a_3^2-1/6*a_6
PCI-CF[8] := 1/12*c_2^3-1/12*a_2^3-1/4*c_2*c_4-1/4*c_4*a_2+1/2*a_2*a_4+1/6*c_6-1/6*a_6
PCI-CF[9] := 0
```

```
PCI-CF[10] := 1/2*b_2*b_4-1/2*a_2*a_4-1/2*b_6+1/2*a_6
PCI-CF[11] := 1/2*c_4*a_2-1/2*a_2*a_4
PCI-CF[12] := 1/2*a_1^2*a_2^2-1/2*a_2*a_4-1/2*a_3^2+1/2*a_6
PCI-CF[13] := 1/2*a_2^3-1/2*a_2*a_4
PCI-CF[14] := 1/6*a_2^3-1/2*a_2*a_4+1/3*a_6
PCI-CF[15] := 1/2*c_2*c_4-1/2*a_2*a_4-1/2*c_6+1/2*a_6
PCI-CF[16] := 1/2*c_4*a_2-1/2*a_2*a_4
PCI-CF[17] := 0
PCI-CF[18] := 1/4*b_3^2-1/4*a_3^2-1/4*c_6-1/4*b_6+1/2*a_6
PCI-CF[19] := 0
PCI-CF[20] := 0
PCI-CF[21] := 0
PCI-CF[22] := 0
PCI-CF[23] := 0
PCI-CF[24] := a_2*a_4-a_6
PCI-CF[25] := 1/2*b_6-1/2*a_6
PCI-CF[26] := 0
PCI-CF[27] := 0
PCI-CF[28] := 1/2*a_3^2-1/2*a_6
PCI-CF[29] := 0
PCI-CF[30] := 1/2*c_6-1/2*a_6
PCI-CF[31] := 0
PCI-CF[32] := a_6
```

The i-th element `PCI-CF[`i`]` ($i = 1, 2, \cdots, 32$) corresponds to the respective subgroups numbered sequentially, as shown in $\mathrm{SSG}_{\boldsymbol{D}_{6h}}$ (Eq. 1). Hence, the above PCI-CFs (`PCI-CF[`i`]`, $i = 1, 2, \ldots, 32$) for the benzene skeleton **1** can be written in usual mathematical notation (cf. Definition 19.6 of Ref. [4]):

$$\begin{aligned}\text{PCI-CF}_{\mathbf{1}}(\boldsymbol{C}_1, \$_d) &= \frac{1}{24}b_1^6 - \frac{1}{24}a_1^6 - \frac{1}{8}b_1^2b_2^2 - \frac{1}{8}c_2^2a_1^2 + \frac{1}{4}a_1^2a_2^2 - \frac{1}{6}b_2^3 - \frac{1}{6}c_2^3 + \frac{1}{3}a_2^3 + \frac{1}{4}b_2b_4 \\ &\quad + \frac{1}{4}c_2c_4 + \frac{1}{12}b_3^2 + \frac{1}{2}c_4a_2 - a_2a_4 - \frac{1}{12}a_3^2 - \frac{1}{12}c_6 - \frac{1}{12}b_6 + \frac{1}{6}a_6 \end{aligned} \tag{7}$$

$$\text{PCI-CF}_{\mathbf{1}}(\boldsymbol{C}_2, \$_d) = \frac{1}{12}b_2^3 - \frac{1}{12}a_2^3 - \frac{1}{4}b_2b_4 - \frac{1}{4}c_4a_2 + \frac{1}{2}a_2a_4 + \frac{1}{6}b_6 - \frac{1}{6}a_6 \tag{8}$$

$$\begin{aligned}\text{PCI-CF}_{\mathbf{1}}(\boldsymbol{C}_2', \$_d) &= \frac{1}{4}b_1^2b_2^2 - \frac{1}{4}a_1^2a_2^2 - \frac{1}{4}b_2b_4 - \frac{1}{4}c_2c_4 - \frac{1}{4}b_3^2 + \frac{1}{2}a_2a_4 + \frac{1}{4}a_3^2 \\ &\quad + \frac{1}{4}c_6 + \frac{1}{4}b_6 - \frac{1}{2}a_6 \end{aligned} \tag{9}$$

$$\text{PCI-CF}_{\mathbf{1}}(\boldsymbol{C}_2'', \$_d) = \frac{1}{4}b_2^3 - \frac{1}{4}a_2^3 - \frac{1}{4}b_2b_4 - \frac{1}{4}c_4a_2 + \frac{1}{2}a_2a_4 \tag{10}$$

$$\text{PCI-CF}_{\mathbf{1}}(\boldsymbol{C}_s, \$_d) = \frac{1}{4}c_2^2a_1^2 - \frac{1}{4}a_1^2a_2^2 - \frac{1}{2}c_4a_2 + \frac{1}{2}a_2a_4 \tag{11}$$

$$\text{PCI-CF}_{\mathbf{1}}(\boldsymbol{C}_s', \$_d) = \frac{1}{4}c_2^3 - \frac{1}{4}a_2^3 - \frac{1}{4}c_2c_4 - \frac{1}{4}c_4a_2 + \frac{1}{2}a_2a_4 \tag{12}$$

$$\text{PCI-CF}_{\mathbf{1}}(\boldsymbol{C}_s'', \$_d) = \frac{1}{12}a_1^6 - \frac{1}{4}a_1^2a_2^2 - \frac{1}{3}a_2^3 + \frac{1}{2}a_2a_4 + \frac{1}{6}a_3^2 - \frac{1}{6}a_6 \tag{13}$$

$$\text{PCI-CF}_{\mathbf{1}}(\boldsymbol{C}_i, \$_d) = \frac{1}{12}c_2^3 - \frac{1}{12}a_2^3 - \frac{1}{4}c_2c_4 - \frac{1}{4}c_4a_2 + \frac{1}{2}a_2a_4 + \frac{1}{6}c_6 - \frac{1}{6}a_6 \tag{14}$$

$$\text{PCI-CF}_{\mathbf{1}}(\boldsymbol{C}_3, \$_d) = 0 \tag{15}$$

$$\text{PCI-CF}_{\mathbf{1}}(\boldsymbol{D}_2, \$_d) = \frac{1}{2}b_2b_4 - \frac{1}{2}a_2a_4 - \frac{1}{2}b_6 + \frac{1}{2}a_6 \tag{16}$$

$$\text{PCI-CF}_{\mathbf{1}}(\boldsymbol{C}_{2v}, \$_d) = \frac{1}{2}c_4a_2 - \frac{1}{2}a_2a_4 \tag{17}$$

$$\text{PCI-CF}_{\mathbf{1}}(\boldsymbol{C}'_{2v}, \$_d) = \frac{1}{2}a_1^2a_2^2 - \frac{1}{2}a_2a_4 - \frac{1}{2}a_3^2 + \frac{1}{2}a_6 \tag{18}$$

$$\text{PCI-CF}_{\mathbf{1}}(\boldsymbol{C}''_{2v}, \$_d) = \frac{1}{2}a_2^3 - \frac{1}{2}a_2a_4 \tag{19}$$

$$\text{PCI-CF}_{\mathbf{1}}(\boldsymbol{C}_{2h}, \$_d) = \frac{1}{6}a_2^3 - \frac{1}{2}a_2a_4 + 1/3a_6 \tag{20}$$

$$\text{PCI-CF}_{\mathbf{1}}(\boldsymbol{C}'_{2h}, \$_d) = \frac{1}{2}c_2c_4 - \frac{1}{2}a_2a_4 - \frac{1}{2}c_6 + \frac{1}{2}a_6 \tag{21}$$

$$\text{PCI-CF}_{\mathbf{1}}(\boldsymbol{C}''_{2h}, \$_d) = \frac{1}{2}c_4a_2 - \frac{1}{2}a_2a_4 \tag{22}$$

$$\text{PCI-CF}_{\mathbf{1}}(\boldsymbol{C}_6, \$_d) = 0 \tag{23}$$

$$\text{PCI-CF}_{\mathbf{1}}(\boldsymbol{D}_3, \$_d) = \frac{1}{4}b_3^2 - \frac{1}{4}a_3^2 - \frac{1}{4}c_6 - \frac{1}{4}b_6 + \frac{1}{2}a_6 \tag{24}$$

$$\text{PCI-CF}_{\mathbf{1}}(\boldsymbol{D}'_3, \$_d) = 0 \tag{25}$$

$$\text{PCI-CF}_{\mathbf{1}}(\boldsymbol{C}_{3v}, \$_d) = 0 \tag{26}$$

$$\text{PCI-CF}_{\mathbf{1}}(\boldsymbol{C}'_{3v}, \$_d) = 0 \tag{27}$$

$$\text{PCI-CF}_{\mathbf{1}}(\boldsymbol{C}_{3h}, \$_d) = 0 \tag{28}$$

$$\text{PCI-CF}_{\mathbf{1}}(\boldsymbol{C}_{3i}, \$_d) = 0 \tag{29}$$

$$\text{PCI-CF}_{\mathbf{1}}(\boldsymbol{D}_{3h}, \$_d) = a_2a_4 - a_6 \tag{30}$$

$$\text{PCI-CF}_{\mathbf{1}}(\boldsymbol{D}_6, \$_d) = \frac{1}{2}b_6 - \frac{1}{2}a_6 \tag{31}$$

$$\text{PCI-CF}_{\mathbf{1}}(\boldsymbol{C}_{6v}, \$_d) = 0 \tag{32}$$

$$\text{PCI-CF}_{\mathbf{1}}(\boldsymbol{C}_{6h}, \$_d) = 0 \tag{33}$$

$$\text{PCI-CF}_{\mathbf{1}}(\boldsymbol{D}_{3h}, \$_d) = \frac{1}{2}a_3^2 - \frac{1}{2}a_6 \tag{34}$$

$$\text{PCI-CF}_{\mathbf{1}}(\boldsymbol{D}'_{3h}, \$_d) = 0 \tag{35}$$

$$\text{PCI-CF}_{\mathbf{1}}(\boldsymbol{D}_{3d}, \$_d) = \frac{1}{2}c_6 - \frac{1}{2}a_6 \tag{36}$$

$$\text{PCI-CF}_{\mathbf{1}}(\boldsymbol{D}'_{3d}, \$_d) = 0 \tag{37}$$

$$\text{PCI-CF}_{\mathbf{1}}(\boldsymbol{D}_{6h}, \$_d) = a_6 \tag{38}$$

where the symbol `a_d` is replaced by the sphericity index (SI) a_d for a d-membered homospheric orbit; the symbol `c_d` is replaced by the SI c_d for a d-membered enantiospheric orbit; the symbol `b_d` is replaced by the SI b_d for a d-membered hemispheric orbit; and totally the symbol $\$_d$ is used to designate a_d, c_d, and b_d.

6.2 PCI-CFs for the Haworth-projected skeleton (2)

The above procedure of Source Code 1 (`SubDh6h6-X.gap`, Appendix A) for calculating PCI-CFs of the benzene skeleton (Eqs. 7–38) via `l_SCICF_benz` and `l_PCICF_benz` is applicable to the other skeletons.

The use of the set of generators `gen_haworth` in place of `gen_benz` of Source Code 1 (`SubDh6h6-X.gap`) generates the CPR `D6h_haworth` for calculating the Haworth-projected skeleton **2**. After the selection of the set of subgroups `gen[`i`]` ($i = 1, 2, \cdots, 32$) according to the $\mathrm{SSG}^{haworth}_{\boldsymbol{D}_{6h}}$ (Eq. 4), the corresponding FPV and the corresponding list of SCI-CFs (Table 1) are calculated as described above. Thereby, the list of PCI-CFs is calculated, so as to give the respective PCI-CFs for the enumeration based on the Haworth-projected skeleton **2**. These PCI-CFs in GAP expressions are converted into usual mathematical formats as follows:

$$\begin{aligned}
\text{PCI-CF}_{\mathbf{2}}(\boldsymbol{C}_1, \$_d) &= \frac{1}{24}b_1^{12} - \frac{1}{8}c_2^4a_1^4 - \frac{7}{24}b_2^6 - \frac{5}{24}c_2^6 - \frac{1}{24}b_3^4 + \frac{3}{4}c_4^2a_2^2 + \frac{1}{8}a_3^4 + \frac{7}{12}c_4^3 \\
&\quad + \frac{1}{4}b_4^3 + \frac{5}{24}c_6^2 + \frac{7}{24}b_6^2 - c_8a_4 - \frac{3}{4}a_6^2 - \frac{7}{12}c_{12} - \frac{1}{4}b_{12} + a_{12} \qquad (39)
\end{aligned}$$

$$\begin{aligned}
\text{PCI-CF}_{\mathbf{2}}(\boldsymbol{C}_2, \$_d) &= \frac{1}{12}b_2^6 - \frac{1}{4}c_4^2a_2^2 - \frac{1}{12}c_4^3 - \frac{1}{4}b_4^3 - \frac{1}{12}b_6^2 + \frac{1}{2}c_8a_4 + \frac{1}{4}a_6^2 \\
&\quad + \frac{1}{12}c_{12} + \frac{1}{4}b_{12} - \frac{1}{2}a_{12} \qquad (40)
\end{aligned}$$

$$\begin{aligned}
\text{PCI-CF}_{\mathbf{2}}(\boldsymbol{C}_2', \$_d) &= \frac{1}{4}b_2^6 - \frac{1}{4}c_4^2a_2^2 - \frac{1}{4}c_4^3 - \frac{1}{4}b_4^3 - \frac{1}{4}b_6^2 + \frac{1}{2}c_8a_4 + \frac{1}{4}a_6^2 + \frac{1}{4}c_{12} \\
&\quad + \frac{1}{4}b_{12} - \frac{1}{2}a_{12} \qquad (41)
\end{aligned}$$

$$\begin{aligned}
\text{PCI-CF}_{\mathbf{2}}(\boldsymbol{C}_2'', \$_d) &= \frac{1}{4}b_2^6 - \frac{1}{4}c_4^2a_2^2 - \frac{1}{4}c_4^3 - \frac{1}{4}b_4^3 - \frac{1}{4}b_6^2 + \frac{1}{2}c_8a_4 + \frac{1}{4}a_6^2 \\
&\quad + \frac{1}{4}c_{12} + \frac{1}{4}b_{12} - \frac{1}{2}a_{12} \qquad (42)
\end{aligned}$$

$$\text{PCI-CF}_{\mathbf{2}}(\boldsymbol{C}_s, \$_d) = \frac{1}{4}c_2^4a_1^4 - \frac{3}{4}c_4^2a_2^2 - \frac{1}{4}a_3^4 + \frac{1}{2}c_8a_4 + \frac{3}{4}a_6^2 - \frac{1}{2}a_{12} \qquad (43)$$

$$\text{PCI-CF}_{\mathbf{2}}(\boldsymbol{C}_s', \$_d) = \frac{1}{4}c_2^6 - \frac{1}{4}c_4^2a_2^2 - \frac{1}{2}c_4^3 - \frac{1}{4}c_6^2 + \frac{1}{2}c_8a_4 + \frac{1}{4}a_6^2 + \frac{1}{2}c_{12} - \frac{1}{2}a_{12} \qquad (44)$$

$$\text{PCI-CF}_{\mathbf{2}}(\boldsymbol{C}_s'', \$_d) = \frac{1}{12}c_2^6 - \frac{1}{4}c_4^2a_2^2 - \frac{1}{3}c_4^3 - \frac{1}{12}c_6^2 + \frac{1}{2}c_8a_4 + \frac{1}{4}a_6^2 + \frac{1}{3}c_{12} - \frac{1}{2}a_{12} \qquad (45)$$

$$\text{PCI-CF}_{\mathbf{2}}(\boldsymbol{C}_i, \$_d) = \frac{1}{12}c_2^6 - \frac{1}{4}c_4^2a_2^2 - \frac{1}{3}c_4^3 - \frac{1}{12}c_6^2 + \frac{1}{2}c_8a_4 + \frac{1}{4}a_6^2 + \frac{1}{3}c_{12} - \frac{1}{2}a_{12} \qquad (46)$$

$$\text{PCI-CF}\mathbf{2}(\boldsymbol{C}_3, \$_d) = \frac{1}{8}b_3^4 - \frac{1}{8}a_3^4 - \frac{3}{8}c_6^2 - \frac{3}{8}b_6^2 + \frac{3}{4}a_6^2 + \frac{3}{4}c_{12} + \frac{1}{4}b_{12} - a_{12} \tag{47}$$

$$\text{PCI-CF}\mathbf{2}(\boldsymbol{D}_2, \$_d) = \frac{1}{2}b_4^3 - \frac{1}{2}c_8a_4 - \frac{1}{2}b_{12} + \frac{1}{2}a_{12} \tag{48}$$

$$\text{PCI-CF}\mathbf{2}(\boldsymbol{C}_{2v}, \$_d) = \frac{1}{2}c_4^2a_2^2 - \frac{1}{2}c_8a_4 - \frac{1}{2}a_6^2 + \frac{1}{2}a_{12} \tag{49}$$

$$\text{PCI-CF}\mathbf{2}(\boldsymbol{C}'_{2v}, \$_d) = \frac{1}{2}c_4^2a_2^2 - \frac{1}{2}c_8a_4 - \frac{1}{2}a_6^2 + \frac{1}{2}a_{12} \tag{50}$$

$$\text{PCI-CF}\mathbf{2}(\boldsymbol{C}''_{2v}, \$_d) = \frac{1}{2}c_4^3 - \frac{1}{2}c_8a_4 - \frac{1}{2}c_{12} + \frac{1}{2}a_{12} \tag{51}$$

$$\text{PCI-CF}\mathbf{2}(\boldsymbol{C}_{2h}, \$_d) = \frac{1}{6}c_4^3 - \frac{1}{2}c_8a_4 - \frac{1}{6}c_{12} + \frac{1}{2}a_{12} \tag{52}$$

$$\text{PCI-CF}\mathbf{2}(\boldsymbol{C}'_{2h}, \$_d) = \frac{1}{2}c_4^3 - \frac{1}{2}c_8a_4 - \frac{1}{2}c_{12} + \frac{1}{2}a_{12} \tag{53}$$

$$\text{PCI-CF}\mathbf{2}(\boldsymbol{C}''_{2h}, \$_d) = \frac{1}{2}c_4^2a_2^2 - \frac{1}{2}c_8a_4 - \frac{1}{2}a_6^2 + \frac{1}{2}a_{12} \tag{54}$$

$$\text{PCI-CF}\mathbf{2}(\boldsymbol{C}_6, \$_d) = \frac{1}{4}b_6^2 - \frac{1}{4}a_6^2 - \frac{1}{4}c_{12} - \frac{1}{4}b_{12} + \frac{1}{2}a_{12} \tag{55}$$

$$\text{PCI-CF}\mathbf{2}(\boldsymbol{D}_3, \$_d) = \frac{1}{4}b_6^2 - \frac{1}{4}a_6^2 - \frac{1}{4}c_{12} - \frac{1}{4}b_{12} + \frac{1}{2}a_{12} \tag{56}$$

$$\text{PCI-CF}\mathbf{2}(\boldsymbol{D}'_3, \$_d) = \frac{1}{4}b_6^2 - \frac{1}{4}a_6^2 - \frac{1}{4}c_{12} - \frac{1}{4}b_{12} + \frac{1}{2}a_{12} \tag{57}$$

$$\text{PCI-CF}\mathbf{2}(\boldsymbol{C}_{3v}, \$_d) = \frac{1}{4}a_3^4 - \frac{3}{4}a_6^2 + \frac{1}{2}a_{12} \tag{58}$$

$$\text{PCI-CF}\mathbf{2}(\boldsymbol{C}'_{3v}, \$_d) = \frac{1}{4}c_6^2 - \frac{1}{4}a_6^2 - \frac{1}{2}c_{12} + \frac{1}{2}a_{12} \tag{59}$$

$$\text{PCI-CF}\mathbf{2}(\boldsymbol{C}_{3h}, \$_d) = \frac{1}{4}c_6^2 - \frac{1}{4}a_6^2 - \frac{1}{2}c_{12} + \frac{1}{2}a_{12} \tag{60}$$

$$\text{PCI-CF}\mathbf{2}(\boldsymbol{C}_{3i}, \$_d) = \frac{1}{4}c_6^2 - \frac{1}{4}a_6^2 - \frac{1}{2}c_{12} + \frac{1}{2}a_{12} \tag{61}$$

$$\text{PCI-CF}\mathbf{2}(\boldsymbol{D}_{3h}, \$_d) = c_8a_4 - a_{12} \tag{62}$$

$$\text{PCI-CF}\mathbf{2}(\boldsymbol{D}_6, \$_d) = \frac{1}{2}b_{12} - \frac{1}{2}a_{12} \tag{63}$$

$$\text{PCI-CF}\mathbf{2}(\boldsymbol{C}_{6v}, \$_d) = \frac{1}{2}a_6^2 - \frac{1}{2}a_{12} \tag{64}$$

$$\text{PCI-CF}\mathbf{2}(\boldsymbol{C}_{6h}, \$_d) = \frac{1}{2}c_{12} - \frac{1}{2}a_{12} \tag{65}$$

$$\text{PCI-CF}\mathbf{2}(\boldsymbol{D}_{3h}, \$_d) = \frac{1}{2}a_6^2 - \frac{1}{2}a_{12} \tag{66}$$

$$\text{PCI-CF}\mathbf{2}(\boldsymbol{D}'_{3h}, \$_d) = \frac{1}{2}c_{12} - \frac{1}{2}a_{12} \tag{67}$$

$$\text{PCI-CF}\mathbf{2}(\boldsymbol{D}_{3d}, \$_d) = \frac{1}{2}c_{12} - \frac{1}{2}a_{12} \tag{68}$$

$$\text{PCI-CF}\mathbf{2}(\boldsymbol{D}'_{3d}, \$_d) = \frac{1}{2}a_6^2 - \frac{1}{2}a_{12} \tag{69}$$

$$\text{PCI-CF}\mathbf{2}(\boldsymbol{D}_{6h}, \$_d) = a_{12} \tag{70}$$

6.3 PCI-CFs for the superphane skeleton (3)

The set of generators `gen_phane` for characterizing the superphane skeleton (**3**) is identical with the set of generators `gen_haworth` for characterizning the Haworth-projected skeleton (**2**) (Figure 1). As a result, the set of FPV, CR, and SCI-CF for the superphane skeleton (**3**) is equal to the corresponding set for the Haworth-projected skeleton (**2**), as collected in Table 1. Moreover, the PCI-CFs expressed by usual mathematical formats for the Haworth-projected skeleton (**2**), i.e., PCI-CF$_{\mathbf{2}}(\boldsymbol{C}_1, \$_d)$ –PCI-CF$_{\mathbf{2}}(\boldsymbol{D}_{6h}, \$_d)$ (Eqs. 39–70), are identical with the counterparts for the superphane skeleton (**3**), i.e., PCI-CF$_{\mathbf{3}}(\boldsymbol{C}_1, \$_d)$ –PCI-CF$_{\mathbf{3}}(\boldsymbol{D}_{6h}, \$_d)$ (which are omitted).

6.4 PCI-CFs for the coronene skeleton (4)

In the above procedure of Source Code 1 (`SubDh6h6-X.gap`, Appendix A), the set of generators `gen_coronene` is used in place of `gen_benz`, so as to gain the corresponding CPR (`D6h_coronene`), which is adopted to employ further calculations for the coronene skeleton **4**. After the selection of the set of subgroups `gen[`i`]` ($i = 1, 2, \cdots, 32$) according to the SSG$^{coronene}_{\boldsymbol{D}_{6h}}$ (Eq. 6), the corresponding FPV and the corresponding list of SCI-CFs for the coronene skeleton **4** are calculated, as collected in Table 1. Thereby, the list of PCI-CFs is calculated, so as to give the respective PCI-CFs for the enumeration based on the coronene skeleton **4**. These PCI-CFs in GAP expressions are converted into usual mathematical formats as follows:

$$\begin{aligned}\text{PCI-CF}_{\mathbf{4}}(\boldsymbol{C}_1, \$_d) &= \frac{1}{24}b_1^{12} - \frac{1}{24}a_1^{12} - \frac{7}{24}b_2^6 - \frac{7}{24}c_2^6 + \frac{7}{12}a_2^6 - \frac{1}{24}b_3^4 + \frac{1}{24}a_3^4 + \frac{3}{4}c_4^3 \\ &\quad + \frac{1}{4}b_4^3 - a_4^3 + \frac{7}{24}c_6^2 + \frac{7}{24}b_6^2 - \frac{7}{12}a_6^2 - \frac{3}{4}c_{12} - \frac{1}{4}b_{12} + a_{12} \qquad (71)\end{aligned}$$

$$\begin{aligned}\text{PCI-CF}_{\mathbf{4}}(\boldsymbol{C}_2, \$_d) &= \frac{1}{12}b_2^6 - \frac{1}{12}a_2^6 - \frac{1}{4}c_4^3 - \frac{1}{4}b_4^3 + \frac{1}{2}a_4^3 - \frac{1}{12}b_6^2 + \frac{1}{12}a_6^2 + \frac{1}{4}c_{12} \\ &\quad + \frac{1}{4}b_{12} - \frac{1}{2}a_{12} \qquad (72)\end{aligned}$$

$$\begin{aligned}\text{PCI-CF}_{\mathbf{4}}(\boldsymbol{C}_2', \$_d) &= \frac{1}{4}b_2^6 - \frac{1}{4}a_2^6 - \frac{1}{4}c_4^3 - \frac{1}{4}b_4^3 + \frac{1}{2}a_4^3 - \frac{1}{4}b_6^2 + \frac{1}{4}a_6^2 + \frac{1}{4}c_{12} \\ &\quad + \frac{1}{4}b_{12} - \frac{1}{2}a_{12} \qquad (73)\end{aligned}$$

$$\begin{aligned}\text{PCI-CF}_{\mathbf{4}}(\boldsymbol{C}_2'', \$_d) &= \frac{1}{4}b_2^6 - \frac{1}{4}a_2^6 - \frac{1}{4}c_4^3 - \frac{1}{4}b_4^3 + \frac{1}{2}a_4^3 - \frac{1}{4}b_6^2 + \frac{1}{4}a_6^2 + \frac{1}{4}c_{12} \\ &\quad + \frac{1}{4}b_{12} - \frac{1}{2}a_{12} \qquad (74)\end{aligned}$$

$$\text{PCI-CF}_{\mathbf{4}}(\boldsymbol{C}_s, \$_d) = \frac{1}{4}c_2^6 - \frac{1}{4}a_2^6 - \frac{1}{2}c_4^3 + \frac{1}{2}a_4^3 - \frac{1}{4}c_6^2 + \frac{1}{4}a_6^2 + \frac{1}{2}c_{12} - \frac{1}{2}a_{12} \tag{75}$$

$$\text{PCI-CF}_{\mathbf{4}}(\boldsymbol{C}_s', \$_d) = \frac{1}{4}c_2^6 - \frac{1}{4}a_2^6 - \frac{1}{2}c_4^3 + \frac{1}{2}a_4^3 - \frac{1}{4}c_6^2 + \frac{1}{4}a_6^2 + \frac{1}{2}c_{12} - \frac{1}{2}a_{12} \tag{76}$$

$$\text{PCI-CF}_{\mathbf{4}}(\boldsymbol{C}_s'', \$_d) = \frac{1}{12}a_1^{12} - \frac{7}{12}a_2^6 - \frac{1}{12}a_3^4 + \frac{1}{2}a_4^3 + \frac{7}{12}a_6^2 - \frac{1}{2}a_{12} \tag{77}$$

$$\text{PCI-CF}_{\mathbf{4}}(\boldsymbol{C}_i, \$_d) = \frac{1}{12}c_2^6 - \frac{1}{12}a_2^6 - \frac{1}{2}c_4^3 + \frac{1}{2}a_4^3 - \frac{1}{12}c_6^2 + \frac{1}{12}a_6^2 + \frac{1}{2}c_{12} - \frac{1}{2}a_{12} \tag{78}$$

$$\text{PCI-CF}_{\mathbf{4}}(\boldsymbol{C}_3,\$_d) = \frac{1}{8}b_3^4 - \frac{1}{8}a_3^4 - \frac{3}{8}c_6^2 - \frac{3}{8}b_6^2 + \frac{3}{4}a_6^2 + \frac{3}{4}c_{12} + \frac{1}{4}b_{12} - a_{12} \tag{79}$$

$$\text{PCI-CF}_{\mathbf{4}}(\boldsymbol{D}_2, \$_d) = \frac{1}{2}b_4^3 - \frac{1}{2}a_4^3 - \frac{1}{2}b_{12} + \frac{1}{2}a_{12} \tag{80}$$

$$\text{PCI-CF}_{\mathbf{4}}(\boldsymbol{C}_{2v}, \$_d) = \frac{1}{2}c_4^3 - \frac{1}{2}a_4^3 - \frac{1}{2}c_{12} + \frac{1}{2}a_{12} \tag{81}$$

$$\text{PCI-CF}_{\mathbf{4}}(\boldsymbol{C}_{2v}', \$_d) = \frac{1}{2}a_2^6 - \frac{1}{2}a_4^3 - \frac{1}{2}a_6^2 + \frac{1}{2}a_{12} \tag{82}$$

$$\text{PCI-CF}_{\mathbf{4}}(\boldsymbol{C}_{2v}'', \$_d) = \frac{1}{2}a_2^6 - \frac{1}{2}a_4^3 - \frac{1}{2}a_6^2 + \frac{1}{2}a_{12} \tag{83}$$

$$\text{PCI-CF}_{\mathbf{4}}(\boldsymbol{C}_{2h}, \$_d) = \frac{1}{6}a_2^6 - \frac{1}{2}a_4^3 - \frac{1}{6}a_6^2 + \frac{1}{2}a_{12} \tag{84}$$

$$\text{PCI-CF}_{\mathbf{4}}(\boldsymbol{C}_{2h}', \$_d) = \frac{1}{2}c_4^3 - \frac{1}{2}a_4^3 - \frac{1}{2}c_{12} + \frac{1}{2}a_{12} \tag{85}$$

$$\text{PCI-CF}_{\mathbf{4}}(\boldsymbol{C}_{2h}'', \$_d) = \frac{1}{2}c_4^3 - \frac{1}{2}a_4^3 - \frac{1}{2}c_{12} + \frac{1}{2}a_{12} \tag{86}$$

$$\text{PCI-CF}_{\mathbf{4}}(\boldsymbol{C}_6, \$_d) = \frac{1}{4}b_6^2 - \frac{1}{4}a_6^2 - \frac{1}{4}c_{12} - \frac{1}{4}b_{12} + \frac{1}{2}a_{12} \tag{87}$$

$$\text{PCI-CF}_{\mathbf{4}}(\boldsymbol{D}_3, \$_d) = \frac{1}{4}b_6^2 - \frac{1}{4}a_6^2 - \frac{1}{4}c_{12} - \frac{1}{4}b_{12} + \frac{1}{2}a_{12} \tag{88}$$

$$\text{PCI-CF}_{\mathbf{4}}(\boldsymbol{D}_3', \$_d) = \frac{1}{4}b_6^2 - \frac{1}{4}a_6^2 - \frac{1}{4}c_{12} - \frac{1}{4}b_{12} + \frac{1}{2}a_{12} \tag{89}$$

$$\text{PCI-CF}_{\mathbf{4}}(\boldsymbol{C}_{3v}, \$_d) = \frac{1}{4}c_6^2 - \frac{1}{4}a_6^2 - \frac{1}{2}c_{12} + \frac{1}{2}a_{12} \tag{90}$$

$$\text{PCI-CF}_{\mathbf{4}}(\boldsymbol{C}_{3v}', \$_d) = \frac{1}{4}c_6^2 - \frac{1}{4}a_6^2 - \frac{1}{2}c_{12} + \frac{1}{2}a_{12} \tag{91}$$

$$\text{PCI-CF}_{\mathbf{4}}(\boldsymbol{C}_{3h}, \$_d) = \frac{1}{4}a_3^4 - \frac{3}{4}a_6^2 + \frac{1}{2}a_{12} \tag{92}$$

$$\text{PCI-CF}_{\mathbf{4}}(\boldsymbol{C}_{3i}, \$_d) = \frac{1}{4}c_6^2 - \frac{1}{4}a_6^2 - \frac{1}{2}c_{12} + \frac{1}{2}a_{12} \tag{93}$$

$$\text{PCI-CF}_{\mathbf{4}}(\boldsymbol{D}_{3h}, \$_d) = a_4^3 - a_{12} \tag{94}$$

$$\text{PCI-CF}_{\mathbf{4}}(\boldsymbol{D}_6, \$_d) = \frac{1}{2}b_{12} - \frac{1}{2}a_{12} \tag{95}$$

$$\text{PCI-CF}_{\mathbf{4}}(\boldsymbol{C}_{6v}, \$_d) = \frac{1}{2}c_{12} - \frac{1}{2}a_{12} \tag{96}$$

$$\text{PCI-CF}_{\mathbf{4}}(\boldsymbol{C}_{6h}, \$_d) = \frac{1}{2}a_6^2 - \frac{1}{2}a_{12} \tag{97}$$

$$\text{PCI-CF}_{\mathbf{4}}(\boldsymbol{D}_{3h}, \$_d) = \frac{1}{2}a_6^2 - \frac{1}{2}a_{12} \tag{98}$$

$$\text{PCI-CF}_{\mathbf{4}}(\boldsymbol{D}'_{3h}, \$_d) = \frac{1}{2}a_6^2 - \frac{1}{2}a_{12} \tag{99}$$

$$\text{PCI-CF}_{\mathbf{4}}(\boldsymbol{D}_{3d}, \$_d) = \frac{1}{2}c_{12} - \frac{1}{2}a_{12} \tag{100}$$

$$\text{PCI-CF}_{\mathbf{4}}(\boldsymbol{D}'_{3d}, \$_d) = \frac{1}{2}c_{12} - \frac{1}{2}a_{12} \tag{101}$$

$$\text{PCI-CF}_{\mathbf{4}}(\boldsymbol{D}_{6h}, \$_d) = a_{12} \tag{102}$$

7 Application of the PCI-CF method to symmetry-itemized enumeration of $\boldsymbol{D}_{6h}$-derivatives

Source Code 2 (`enumoctaX`) for enumeration of $\boldsymbol{O}_h$-derivatives has been reported by the present author (Fujita) on page 362 of Ref. [25]. It is here applied to the enumeration of $\boldsymbol{D}_{6h}$-derivatives. Source Code 2 (`enumoctaX`) has shown the GAP code for practical enumeration based on the PCI-CF method, where the GAP functions developed to treat CI-CFs [22], e.g., `calcCoeffGen`, are capable of treating PCI-CFs as they are. In order to use the function `calcCoeffGen`, the file `CICFgenCC.gapfunc` (Appendix A of [22]) should be loaded along a similar way to Appendix B of [22].

In order to show practices of enumeration procedures based on the PCI method of Fujita's USCI approach ([4]), let us examine enumerations of several selected skeletons.

7.1 Enumeration of benzene derivatives

7.1.1 Calculation of symmetry-itemized numbers of benzene derivatives with given compositions

Let us select six proligands for the benzene skeleton **1** from the following ligand inventory:

$$\boldsymbol{L} = \{\mathrm{H}, \mathrm{A}, \mathrm{B}, \mathrm{C}; \mathrm{p}/\mathrm{P}, \mathrm{q}/\mathrm{Q}, \mathrm{r}/\mathrm{R}, \mathrm{s}/\mathrm{S}\}, \tag{103}$$

where H, A, B, and C represent achiral proligands, while p/P $\cdots$ s/S represents a pair of enantiomeric proligands when detached. The uppercase letter P etc. is used in place of the symbol $\overline{\mathrm{p}}$ etc. to simplify the source code. The letter H is used to show the substitution of a hydrogen atom, which is usually omitted in structural formulas. For the sake of simplicity, only four achiral proligands and only four pairs of chiral proligands are adopted for substituting the six positions of the benzene skeleton. Then, the following ligand-inventory functions are calculated:

$$a_d = H^d + A^d + B^d + C^d \tag{104}$$

$$c_d = H^d + A^d + B^d + C^d \\ + 2p^{d/2}P^{d/2} + 2q^{d/2}Q^{d/2} + 2r^{d/2}R^{d/2} + 2s^{d/2}S^{d/2} \tag{105}$$

$$b_d = H^d + A^d + B^d + C^d \\ + p^d + P^d + q^d + Q^d + r^d + R^d + s^d + S^d \tag{106}$$

These ligand-inventory functions are introduced into the right-hand side of each PCI-CF for the benzene skeleton **1**, i.e., Eqs. 7–38. The resulting equations are expanded to give generating functions, in which the coefficient of each term corresponding to the composition $\mathrm{H}^H\mathrm{A}^A\mathrm{B}^B\mathrm{C}^C\mathrm{p}^p\mathrm{P}^P\mathrm{q}^q\mathrm{Q}^Q\mathrm{r}^r\mathrm{R}^R\mathrm{s}^s\mathrm{S}^S$ represents the number of the corresponding derivatives. The non-negative superscripts satisfy the following condition:

$$H + A + B + C + p + P + q + Q + r + R + s + S = 6. \tag{107}$$

For practical enumeration, the GAP code is obtained by modifying Source Code 2 (`enumoctaX`) reported on page 362 of Ref. [25], where the function `calcCoeffGen` is used in the subroutine function `calcCoeffGenbenz` for outputting enumeration results in a tabular form. The composition $\mathrm{H}^H\mathrm{A}^A\mathrm{B}^B\mathrm{C}^C\mathrm{p}^p\mathrm{P}^P\mathrm{q}^q\mathrm{Q}^Q\mathrm{r}^r\mathrm{R}^R\mathrm{s}^s\mathrm{S}^S$ is represented by the following partition during the process of tabulation:

$$[\theta] = [H, A, B, C, p, P, q, Q, r, R, s, S], \tag{108}$$

which is used as the argument of the function `calcCoeffGen` and the subroutine function `calcCoeffGenbenz`. Thereby, the coefficient of the term $\mathrm{H}^H\mathrm{A}^A\mathrm{B}^B\mathrm{C}^C\mathrm{p}^p\mathrm{P}^P\mathrm{q}^q\mathrm{Q}^Q\mathrm{r}^r\mathrm{R}^R\mathrm{s}^s\mathrm{S}^S$ appearing in each of the generating functions is extracted to give the number of promolecules with the composition $\mathrm{H}^H\mathrm{A}^A\mathrm{B}^B\mathrm{C}^C\mathrm{p}^p\mathrm{P}^P\mathrm{q}^q\mathrm{Q}^Q\mathrm{r}^r\mathrm{R}^R\mathrm{s}^s\mathrm{S}^S$ and with the assigned subgroup of $\boldsymbol{D}_{6h}$.

Table 2 collects the symmetry-itemized numbers of isomeric benzene derivatives with achiral and chiral proligands, where the symmetry-itemized values for each selected composition (the partition $[\theta]$) are shown in accord with the $\mathrm{SSG}_{\boldsymbol{D}_{6h}}$ (Eq. 1). The data collected in Table 2 are consistent with those reported previously [27], which have not relied on the GAP system.

Each row with an asterisk should be duplicated, because a pair of enantiomers is counted once under the present enumeration of the PCI-CF method. For example, the

Table 2. Symmetry-Itemized Numbers of Derivatives Derived from the Benzene Skeleton **1**

	$\boldsymbol{C}_1$	$\boldsymbol{C}_2$	$\boldsymbol{C}_2'$	$\boldsymbol{C}_2''$	$\boldsymbol{C}_s$	$\boldsymbol{C}_s'$	$\boldsymbol{C}_s''$	$\boldsymbol{C}_i$	$\boldsymbol{D}_2$	$\boldsymbol{C}_{2v}$	$\boldsymbol{C}_{2v}'$	$\boldsymbol{C}_{2v}''$	$\boldsymbol{C}_{2h}$	$\boldsymbol{C}_{2h}'$	$\boldsymbol{C}_{2h}''$	$\boldsymbol{D}_3$	$\boldsymbol{D}_{2h}$	$\boldsymbol{D}_6$	$\boldsymbol{D}_{3h}$	$\boldsymbol{D}_{3d}$	$\boldsymbol{D}_{6h}$
	1	2	3	4	5	6	7	8	10	11	12	13	14	15	16	18	24	25	28	30	32
$[6,0,0,0,0,0,0,0,0,0,0,0]$	0	0	0	0	0	0	0	0	0	0	0	0	0	0	0	0	0	0	0	0	1
$[5,1,0,0,0,0,0,0,0,0,0,0]$	0	0	0	0	0	0	0	0	0	0	1	0	0	0	0	0	0	0	0	0	0
$[5,0,0,0,1,0,0,0,0,0,0,0]*$	0	0	1/2	0	0	0	0	0	0	0	0	0	0	0	0	0	0	0	0	0	0
$[4,2,0,0,0,0,0,0,0,0,0,0]$	0	0	0	0	0	0	0	0	0	0	1	1	0	0	0	0	1	0	0	0	0
$[4,0,0,0,2,0,0,0,0,0,0,0]*$	0	0	1/2	1/2	0	0	0	0	1/2	0	0	0	0	0	0	0	0	0	0	0	0
$[4,1,1,0,0,0,0,0,0,0,0,0]$	0	0	0	0	0	0	2	0	0	0	1	0	0	0	0	0	0	0	0	0	0
$[4,1,0,0,1,0,0,0,0,0,0,0]*$	1	0	1/2	0	0	0	0	0	0	0	0	0	0	0	0	0	0	0	0	0	0
$[4,0,0,0,1,1,0,0,0,0,0,0]$	0	0	0	0	1	1	0	0	0	0	0	0	0	1	0	0	0	0	0	0	0
$[4,0,0,0,1,0,1,0,0,0,0,0]*$	1	0	1/2	0	0	0	0	0	0	0	0	0	0	0	0	0	0	0	0	0	0
$[3,3,0,0,0,0,0,0,0,0,0,0]$	0	0	0	0	0	0	1	0	0	0	1	0	0	0	0	0	0	0	1	0	0
$[3,0,0,0,3,0,0,0,0,0,0,0]*$	1/2	0	1/2	0	0	0	0	0	0	0	0	0	0	0	0	1/2	0	0	0	0	0
$[3,2,1,0,0,0,0,0,0,0,0,0]$	0	0	0	0	0	0	4	0	0	0	2	0	0	0	0	0	0	0	0	0	0
$[3,2,0,0,1,0,0,0,0,0,0,0]*$	2	0	1	0	0	0	0	0	0	0	0	0	0	0	0	0	0	0	0	0	0
$[3,1,0,0,2,0,0,0,0,0,0,0]*$	2	0	1	0	0	0	0	0	0	0	0	0	0	0	0	0	0	0	0	0	0
$[3,0,0,0,2,1,0,0,0,0,0,0]*$	2	0	1	0	0	0	0	0	0	0	0	0	0	0	0	0	0	0	0	0	0
$[3,1,1,1,0,0,0,0,0,0,0,0]$	0	0	0	0	0	0	10	0	0	0	0	0	0	0	0	0	0	0	0	0	0
$[3,1,1,0,1,0,0,0,0,0,0,0]*$	5	0	0	0	0	0	0	0	0	0	0	0	0	0	0	0	0	0	0	0	0
$[3,1,0,0,1,1,0,0,0,0,0,0]$	4	0	0	0	2	0	0	0	0	0	0	0	0	0	0	0	0	0	0	0	0
$[3,0,0,0,1,1,1,0,0,0,0,0]*$	5	0	0	0	0	0	0	0	0	0	0	0	0	0	0	0	0	0	0	0	0
$[2,2,2,0,0,0,0,0,0,0,0,0]$	0	0	0	0	0	0	4	0	0	0	3	3	1	0	0	0	0	0	0	0	0
$[2,2,0,0,2,0,0,0,0,0,0,0]*$	2	1/2	3/2	3/2	0	0	0	0	0	0	0	0	0	0	0	0	0	0	0	0	0
$[2,0,0,0,2,2,0,0,0,0,0,0]$	1	0	1	1	0	2	0	0	0	1	0	0	0	1	1	0	0	0	0	0	0
$[2,0,0,0,2,0,2,0,0,0,0,0]*$	2	1/2	3/2	3/2	0	0	0	0	0	0	0	0	0	0	0	0	0	0	0	0	0
$[2,2,1,1,0,0,0,0,0,0,0,0]$	0	0	0	0	0	0	14	0	0	0	2	0	0	0	0	0	0	0	0	0	0
$[2,2,1,0,1,0,0,0,0,0,0,0]*$	7	0	1	0	0	0	0	0	0	0	0	0	0	0	0	0	0	0	0	0	0
$[2,2,0,0,1,1,0,0,0,0,0,0]$	4	0	1	0	2	3	0	1	0	0	0	0	0	0	0	0	0	0	0	0	0
$[2,1,1,0,2,0,0,0,0,0,0,0]*$	7	0	1	0	0	0	0	0	0	0	0	0	0	0	0	0	0	0	0	0	0
$[2,1,1,0,1,1,0,0,0,0,0,0]$	14	0	0	0	2	0	0	0	0	0	0	0	0	0	0	0	0	0	0	0	0
$[2,1,0,0,2,1,0,0,0,0,0,0]*$	7	0	1	0	0	0	0	0	0	0	0	0	0	0	0	0	0	0	0	0	0
$[2,1,0,0,1,1,1,0,0,0,0,0]*$	15	0	0	0	0	0	0	0	0	0	0	0	0	0	0	0	0	0	0	0	0
$[2,0,0,0,2,1,1,0,0,0,0,0]*$	7	0	1	0	0	0	0	0	0	0	0	0	0	0	0	0	0	0	0	0	0
$[2,0,0,0,1,1,1,1,0,0,0,0]$	10	0	0	0	2	6	0	2	0	0	0	0	0	0	0	0	0	0	0	0	0
$[2,0,0,0,1,1,1,0,1,0,0,0]*$	15	0	0	0	0	0	0	0	0	0	0	0	0	0	0	0	0	0	0	0	0
$[2,0,0,0,1,0,1,0,1,0,1,0]*$	15	0	0	0	0	0	0	0	0	0	0	0	0	0	0	0	0	0	0	0	0

partition $[5,0,0,0,1,0,0,0,0,0,0,0]*$ of the third row (Table 2) is paired with the partition $[5,0,0,0,0,1,0,0,0,0,0,0]*$, so that these paired partitions correspond to $1/2(\mathrm{H}_5\mathrm{p}+\mathrm{H}_5\overline{\mathrm{p}})$; then the value 1/2 at the intersection between the third row and the third column ($\boldsymbol{C}_2'$) should be duplicated to give 1 ($= 1/2 \times 2$). Note that the columns for the respective subgroups of an inherent zero value (Eqs. 15, 23, 25–29, 32, 33, 35, and 37) are omitted from Table 2.

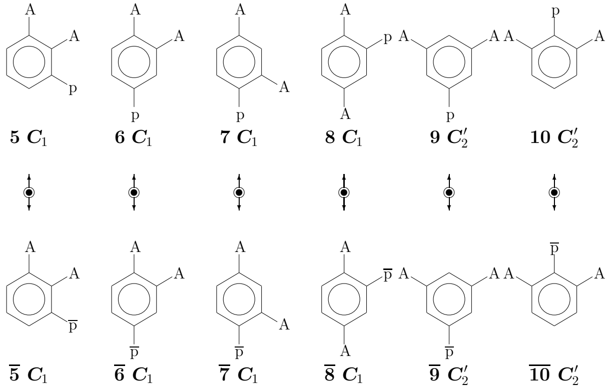
5 $\boldsymbol{C}_1$
6 $\boldsymbol{C}_1$
7 $\boldsymbol{C}_1$
8 $\boldsymbol{C}_1$
9 $\boldsymbol{C}_2'$
10 $\boldsymbol{C}_2'$
$\overline{5}$ $\boldsymbol{C}_1$
$\overline{6}$ $\boldsymbol{C}_1$
$\overline{7}$ $\boldsymbol{C}_1$
$\overline{8}$ $\boldsymbol{C}_1$
$\overline{9}$ $\boldsymbol{C}_2'$
$\overline{10}$ $\boldsymbol{C}_2'$

Figure 7. Symmetry-itemized enumeration of benzene derivatives with the composition H_3A_2p (partition: $[3, 2, 0, 0, 1, 0, 0, 0, 0, 0, 0, 0]$), which shows the presence of four pairs of enantiomeric $\boldsymbol{C}_1$-derivatives and two pairs of enantiomeric $\boldsymbol{C}_2'$-derivatives.

7.1.2 Diagrammatical examination of calculation results concerning benzene derivatives

For the purpose of confirming the validity of the PCI-CF method, let us examine several rows among the data of Table 2. It should be noted that each pair of enantiomeric derivative or each achiral derivative is counted once during the present enumerations.

The values at the 13th row of Table 2 with the partition $[3, 2, 0, 0, 1, 0, 0, 0, 0, 0, 0, 0]*$ should be duplicated, so as to indicate the presence of four $(= 2 \times 2)$ pairs of enantiomeric $\boldsymbol{C}_1$-derivatives (**5**/$\overline{\mathbf{5}}$, **6**/$\overline{\mathbf{6}}$, **7**/$\overline{\mathbf{7}}$, and **8**/$\overline{\mathbf{8}}$) and two $(= 1 \times 2)$ pairs of enantiomeric $\boldsymbol{C}_2'$-derivatives (**9**/$\overline{\mathbf{9}}$ and **10**/$\overline{\mathbf{10}}$) of the composition $H_3A_2p/H_3A_2\overline{p}$. These derivatives are depicted in Figure 7. For the sake of rigidity, each pair of enantiomers is connected by a vertical double-headed arrow, because each pair linked with a vertical double-headed arrow is regarded as a hypothetically single object and so counted once during the present enumeration nuder the point group $\boldsymbol{D}_{6h}$.

The values at the 18th row of Table 2 with the partition $[3, 1, 0, 0, 1, 1, 0, 0, 0, 0, 0, 0]$ indicate the presence of four pairs of enantiomeric $\boldsymbol{C}_1$-derivatives (**11**/$\overline{\mathbf{11}}$, **12**/$\overline{\mathbf{12}}$, **13**/$\overline{\mathbf{13}}$, and **14**/$\overline{\mathbf{14}}$) and two $\boldsymbol{C}_s$-derivatives (**15** and **16**) of the composition $H_3Ap\overline{p}$. Note that the antipodal effects of p and $\overline{p}$ are compensated during reflection, so as to result in the appearance of the $\boldsymbol{C}_s$-derivatives. These derivatives are depicted in Figure 8.

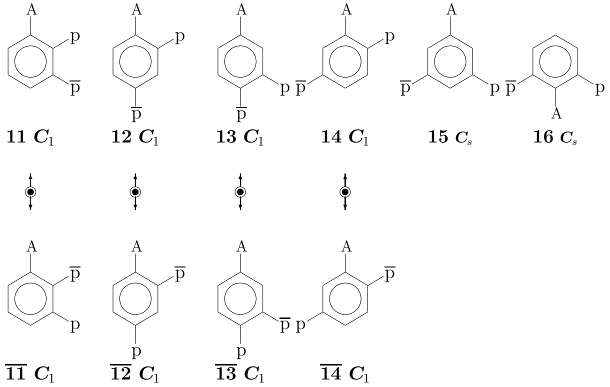

Figure 8. Symmetry-itemized enumeration of benzene derivatives with the composition $H_3Ap\overline{p}$ (partition: $[3,1,0,0,1,1,0,0,0,0,0,0]$), which shows the presence of four pairs of enantiomeric $\boldsymbol{C}_1$-derivatives and two $\boldsymbol{C}_s$-derivatives.

7.2 Enumeration of superphane derivatives

7.2.1 Calculation of symmetry-itemized numbers of superphane derivatives with given compositions

Let us next examine skeletal substitution concerning the twelve methylene moieties of the superphane skeleton **3**. Then, twelve skeletal positions are replaced by bidentate moieties selected from the following ligand inventory:

$$\boldsymbol{L}' = \{\mathrm{C}, \mathrm{N}, \mathrm{O}, \mathrm{S}\}, \tag{109}$$

where C represents a methylene moiety (CH_2), N represents an amine moiety (NH), O and S represent bidentate oxygen and sulfur. Because the absence of no chiral moiety, equal ligand-inventory functions are used as follows:

$$a_d = \mathrm{C}^d + \mathrm{N}^d + \mathrm{O}^d + \mathrm{S}^d \tag{110}$$

$$b_d = \mathrm{C}^d + \mathrm{N}^d + \mathrm{O}^d + \mathrm{S}^d \tag{111}$$

$$c_d = \mathrm{C}^d + \mathrm{N}^d + \mathrm{O}^d + \mathrm{S}^d \tag{112}$$

Because the PCI-CFs for enumerations based on the superphane skeleton (**3**), i.e., PCI-CF$_{\mathbf{3}}(\boldsymbol{C}_1, \$_d)$ –PCI-CF$_{\mathbf{3}}(\boldsymbol{D}_{6h}, \$_d)$, (omitted) are identical with PCI-CF$_{\mathbf{2}}(\boldsymbol{C}_1, \$_d)$ – PCI-CF$_{\mathbf{2}}(\boldsymbol{D}_{6h}, \$_d)$ (Eqs. 39–70), the latter are used for the present calculation.

After the ligand-inventory functions (Eqs. 110–112) are introduced into the right-hand side of each PCI-CF (Eqs. 39–70), the resulting equations are expanded to give generating functions, in which the coefficient of the composition $\mathrm{C}^{C}\mathrm{N}^{A}\mathrm{O}^{O}\mathrm{S}^{S}$ represent the number of the corresponding skeletal derivatives. The superscripts satisfy following equation:

$$C + N + O + S = 12. \tag{113}$$

For practical enumeration, the GAP code obtained previously as Source Code 2 (`enum-octaX`) on page 362 of Ref. [25] is applied to the present enumeration after appropriate modifications, where the function `calcCoeffGen` is used in the subroutine function `calcCoeffGenphane` for outputting enumeration results in a tabular form. During this process of tabulation, the composition $\mathrm{C}^{C}\mathrm{N}^{N}\mathrm{O}^{O}\mathrm{S}^{S}$ is represented by the following partition:

$$[\theta] = [C, N, O, S], \tag{114}$$

which is used as the argument of the function `calcCoeffGen` and the subroutine function `calcCoeffGenphane`. Thereby, the coefficient of the term $\mathrm{C}^{C}\mathrm{N}^{N}\mathrm{O}^{O}\mathrm{S}^{S}$ (partition: Eq. 114) appearing in each of the generating functions is extracted to give the number of promolecules with the composition $\mathrm{C}^{C}\mathrm{N}^{N}\mathrm{O}^{O}\mathrm{S}^{S}$ and with the assigned subgroup of $\boldsymbol{D}_{6h}$. The resulting set of coefficients are collected in Table 3. These data are consistent with those previously reported, which have not relied on the GAP system and have not considered chirality fittingness (PCIs in place of PCI-CFs).

7.2.2 Diagrammatical examination of calculation results concerning superphane derivatives

For the purpose of confirming the validity of the PCI-CF method, let us examine several rows among the data of Table 3, where each pair of enantiomeric derivative or each achiral derivative is counted once during the present enumerations.

The values at the 6th row of Table 3 with the partition $[10, 0, 2, 0]$ indicate the presence of one pair of enantiomeric $\boldsymbol{C}_2'$-derivatives (**17**/$\overline{\mathbf{17}}$), one pair of enantiomeric $\boldsymbol{C}_2''$-derivatives **18**/$\overline{\mathbf{18}}$), one achiral $\boldsymbol{C}_s$-derivative (**19**), one achiral $\boldsymbol{C}_s'$-derivative (**20**), one achiral $\boldsymbol{C}_{2v}$-derivative (**21**), one achiral $\boldsymbol{C}_{2v}'$-derivative (**22**), and one achiral $\boldsymbol{C}_{2h}''$-derivative (**23**), where they have the composition $\mathrm{C}^{10}\mathrm{O}^{2}$ (or alternatively expressed as $\mathrm{C}_{10}\mathrm{O}_{2}$). These derivatives are depicted in Figure 9.

Table 3. Symmetry-Itemized Numbers of Derivatives Derived from the Superphane Skeleton **3**

	$\boldsymbol{C}_1$	$\boldsymbol{C}_2$	$\boldsymbol{C}'_2$	$\boldsymbol{C}''_2$	$\boldsymbol{C}_s$	$\boldsymbol{C}'_s$	$\boldsymbol{C}''_s$	$\boldsymbol{C}_i$	$\boldsymbol{C}_3$	$\boldsymbol{D}_2$	$\boldsymbol{C}_{2v}$	$\boldsymbol{C}'_{2v}$	$\boldsymbol{C}''_{2v}$	$\boldsymbol{C}_{2h}$	$\boldsymbol{C}'_{2h}$	$\boldsymbol{C}''_{2h}$	$\boldsymbol{C}_6$	$\boldsymbol{D}_3$	$\boldsymbol{D}'_3$	$\boldsymbol{C}_{3v}$	$\boldsymbol{C}'_{3v}$	$\boldsymbol{C}_{3h}$	$\boldsymbol{C}_{3i}$	$\boldsymbol{D}_{2h}$	$\boldsymbol{D}_6$	$\boldsymbol{C}_{6v}$	$\boldsymbol{C}_{6h}$	$\boldsymbol{D}_{3h}$	$\boldsymbol{D}'_{3h}$	$\boldsymbol{D}_{3d}$	$\boldsymbol{D}'_{3d}$	$\boldsymbol{D}_{6h}$
	1	2	3	4	5	6	7	8	9	10	11	12	13	14	15	16	17	18	19	20	21	22	23	24	25	26	27	28	29	30	31	32
$[12, 0, 0, 0]$	0	0	0	0	0	0	0	0	0	0	0	0	0	0	0	0	0	0	0	0	0	0	0	0	0	0	0	0	0	0	0	1
$[11, 1, 0, 0]$	0	0	0	0	1	0	0	0	0	0	0	0	0	0	0	0	0	0	0	0	0	0	0	0	0	0	0	0	0	0	0	0
$[11, 0, 1, 0]$	0	0	0	0	1	0	0	0	0	0	0	0	0	0	0	0	0	0	0	0	0	0	0	0	0	0	0	0	0	0	0	0
$[11, 0, 0, 1]$	0	0	0	0	1	0	0	0	0	0	0	0	0	0	0	0	0	0	0	0	0	0	0	0	0	0	0	0	0	0	0	0
$[10, 2, 0, 0]$	0	0	1	1	1	1	0	0	0	0	1	1	0	0	0	1	0	0	0	0	0	0	0	0	0	0	0	0	0	0	0	0
$[10, 0, 2, 0]$	0	0	1	1	1	1	0	0	0	0	1	1	0	0	0	1	0	0	0	0	0	0	0	0	0	0	0	0	0	0	0	0
$[10, 0, 0, 2]$	0	0	1	1	1	1	0	0	0	0	1	1	0	0	0	1	0	0	0	0	0	0	0	0	0	0	0	0	0	0	0	0
$[10, 1, 1, 0]$	4	0	0	0	3	0	0	0	0	0	0	0	0	0	0	0	0	0	0	0	0	0	0	0	0	0	0	0	0	0	0	0
$[10, 1, 0, 1]$	4	0	0	0	3	0	0	0	0	0	0	0	0	0	0	0	0	0	0	0	0	0	0	0	0	0	0	0	0	0	0	0
$[10, 0, 1, 1]$	4	0	0	0	3	0	0	0	0	0	0	0	0	0	0	0	0	0	0	0	0	0	0	0	0	0	0	0	0	0	0	0
$[9, 3, 0, 0]$	7	0	0	0	4	0	0	0	0	0	0	0	0	0	0	0	0	0	0	1	0	0	0	0	0	0	0	0	0	0	0	0
$[9, 0, 3, 0]$	7	0	0	0	4	0	0	0	0	0	0	0	0	0	0	0	0	0	0	1	0	0	0	0	0	0	0	0	0	0	0	0
$[9, 0, 0, 3]$	7	0	0	0	4	0	0	0	0	0	0	0	0	0	0	0	0	0	0	1	0	0	0	0	0	0	0	0	0	0	0	0
$[9, 2, 1, 0]$	24	0	0	0	7	0	0	0	0	0	0	0	0	0	0	0	0	0	0	0	0	0	0	0	0	0	0	0	0	0	0	0
$[9, 2, 0, 1]$	24	0	0	0	7	0	0	0	0	0	0	0	0	0	0	0	0	0	0	0	0	0	0	0	0	0	0	0	0	0	0	0
$[9, 1, 2, 0]$	24	0	0	0	7	0	0	0	0	0	0	0	0	0	0	0	0	0	0	0	0	0	0	0	0	0	0	0	0	0	0	0
$[9, 1, 0, 2]$	24	0	0	0	7	0	0	0	0	0	0	0	0	0	0	0	0	0	0	0	0	0	0	0	0	0	0	0	0	0	0	0
$[9, 1, 1, 1]$	52	0	0	0	6	0	0	0	0	0	0	0	0	0	0	0	0	0	0	0	0	0	0	0	0	0	0	0	0	0	0	0
$[9, 0, 2, 1]$	24	0	0	0	7	0	0	0	0	0	0	0	0	0	0	0	0	0	0	0	0	0	0	0	0	0	0	0	0	0	0	0
$[8, 4, 0, 0]$	13	0	2	2	6	2	0	0	0	1	1	1	1	0	1	1	0	0	0	0	0	0	0	1	0	0	0	0	0	0	0	0
$[8, 0, 4, 0]$	13	0	2	2	6	2	0	0	0	1	1	1	1	0	1	1	0	0	0	0	0	0	0	1	0	0	0	0	0	0	0	0
$[8, 0, 0, 4]$	13	0	2	2	6	2	0	0	0	1	1	1	1	0	1	1	0	0	0	0	0	0	0	1	0	0	0	0	0	0	0	0
$[8, 3, 1, 0]$	76	0	0	0	13	0	0	0	0	0	0	0	0	0	0	0	0	0	0	0	0	0	0	0	0	0	0	0	0	0	0	0
$[8, 3, 0, 1]$	76	0	0	0	13	0	0	0	0	0	0	0	0	0	0	0	0	0	0	0	0	0	0	0	0	0	0	0	0	0	0	0
$[8, 2, 2, 0]$	102	2	7	7	15	7	2	2	0	0	1	1	0	0	0	1	0	0	0	0	0	0	0	0	0	0	0	0	0	0	0	0
$[8, 2, 0, 2]$	102	2	7	7	15	7	2	2	0	0	1	1	0	0	0	1	0	0	0	0	0	0	0	0	0	0	0	0	0	0	0	0
$[8, 2, 1, 1]$	240	0	0	0	15	0	0	0	0	0	0	0	0	0	0	0	0	0	0	0	0	0	0	0	0	0	0	0	0	0	0	0
$[8, 1, 2, 1]$	240	0	0	0	15	0	0	0	0	0	0	0	0	0	0	0	0	0	0	0	0	0	0	0	0	0	0	0	0	0	0	0
$[8, 1, 1, 2]$	240	0	0	0	15	0	0	0	0	0	0	0	0	0	0	0	0	0	0	0	0	0	0	0	0	0	0	0	0	0	0	0
$[8, 0, 3, 1]$	76	0	0	0	13	0	0	0	0	0	0	0	0	0	0	0	0	0	0	0	0	0	0	0	0	0	0	0	0	0	0	0
$[7, 5, 0, 0]$	28	0	0	0	10	0	0	0	0	0	0	0	0	0	0	0	0	0	0	0	0	0	0	0	0	0	0	0	0	0	0	0
$[7, 4, 1, 0]$	156	0	0	0	18	0	0	0	0	0	0	0	0	0	0	0	0	0	0	0	0	0	0	0	0	0	0	0	0	0	0	0
$[7, 4, 0, 1]$	156	0	0	0	18	0	0	0	0	0	0	0	0	0	0	0	0	0	0	0	0	0	0	0	0	0	0	0	0	0	0	0
$[7, 3, 2, 0]$	316	0	0	0	28	0	0	0	0	0	0	0	0	0	0	0	0	0	0	0	0	0	0	0	0	0	0	0	0	0	0	0
$[7, 3, 0, 2]$	316	0	0	0	28	0	0	0	0	0	0	0	0	0	0	0	0	0	0	0	0	0	0	0	0	0	0	0	0	0	0	0
$[7, 2, 3, 0]$	316	0	0	0	28	0	0	0	0	0	0	0	0	0	0	0	0	0	0	0	0	0	0	0	0	0	0	0	0	0	0	0
$[7, 2, 0, 3]$	316	0	0	0	28	0	0	0	0	0	0	0	0	0	0	0	0	0	0	0	0	0	0	0	0	0	0	0	0	0	0	0
$[7, 1, 4, 0]$	156	0	0	0	18	0	0	0	0	0	0	0	0	0	0	0	0	0	0	0	0	0	0	0	0	0	0	0	0	0	0	0
$[7, 1, 0, 4]$	156	0	0	0	18	0	0	0	0	0	0	0	0	0	0	0	0	0	0	0	0	0	0	0	0	0	0	0	0	0	0	0
$[7, 1, 3, 1]$	648	0	0	0	24	0	0	0	0	0	0	0	0	0	0	0	0	0	0	0	0	0	0	0	0	0	0	0	0	0	0	0
$[7, 1, 1, 3]$	648	0	0	0	24	0	0	0	0	0	0	0	0	0	0	0	0	0	0	0	0	0	0	0	0	0	0	0	0	0	0	0
$[6, 6, 0, 0]$	26	1	4	4	8	4	1	1	0	0	1	1	0	0	0	1	0	0	0	0	0	0	0	0	0	1	0	1	0	0	1	0
$[6, 5, 1, 0]$	220	0	0	0	22	0	0	0	0	0	0	0	0	0	0	0	0	0	0	0	0	0	0	0	0	0	0	0	0	0	0	0
$[6, 5, 0, 1]$	220	0	0	0	22	0	0	0	0	0	0	0	0	0	0	0	0	0	0	0	0	0	0	0	0	0	0	0	0	0	0	0
$[6, 4, 2, 0]$	532	4	14	14	34	14	4	4	0	0	2	2	0	0	0	2	0	0	0	0	0	0	0	0	0	0	0	0	0	0	0	0
$[6, 4, 0, 2]$	532	4	14	14	34	14	4	4	0	0	2	2	0	0	0	2	0	0	0	0	0	0	0	0	0	0	0	0	0	0	0	0
$[6, 3, 3, 0]$	749	0	0	0	41	0	0	0	0	0	0	0	0	0	0	0	0	0	0	3	0	0	0	0	0	0	0	0	0	0	0	0
$[6, 3, 0, 3]$	749	0	0	0	41	0	0	0	0	0	0	0	0	0	0	0	0	0	0	3	0	0	0	0	0	0	0	0	0	0	0	0
$[6, 2, 4, 0]$	532	4	14	14	34	14	4	4	0	0	2	2	0	0	0	2	0	0	0	0	0	0	0	0	0	0	0	0	0	0	0	0
$[6, 2, 0, 4]$	532	4	14	14	34	14	4	4	0	0	2	2	0	0	0	2	0	0	0	0	0	0	0	0	0	0	0	0	0	0	0	0
$[6, 2, 3, 1]$	2284	0	0	0	52	0	0	0	0	0	0	0	0	0	0	0	0	0	0	0	0	0	0	0	0	0	0	0	0	0	0	0
$[6, 2, 1, 3]$	2284	0	0	0	52	0	0	0	0	0	0	0	0	0	0	0	0	0	0	0	0	0	0	0	0	0	0	0	0	0	0	0
$[6, 2, 2, 2]$	3366	10	30	30	78	30	10	10	0	0	0	0	0	0	0	0	0	0	0	0	0	0	0	0	0	0	0	0	0	0	0	0
$[6, 1, 5, 0]$	220	0	0	0	22	0	0	0	0	0	0	0	0	0	0	0	0	0	0	0	0	0	0	0	0	0	0	0	0	0	0	0
$[6, 1, 0, 5]$	220	0	0	0	22	0	0	0	0	0	0	0	0	0	0	0	0	0	0	0	0	0	0	0	0	0	0	0	0	0	0	0
$[6, 1, 4, 1]$	1140	0	0	0	30	0	0	0	0	0	0	0	0	0	0	0	0	0	0	0	0	0	0	0	0	0	0	0	0	0	0	0
$[6, 1, 1, 4]$	1140	0	0	0	30	0	0	0	0	0	0	0	0	0	0	0	0	0	0	0	0	0	0	0	0	0	0	0	0	0	0	0
$[6, 1, 3, 2]$	2284	0	0	0	52	0	0	0	0	0	0	0	0	0	0	0	0	0	0	0	0	0	0	0	0	0	0	0	0	0	0	0
$[6, 1, 2, 3]$	2284	0	0	0	52	0	0	0	0	0	0	0	0	0	0	0	0	0	0	0	0	0	0	0	0	0	0	0	0	0	0	0

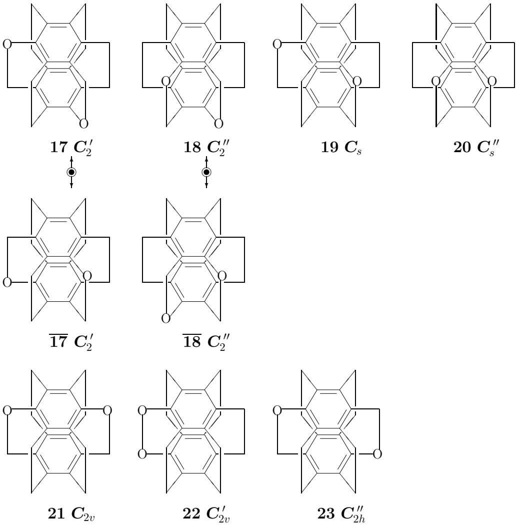
O
17 $\boldsymbol{C}_2'$
18 $\boldsymbol{C}_2''$
19 $\boldsymbol{C}_s$
20 $\boldsymbol{C}_s''$
$\overline{\mathbf{17}}$ $\boldsymbol{C}_2'$
$\overline{\mathbf{18}}$ $\boldsymbol{C}_2''$
21 $\boldsymbol{C}_{2v}$
22 $\boldsymbol{C}_{2v}'$
23 $\boldsymbol{C}_{2h}''$

Figure 9. Symmetry-itemized enumeration of superphane derivatives with the composition $C_{10}O_2$ (partition: $[10, 0, 2, 0]$).

The values at the 10th row of Table 3 with the partition $[10, 0, 1, 1]$ indicate the presence of four pairs of enantiomeric $\boldsymbol{C}_1$-derivatives (**24**/$\overline{\mathbf{24}}$ –**27**/$\overline{\mathbf{27}}$) and three achiral $\boldsymbol{C}_s$-derivatives (**28**, **29**, and **30**), where they have the composition $C^{10}OS$ (or alternatively expressed as $C_{10}OS$). These derivatives are depicted in Figure 10.

7.3 Enumeration of coronene derivatives

7.3.1 Calculation of symmetry-itemized numbers of coronene derivatives with given compositions

Let us select twelve proligands for the coronene skeleton **4** from the following ligand inventory:

$$\boldsymbol{L}'' = \{\mathrm{H}, \mathrm{A}, \mathrm{B}, \mathrm{C}; \mathrm{p}/\mathrm{P}, \mathrm{q}/\mathrm{Q}\}, \tag{115}$$

where H, A, B, and C represent achiral proligands, while p/P or q/Q represents a pair of enantiomeric proligands when detached. This ligand inventory is selected to be smaller than the ligand inventory of Eq. 103. Thus only two pairs of chiral proligands are adopted for substituting the twelve positions of the coronene skeleton, because the usage of Eq. 103 (four pairs of chiral proligands) to the term b_1^{12} causes the GAP error (“Error, reached the pre-set memory limit”). The uppercase letter P etc. is used in place of the symbol

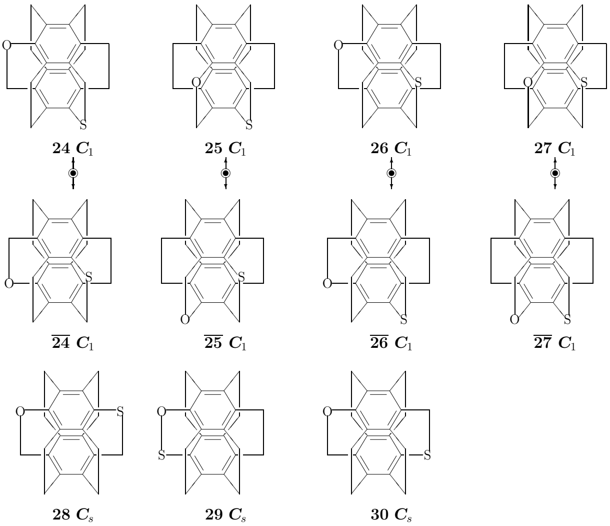

Figure 10. Symmetry-itemized enumeration of superphane derivatives with the composition $C_{10}OS$ (partition: $[10, 0, 1, 1]$).

$\overline{\text{p}}$ etc. to simplify the source code. Then, the following ligand-inventory functions are calculated:

$$a_d = H^d + A^d + B^d + C^d \tag{116}$$

$$c_d = H^d + A^d + B^d + C^d + 2p^{d/2}P^{d/2} + 2q^{d/2}Q^{d/2} \tag{117}$$

$$b_d = H^d + A^d + B^d + C^d + p^d + P^d + q^d + Q^d \tag{118}$$

These ligand-inventory functions are introduced into the right-hand side of each PCI-CF for the coronene skeleton **4**, i.e., Eqs. 71–102. The resulting equations are expanded to give generating functions, in which the coefficient of the composition $\mathrm{H}^H\mathrm{A}^A\mathrm{B}^B\mathrm{C}^C\mathrm{p}^p\mathrm{P}^P\mathrm{q}^q\mathrm{Q}^Q$ represent the number of the corresponding derivatives. The superscripts satisfy following equation:

$$H + A + B + C + p + P + q + Q = 12. \tag{119}$$

For practical enumeration, the GAP code is obtained by modifying Source Code 2 (`enumoctaX`) reported previously on page 362 of Ref. [25], where the function `calcCoeffGen` is used in the subroutine function `calcCoeffGencoronene` for outputting enumeration results in a tabular form. During this process of tabulation, the composition $\mathrm{H}^H\mathrm{A}^A\mathrm{B}^B\mathrm{C}^C$-

$\mathrm{p}^p\mathrm{P}^P\mathrm{q}^q\mathrm{Q}^Q$ is represented by the following partition:

$$[\theta] = [H, A, B, C, p, P, q, Q], \tag{120}$$

which is used as the argument of the function `calcCoeffGen` and the subroutine function `calcCoeffGencoronene`. Thereby, the coefficient of the term $\mathrm{H}^H\mathrm{A}^A\mathrm{B}^B\mathrm{C}^C\mathrm{p}^p\mathrm{P}^P\mathrm{q}^q\mathrm{Q}^Q$ appearing in each of the generating functions is extracted to give the number of promolecules with the composition $\mathrm{H}^H\mathrm{A}^A\mathrm{B}^B\mathrm{C}^C\mathrm{p}^p\mathrm{P}^P\mathrm{q}^q\mathrm{Q}^Q$ and with the assigned subgroup of $\boldsymbol{D}_{6h}$.

Table 4 (Part 1) and Table 5 (Part 2) collect the symmetry-itemized numbers of isomeric coronene derivatives with achiral and chiral proligands, where the symmetry-itemized values for each selected composition (the partition $[\theta]$) are shown in accord with the SSG$_{\boldsymbol{D}_{6h}}$ (Eq. 1). Each row with an asterisk should be duplicated, because a pair of enantiomers (as well as an achiral derivative) is counted once under the present enumeration. The non-asterisked data collected in Tables 4 and 5 are consistent with those reported previously [27], which have been concerned with achiral proligands only.

7.3.2 Diagrammatical examination of calculation results concerning coronene derivatives

For the purpose of confirming the validity of the PCI-CF method, let us examine several rows among the data of Table 4 where each pair of enantiomeric derivative or each achiral derivative is counted once during the present enumerations.

The value 11 at the intersection between the 6th row (the partition $[10, 1, 1, 0, 0, 0, 0, 0]$) and $\boldsymbol{C}_s''$-column in Table 4 shows the presence of eleven $\boldsymbol{C}_s''$-derivatives with the composition $\mathrm{H}_{10}\mathrm{AB}$. These derivatives are depicted in Figure 11. Note that $\boldsymbol{C}_s''$-symmetry is characterized by its horizontal mirror plane which contains the plane of coronene.

The values at the 8th row of Table 4 with the partition $[10, 0, 0, 0, 1, 1, 0, 0]$ (the composition $\mathrm{H}_{10}\mathrm{p}\overline{\mathrm{p}}$) show the presence of two pairs of enantiomeric $\boldsymbol{C}_1$-derivatives ($\mathbf{42}/\overline{\mathbf{42}}$ and $\mathbf{43}/\overline{\mathbf{43}}$), three achiral $\boldsymbol{C}_s$-derivatives (**45**, **46**, and **47**), three achiral $\boldsymbol{C}_s'$-derivatives (**48**, **49**, and **50**), and one achiral $\boldsymbol{C}_i$-derivative (**44**). These derivatives are depicted in Figure 12.

Note that the mirror operation onto **42** (as well as **43**) results in the appearance of its non-superimposable mirror object $\overline{\mathbf{42}}$ (as well as $\overline{\mathbf{43}}$); however, the resulting enantiomeric pair $\mathbf{42}/\overline{\mathbf{42}}$ (as well as $\mathbf{43}/\overline{\mathbf{43}}$) is counted once as a hypothetically single object during the present enumeration under the point group $\boldsymbol{D}_{6h}$. As a result, the value 2 appears at the

Table 4. Symmetry-Itemized Numbers of Derivatives Derived from the Coronene Skeleton **4** (Part 1)

	C_1	C_2	C_2'	C_2''	C_s	C_s'	C_s''	C_i	C_3	D_2	C_{2v}	C_{2v}'	C_{2v}''	C_{2h}	C_{2h}'	C_{2h}''	C_6	D_3	D_3'	C_{3v}	C_{3v}'	C_{3h}	C_{3i}	D_{2h}	D_6	C_{6v}	C_{6h}	D_{3h}	D_{3h}'	D_{3d}	D_{3d}'	D_{6h}
	1	2	3	4	5	6	7	8	9	10	11	12	13	14	15	16	17	18	19	20	21	22	23	24	25	26	27	28	29	30	31	32
$[12,0,0,0,0,0,0,0]$	0	0	0	0	0	0	0	0	0	0	0	0	0	0	0	0	0	0	0	0	0	0	0	0	0	0	0	0	0	0	0	1
$[11,1,0,0,0,0,0,0]$	0	0	0	0	0	0	1	0	0	0	0	0	0	0	0	0	0	0	0	0	0	0	0	0	0	0	0	0	0	0	0	0
$[11,0,0,0,1,0,0,0]*$	1/2	0	0	0	0	0	0	0	0	0	0	0	0	0	0	0	0	0	0	0	0	0	0	0	0	0	0	0	0	0	0	0
$[10,2,0,0,0,0,0,0]$	0	0	0	0	0	0	2	0	0	0	0	3	3	1	0	0	0	0	0	0	0	0	0	0	0	0	0	0	0	0	0	0
$[10,0,0,0,2,0,0,0]*$	1	1/2	3/2	3/2	0	0	0	0	0	0	0	0	0	0	0	0	0	0	0	0	0	0	0	0	0	0	0	0	0	0	0	0
$[10,1,1,0,0,0,0,0]$	0	0	0	0	0	0	11	0	0	0	0	0	0	0	0	0	0	0	0	0	0	0	0	0	0	0	0	0	0	0	0	0
$[10,1,0,0,1,0,0,0]*$	11/2	0	0	0	0	0	0	0	0	0	0	0	0	0	0	0	0	0	0	0	0	0	0	0	0	0	0	0	0	0	0	0
$[10,0,0,0,1,1,0,0]$	2	0	0	0	3	3	0	1	0	0	0	0	0	0	0	0	0	0	0	0	0	0	0	0	0	0	0	0	0	0	0	0
$[10,0,0,0,1,0,1,0]*$	11/2	0	0	0	0	0	0	0	0	0	0	0	0	0	0	0	0	0	0	0	0	0	0	0	0	0	0	0	0	0	0	0
$[9,3,0,0,0,0,0,0]$	0	0	0	0	0	0	18	0	0	0	0	0	0	0	0	0	0	0	0	0	0	1	0	0	0	0	0	0	0	0	0	0
$[9,0,0,0,3,0,0,0]*$	9	0	0	0	0	0	0	0	1/2	0	0	0	0	0	0	0	0	0	0	0	0	0	0	0	0	0	0	0	0	0	0	0
$[9,2,1,0,0,0,0,0]$	0	0	0	0	0	0	55	0	0	0	0	0	0	0	0	0	0	0	0	0	0	0	0	0	0	0	0	0	0	0	0	0
$[9,2,0,0,1,0,0,0]*$	55/2	0	0	0	0	0	0	0	0	0	0	0	0	0	0	0	0	0	0	0	0	0	0	0	0	0	0	0	0	0	0	0
$[9,1,0,0,2,0,0,0]*$	55/2	0	0	0	0	0	0	0	0	0	0	0	0	0	0	0	0	0	0	0	0	0	0	0	0	0	0	0	0	0	0	0
$[9,0,0,0,2,1,0,0]*$	55/2	0	0	0	0	0	0	0	0	0	0	0	0	0	0	0	0	0	0	0	0	0	0	0	0	0	0	0	0	0	0	0
$[9,1,1,1,0,0,0,0]$	0	0	0	0	0	0	110	0	0	0	0	0	0	0	0	0	0	0	0	0	0	0	0	0	0	0	0	0	0	0	0	0
$[9,1,1,0,1,0,0,0]*$	55	0	0	0	0	0	0	0	0	0	0	0	0	0	0	0	0	0	0	0	0	0	0	0	0	0	0	0	0	0	0	0
$[9,1,0,0,1,1,0,0]$	55	0	0	0	0	0	0	0	0	0	0	0	0	0	0	0	0	0	0	0	0	0	0	0	0	0	0	0	0	0	0	0
$[9,0,0,0,1,1,1,0]*$	55	0	0	0	0	0	0	0	0	0	0	0	0	0	0	0	0	0	0	0	0	0	0	0	0	0	0	0	0	0	0	0
$[8,4,0,0,0,0,0,0]$	0	0	0	0	0	0	34	0	0	0	0	6	6	1	0	0	0	0	0	0	0	0	0	3	0	0	0	0	0	0	0	0
$[8,0,0,0,4,0,0,0]*$	17	1/2	3	3	0	0	0	0	0	3/2	0	0	0	0	0	0	0	0	0	0	0	0	0	0	0	0	0	0	0	0	0	0
$[8,3,1,0,0,0,0,0]$	0	0	0	0	0	0	165	0	0	0	0	0	0	0	0	0	0	0	0	0	0	0	0	0	0	0	0	0	0	0	0	0
$[8,3,0,0,1,0,0,0]*$	165/2	0	0	0	0	0	0	0	0	0	0	0	0	0	0	0	0	0	0	0	0	0	0	0	0	0	0	0	0	0	0	0
$[8,2,2,0,0,0,0,0]$	0	0	0	0	0	0	230	0	0	0	0	15	15	5	0	0	0	0	0	0	0	0	0	0	0	0	0	0	0	0	0	0
$[8,2,0,0,2,0,0,0]*$	115	5/2	15/2	15/2	0	0	0	0	0	0	0	0	0	0	0	0	0	0	0	0	0	0	0	0	0	0	0	0	0	0	0	0
$[8,0,0,0,2,2,0,0]$	102	1	6	6	12	12	0	2	0	0	3	0	0	0	3	3	0	0	0	0	0	0	0	0	0	0	0	0	0	0	0	0
$[8,0,0,0,2,0,2,0]*$	115	5/2	15/2	15/2	0	0	0	0	0	0	0	0	0	0	0	0	0	0	0	0	0	0	0	0	0	0	0	0	0	0	0	0
$[8,2,1,1,0,0,0,0]$	0	0	0	0	0	0	495	0	0	0	0	0	0	0	0	0	0	0	0	0	0	0	0	0	0	0	0	0	0	0	0	0
$[8,2,1,0,1,0,0,0]*$	495/2	0	0	0	0	0	0	0	0	0	0	0	0	0	0	0	0	0	0	0	0	0	0	0	0	0	0	0	0	0	0	0
$[8,2,0,0,1,1,0,0]$	230	0	0	0	15	15	0	5	0	0	0	0	0	0	0	0	0	0	0	0	0	0	0	0	0	0	0	0	0	0	0	0
$[8,1,1,0,2,0,0,0]*$	495/2	0	0	0	0	0	0	0	0	0	0	0	0	0	0	0	0	0	0	0	0	0	0	0	0	0	0	0	0	0	0	0
$[8,1,1,0,1,1,0,0]$	495	0	0	0	0	0	0	0	0	0	0	0	0	0	0	0	0	0	0	0	0	0	0	0	0	0	0	0	0	0	0	0
$[8,1,0,0,2,1,0,0]*$	495/2	0	0	0	0	0	0	0	0	0	0	0	0	0	0	0	0	0	0	0	0	0	0	0	0	0	0	0	0	0	0	0
$[8,1,0,0,1,1,1,0]*$	495	0	0	0	0	0	0	0	0	0	0	0	0	0	0	0	0	0	0	0	0	0	0	0	0	0	0	0	0	0	0	0
$[8,0,0,0,2,1,1,0]*$	495/2	0	0	0	0	0	0	0	0	0	0	0	0	0	0	0	0	0	0	0	0	0	0	0	0	0	0	0	0	0	0	0
$[8,0,0,0,1,1,1,1]$	460	0	0	0	30	30	0	10	0	0	0	0	0	0	0	0	0	0	0	0	0	0	0	0	0	0	0	0	0	0	0	0

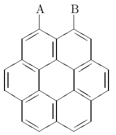

31 C_s''

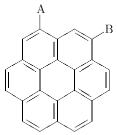

32 C_s''

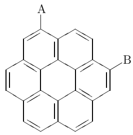

33 C_s''

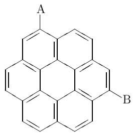

34 C_s''

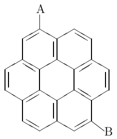

35 C_s''

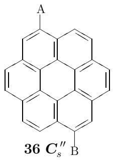

36 C_s''

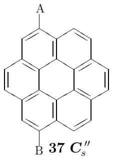

37 C_s''

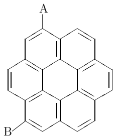

38 C_s''

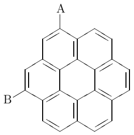

39 C_s''

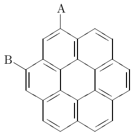

40 C_s''

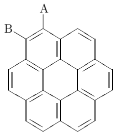

41 C_s''

Figure 11. Symmetry-itemized enumeration of coronene derivatives with the composition $H_{10}AB$ (partition: $[10,1,1,0,0,0,0,0]$), which shows the presence of eleven C_s''-derivatives.

Table 5. Symmetry-Itemized Numbers of Derivatives Derived from the Coronene Skeleton **4** (Part2)

	$\boldsymbol{C}_1$	$\boldsymbol{C}_2$	$\boldsymbol{C}_2'$	$\boldsymbol{C}_2''$	$\boldsymbol{C}_s$	$\boldsymbol{C}_s'$	$\boldsymbol{C}_s''$	$\boldsymbol{C}_i$	$\boldsymbol{C}_3$	$\boldsymbol{D}_2$	$\boldsymbol{C}_{2v}$	$\boldsymbol{C}_{2v}'$	$\boldsymbol{C}_{2v}''$	$\boldsymbol{C}_{2h}$	$\boldsymbol{C}_{2h}'$	$\boldsymbol{C}_{2h}''$	$\boldsymbol{C}_6$	$\boldsymbol{D}_3$	$\boldsymbol{D}_3'$	$\boldsymbol{C}_{3v}$	$\boldsymbol{C}_{3v}'$	$\boldsymbol{C}_{3h}$	$\boldsymbol{C}_{3i}$	$\boldsymbol{D}_{2h}$	$\boldsymbol{D}_6$	$\boldsymbol{C}_{6v}$	$\boldsymbol{C}_{6h}$	$\boldsymbol{D}_{3h}$	$\boldsymbol{D}_{3h}'$	$\boldsymbol{D}_{3d}$	$\boldsymbol{D}_{3d}'$	$\boldsymbol{D}_{6h}$
	1	2	3	4	5	6	7	8	9	10	11	12	13	14	15	16	17	18	19	20	21	22	23	24	25	26	27	28	29	30	31	32
[7, 5, 0, 0, 0, 0, 0, 0]	0	0	0	0	0	0	66	0	0	0	0	0	0	0	0	0	0	0	0	0	0	0	0	0	0	0	0	0	0	0	0	0
[7, 0, 0, 0, 5, 0, 0, 0]*	33	0	0	0	0	0	0	0	0	0	0	0	0	0	0	0	0	0	0	0	0	0	0	0	0	0	0	0	0	0	0	0
[7, 4, 1, 0, 0, 0, 0, 0]	0	0	0	0	0	0	330	0	0	0	0	0	0	0	0	0	0	0	0	0	0	0	0	0	0	0	0	0	0	0	0	0
[7, 4, 0, 0, 1, 0, 0, 0]*	165	0	0	0	0	0	0	0	0	0	0	0	0	0	0	0	0	0	0	0	0	0	0	0	0	0	0	0	0	0	0	0
[7, 0, 0, 0, 4, 1, 0, 0]*	165	0	0	0	0	0	0	0	0	0	0	0	0	0	0	0	0	0	0	0	0	0	0	0	0	0	0	0	0	0	0	0
[7, 0, 0, 0, 4, 0, 1, 0]*	165	0	0	0	0	0	0	0	0	0	0	0	0	0	0	0	0	0	0	0	0	0	0	0	0	0	0	0	0	0	0	0
[7, 3, 2, 0, 0, 0, 0, 0]	0	0	0	0	0	0	660	0	0	0	0	0	0	0	0	0	0	0	0	0	0	0	0	0	0	0	0	0	0	0	0	0
[7, 3, 0, 0, 2, 0, 0, 0]*	330	0	0	0	0	0	0	0	0	0	0	0	0	0	0	0	0	0	0	0	0	0	0	0	0	0	0	0	0	0	0	0
[7, 0, 0, 0, 3, 2, 0, 0]*	330	0	0	0	0	0	0	0	0	0	0	0	0	0	0	0	0	0	0	0	0	0	0	0	0	0	0	0	0	0	0	0
[7, 0, 0, 0, 3, 0, 2, 0]*	330	0	0	0	0	0	0	0	0	0	0	0	0	0	0	0	0	0	0	0	0	0	0	0	0	0	0	0	0	0	0	0
[7, 3, 1, 1, 0, 0, 0, 0]	0	0	0	0	0	0	1320	0	0	0	0	0	0	0	0	0	0	0	0	0	0	0	0	0	0	0	0	0	0	0	0	0
[7, 3, 1, 0, 1, 0, 0, 0]*	660	0	0	0	0	0	0	0	0	0	0	0	0	0	0	0	0	0	0	0	0	0	0	0	0	0	0	0	0	0	0	0
[7, 3, 0, 0, 1, 1, 0, 0]	660	0	0	0	0	0	0	0	0	0	0	0	0	0	0	0	0	0	0	0	0	0	0	0	0	0	0	0	0	0	0	0
[7, 2, 2, 1, 0, 0, 0, 0]	0	0	0	0	0	0	1980	0	0	0	0	0	0	0	0	0	0	0	0	0	0	0	0	0	0	0	0	0	0	0	0	0
[7, 2, 2, 0, 1, 0, 0, 0]*	990	0	0	0	0	0	0	0	0	0	0	0	0	0	0	0	0	0	0	0	0	0	0	0	0	0	0	0	0	0	0	0
[7, 2, 1, 1, 1, 0, 0, 0]*	1980	0	0	0	0	0	0	0	0	0	0	0	0	0	0	0	0	0	0	0	0	0	0	0	0	0	0	0	0	0	0	0
[7, 2, 1, 0, 2, 0, 0, 0]*	990	0	0	0	0	0	0	0	0	0	0	0	0	0	0	0	0	0	0	0	0	0	0	0	0	0	0	0	0	0	0	0
[7, 2, 1, 0, 1, 1, 0, 0]	1980	0	0	0	0	0	0	0	0	0	0	0	0	0	0	0	0	0	0	0	0	0	0	0	0	0	0	0	0	0	0	0
[7, 2, 1, 0, 1, 0, 1, 0]*	1980	0	0	0	0	0	0	0	0	0	0	0	0	0	0	0	0	0	0	0	0	0	0	0	0	0	0	0	0	0	0	0
[7, 2, 0, 0, 2, 1, 0, 0]*	990	0	0	0	0	0	0	0	0	0	0	0	0	0	0	0	0	0	0	0	0	0	0	0	0	0	0	0	0	0	0	0
[7, 2, 0, 0, 2, 0, 1, 0]*	990	0	0	0	0	0	0	0	0	0	0	0	0	0	0	0	0	0	0	0	0	0	0	0	0	0	0	0	0	0	0	0
[7, 2, 0, 0, 1, 1, 1, 0]*	1980	0	0	0	0	0	0	0	0	0	0	0	0	0	0	0	0	0	0	0	0	0	0	0	0	0	0	0	0	0	0	0
[7, 1, 1, 1, 1, 1, 0, 0]	3960	0	0	0	0	0	0	0	0	0	0	0	0	0	0	0	0	0	0	0	0	0	0	0	0	0	0	0	0	0	0	0
[7, 1, 1, 1, 1, 0, 1, 0]*	3960	0	0	0	0	0	0	0	0	0	0	0	0	0	0	0	0	0	0	0	0	0	0	0	0	0	0	0	0	0	0	0
[7, 1, 1, 0, 1, 1, 1, 0]*	3960	0	0	0	0	0	0	0	0	0	0	0	0	0	0	0	0	0	0	0	0	0	0	0	0	0	0	0	0	0	0	0
[7, 1, 0, 0, 1, 1, 1, 1]	3960	0	0	0	0	0	0	0	0	0	0	0	0	0	0	0	0	0	0	0	0	0	0	0	0	0	0	0	0	0	0	0
[6, 6, 0, 0, 0, 0, 0, 0]	0	0	0	0	0	0	66	0	0	0	0	9	9	3	0	0	0	0	0	0	0	0	0	0	0	0	1	1	1	0	0	0
[6, 0, 0, 0, 6, 0, 0, 0]*	33	3/2	9/2	9/2	0	0	0	0	0	0	0	0	0	0	0	0	1/2	1/2	1/2	0	0	0	0	0	0	0	0	0	0	0	0	0
[6, 5, 1, 0, 0, 0, 0, 0]	0	0	0	0	0	0	462	0	0	0	0	0	0	0	0	0	0	0	0	0	0	0	0	0	0	0	0	0	0	0	0	0
[6, 5, 0, 0, 1, 0, 0, 0]*	231	0	0	0	0	0	0	0	0	0	0	0	0	0	0	0	0	0	0	0	0	0	0	0	0	0	0	0	0	0	0	0
[6, 0, 0, 0, 5, 1, 0, 0]*	231	0	0	0	0	0	0	0	0	0	0	0	0	0	0	0	0	0	0	0	0	0	0	0	0	0	0	0	0	0	0	0
[6, 4, 2, 0, 0, 0, 0, 0]	0	0	0	0	0	0	1120	0	0	0	0	30	30	10	0	0	0	0	0	0	0	0	0	0	0	0	0	0	0	0	0	0
[6, 4, 0, 0, 2, 0, 0, 0]*	560	5	15	15	0	0	0	0	0	0	0	0	0	0	0	0	0	0	0	0	0	0	0	0	0	0	0	0	0	0	0	0
[6, 0, 0, 4, 2, 0, 0, 0]*	560	5	15	15	0	0	0	0	0	0	0	0	0	0	0	0	0	0	0	0	0	0	0	0	0	0	0	0	0	0	0	0
[6, 3, 3, 0, 0, 0, 0, 0]	0	0	0	0	0	0	1539	0	0	0	0	0	0	0	0	0	0	0	0	0	0	3	0	0	0	0	0	0	0	0	0	0
[6, 3, 0, 0, 3, 0, 0, 0]*	1539/2	0	0	0	0	0	0	0	3/2	0	0	0	0	0	0	0	0	0	0	0	0	0	0	0	0	0	0	0	0	0	0	0
[6, 0, 0, 0, 3, 3, 0, 0]	724	0	0	0	39	39	0	13	0	0	0	0	0	0	0	0	0	0	0	1	1	0	1	0	0	0	0	0	0	0	0	0
[6, 2, 2, 2, 0, 0, 0, 0]	0	0	0	0	0	0	6860	0	0	0	0	60	60	20	0	0	0	0	0	0	0	0	0	0	0	0	0	0	0	0	0	0
[6, 2, 2, 0, 2, 0, 0, 0]*	3430	10	30	30	0	0	0	0	0	0	0	0	0	0	0	0	0	0	0	0	0	0	0	0	0	0	0	0	0	0	0	0
[6, 2, 0, 0, 2, 2, 0, 0]	3360	10	30	30	60	60	0	20	0	0	0	0	0	0	0	0	0	0	0	0	0	0	0	0	0	0	0	0	0	0	0	0
[6, 0, 0, 0, 2, 2, 2, 0]*	3430	10	30	30	0	0	0	0	0	0	0	0	0	0	0	0	0	0	0	0	0	0	0	0	0	0	0	0	0	0	0	0
[6, 2, 1, 1, 2, 0, 0, 0]*	6930	0	0	0	0	0	0	0	0	0	0	0	0	0	0	0	0	0	0	0	0	0	0	0	0	0	0	0	0	0	0	0
[6, 2, 1, 0, 2, 1, 0, 0]*	6930	0	0	0	0	0	0	0	0	0	0	0	0	0	0	0	0	0	0	0	0	0	0	0	0	0	0	0	0	0	0	0
[6, 2, 0, 0, 2, 1, 1, 0]*	6930	0	0	0	0	0	0	0	0	0	0	0	0	0	0	0	0	0	0	0	0	0	0	0	0	0	0	0	0	0	0	0
[6, 0, 0, 0, 2, 2, 1, 1]	6790	0	0	0	120	120	0	40	0	0	0	0	0	0	0	0	0	0	0	0	0	0	0	0	0	0	0	0	0	0	0	0
[6, 1, 1, 1, 3, 0, 0, 0]*	4620	0	0	0	0	0	0	0	0	0	0	0	0	0	0	0	0	0	0	0	0	0	0	0	0	0	0	0	0	0	0	0
[6, 1, 1, 1, 2, 1, 0, 0]*	13860	0	0	0	0	0	0	0	0	0	0	0	0	0	0	0	0	0	0	0	0	0	0	0	0	0	0	0	0	0	0	0
[6, 1, 1, 1, 1, 1, 1, 0]*	27720	0	0	0	0	0	0	0	0	0	0	0	0	0	0	0	0	0	0	0	0	0	0	0	0	0	0	0	0	0	0	0
[6, 1, 1, 0, 1, 1, 1, 1]	27720	0	0	0	0	0	0	0	0	0	0	0	0	0	0	0	0	0	0	0	0	0	0	0	0	0	0	0	0	0	0	0

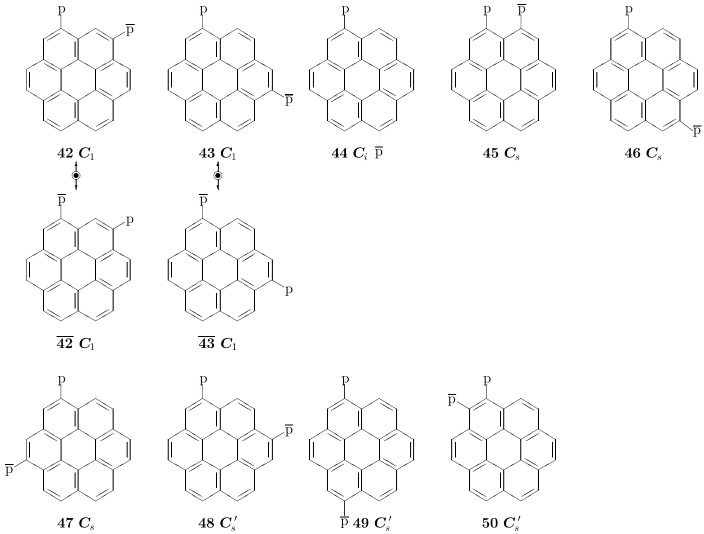

Figure 12. Symmetry-itemized enumeration of coronene derivatives with the composition $H_{10}p\overline{p}$ (partition: $[10, 0, 0, 0, 1, 1, 0, 0]$), which shows the presence of two pairs of enantiomeric $\boldsymbol{C}_1$-derivatives, three achiral $\boldsymbol{C}_s$-derivatives, three achiral $\boldsymbol{C}'_s$-derivatives. and one achiral $\boldsymbol{C}_i$-derivative.

intersection between the 8th $[10, 0, 0, 0, 1, 1, 0, 0]$-row and the $\boldsymbol{C}_1$-column. The inversion operation i means the successive action of the rotation C_2 around the vertical two-fold axis and the horizontal reflection; thereby, the i operation stabilizes (fixes) the $\boldsymbol{C}_i$-derivative (**44**). Three vertical reflection groups for stabilizing the three achiral $\boldsymbol{C}_s$-derivatives (**45**, **46**, and **47**) are conjugate under $\boldsymbol{D}_{6h}$.

This fact can be confirmed by the GAP function `ConjugateSubgroups`, which is operated onto `Cs` ($\boldsymbol{C}_s$) for stabilizing **45** as follows.

```
gap> gen_coronene := [(1,3,5,7,9,11)(2,4,6,8,10,12),
> (1,6)(2,5)(3,4)(7,12)(8,11)(9,10), (13,14)];;
gap> D6h_coronene := Group(gen_coronene);; #coronene skeleton
gap> gen_Cs := [(1,12)(2,11)(3,10)(4,9)(5,8)(6,7)(13,14)];;
gap> Cs := Group(gen_Cs);;
gap> ConjugateSubgroups(D6h_coronene,Cs);
[ Group([ (1,12)(2,11)(3,10)(4,9)(5,8)(6,7)(13,14) ]),
  Group([ (1,4)(2,3)(5,12)(6,11)(7,10)(8,9)(13,14) ]),
  Group([ (1,8)(2,7)(3,6)(4,5)(9,12)(10,11)(13,14) ]) ]
gap>
```

The resulting two-fold reflection groups stabilize **46** and **47**, respectively.

Similarly, three vertical reflection groups for stabilizing the three achiral $\boldsymbol{C}'_s$-derivatives (**48**, **49**, and **50**) are conjugate under $\boldsymbol{D}_{6h}$.

8 Conclusions

To systematize symmetry-itemized enumeration under a point group by using the GAP (Groups, Algorithms, Programming) system, the applicability of combined-permutation representations (CPRs) with an additional 2-cycle due to a mirror-permutation are examined by adopting several skeletons of the $\boldsymbol{D}_{6h}$-point group as probes. Thereby, the GAP functions `MarkTableforUSCI` and `constructUSCITable`, which have been newly devised to systematize the concordant construction of a standard mark table and a standard USCI-CF (unit-subduced-cycle-index-with-chirality-fittingness) table in a previous report [25], are applied to four representative $\boldsymbol{D}_{6h}$-skeletons, i.e., a benzene skeleton, a Haward-projected skeleton, a superphane skeleton, and a coronene skeleton. Thereby, we are able to construct the standard mark table and the standard USCI-CF table even if we start from any of CPRs for characterizing these skeletons, i.e. the CPR of degree 8 (= 6 + 2) for the benzene skeleton, the CPR of degree 14 (= 12 + 2) for the Haward-projected skeleton, the CPR of degree 14 (= 12 + 2) for the superphane skeleton, and the CPR of degree 14 (= 12 + 2) for the coronene skeleton. After a set of PCI-CFs (partial cycle indices with chirality fittingness) is calculated for each skeleton, symmetry-itemized combinatorial enumeration is conducted by means of the PCI method of Fujita's USCI approach.

References

[1] W. Burnside, *Theory of Groups of Finite Order*, Cambridge Univ. Press, Cambridge, 1911.

[2] G. Pólya, Kombinatorische Anzahlbestimmungen für Gruppen, Graphen und chemische Verbindungen, *Acta Math.* **68** (1937) 145–254.

[3] G. Pólya, R. C. Read, *Combinatorial Enumeration of Groups, Graphs, and Chemical Compounds*, Springer, New York, 1987.

[4] S. Fujita, *Symmetry and Combinatorial Enumeration in Chemistry*, Springer-Verlag, Berlin, 1991.

[5] S. Fujita, *Combinatorial Enumeration of Graphs, Three-Dimensional Structures, and Chemical Compounds*, Univ. Kragujevac, Kragujevac, 2013.

[6] S. Fujita, Chirality fittingness of an orbit governed by a coset representation. Integration of point-group and permutation-group theories to treat local chirality and prochirality, *J. Am. Chem. Soc.* **112** (1990) 3390–3397.

[7] S. Fujita, Subduction of coset representations. An application to enumeration of chemical structures, *Theor. Chim. Acta* **76** (1989) 247–268.

[8] S. Fujita, Subduction of coset representations. An application to enumeration of chemical structures with achiral and chiral ligands, *J. Math. Chem.* **5** (1990) 121–156.

[9] S. Fujita, Systematic enumeration of high symmetry molecules by means of unit subduced cycle indices with and without chirality fittingness, *Bull. Chem. Soc. Jpn.* **63** (1990) 203–215.

[10] S. Fujita, *Diagrammatical Approach to Molecular Symmetry and Enumeration of Stereoisomers*, Univ. Kragujevac, Kragujevac, 2007.

[11] S. Fujita, *Mathematical Stereochemistry*, De Gruyter, Berlin, 2015.

[12] S. Fujita, *Mathematical Stereochemistry*, De Gruyter, Berlin, 2021.

[13] S. Fujita, Graphs to chemical structures 1. Sphericity indices of cycles for stereochemical extension of Pólya's theorem, *Theor. Chem. Acc.* **113** (2005) 73–79.

[14] S. Fujita, Graphs to chemical structures 2. Extended sphericity indices of cycles for stereochemical extension of Pólya's coronas, *Theor. Chem. Acc.* **113** (2005) 80–86.

[15] S. Fujita, Graphs to chemical structures 3. General theorems with the use of different sets of sphericity indices for combinatorial enumeration of nonrigid stereoisomers, *Theor. Chem. Acc.* **115** (2006) 37–53.

[16] S. Fujita, Stereogenicity revisited. Proposal of holantimers for comprehending the relationship between stereogenicity and chirality, *J. Org. Chem.* **69** (2004) 3158–3165.

[17] S. Fujita, Pseudoasymmetry, stereogenicity, and the RS-nomenclature comprehended by the concepts of holantimers and stereoisograms, *Tetrahedron* **60** (2004) 11629–11638.

[18] S. Fujita, Chirality and RS-stereogenicity as two kinds of handedness. Their aufheben by Fujita's stereoisogram approach for giving new insights into classification of isomers, *Bull. Chem. Soc. Jpn.* **89** (2016) 987–1017.

[19] S. Fujita, Unit subduced cycle indices with and without chirality fittingness for $\mathbf{I}_h$ group. An application to systematic enumeration of dodecahedrane derivatives, *Bull. Chem. Soc. Jpn.* **63** (1990) 2759–2769.

[20] https://www.gap-system.org/.

[21] S. Fujita, Computer-oriented representations of point groups and cycle indices with chirality fittingness (CI-CFs) calculated by the GAP system. Enumeration of three-dimensional structures of ligancy 4 by Fujita's proligand method, *MATCH Commun. Math. Comput. Chem.* **76** (2016) 379–400.

[22] S. Fujita, Computer-oriented representations of $\mathbf{O}_h$-skeletons for supporting combinatorial enumeration by Fujita's proligand method. GAP calculation of cycle indices with chirality fittingness (CI-CFs), *MATCH Commun. Math. Comput. Chem.* **77** (2017) 409–442.

[23] S. Fujita, Hierarchical enumeration based on skeletons of ligancy 6 by using combined-permutation representations. Part 1. Cyclopropane derivatives, *MATCH Commun. Math. Comput. Chem.* **79** (2018) 103–142.

[24] S. Fujita, Concordant generation of mark tables and USCI-CF (unit subduced cycle indices with chirality fittingness) tables on the basis of combined-permutation representations, *MATCH Commun. Math. Comput. Chem.* **82** (2019) 295–326.

[25] S. Fujita, Standardization of mark tables and USCI-CF (unit subduced cycle indices with chirality fittingness) tables derived from different $\mathbf{O}_h$-skeletons, *MATCH Commun. Math. Comput. Chem.* **82** (2019) 327–373.

[26] S. Fujita, Standardization of mark tables and USCI-CF (unit subduced cycle indices with chirality fittingness) tables derived from different $\mathbf{D}_{3h}$-skeletons, *Bull. Chem. Soc. Jpn.* **93** (2020) 880–897.

[27] S. Fujita, Benzene derivatives with achiral and chiral substituents and relevant derivatives derived from $\mathbf{D}_{6h}$-skeletons. Symmetry-itemized enumeration and symmetry characterization by the unit-subduced-cycle-index approach, *J. Chem. Inf. Comput. Sci.* **39** (1999) 151–163.

[28] S. Fujita, α, β-itemized enumeration of inositol derivatives and m-gonal homologs by extending Fujita's proligand method, *Bull. Chem. Soc. Jpn.* **90** (2017) 343–366.

[29] S. Fujita, Subsymmetry-itemized enumeration of flexible cyclohexane derivatives, *Bull. Chem. Soc. Jpn.* **67** (1994) 2935–2948.

[30] S. Fujita, Pseudo-point group approach to stereochemistry and stereoisomerism of cyclohexane derivatives, *Proc. Jpn. Acad. Ser. B* **77** (2001) 197–202.

[31] S. Fujita, Systematic design of high-symmetry cyclohexane derivatives and characteration of their energetic and symmetric equivalency, *MATCH Commun. Math. Comput. Chem.* **46** (2002) 25–44.

[32] S. Fujita, The SCR notation for systematic classification of molecular symmetries, *Memoirs of the Faculty of Engineering and Design, Kyoto Institute of Technology* **47** (1999) 111–126.

[33] S. Fujita, Promolecules with a subsymmetry of $\mathbf{O}_h$. Combinatorial enumeration and stereochemical properties, *Polyhedron* **12** (1993) 95–110.

[34] S. Fujita, Enumeration of digraphs with a given automorphism group, *J. Math. Chem.* **12** (1993) 173–195.

[35] S. Fujita, Generalization of partial cycle indices and modified bisected mark tables for combinatorial enumeration, *Bull. Chem. Soc. Jpn.* **73** (2000) 329–339.

[36] S. Fujita, The USCI approach and elementary superposition for combinatorial enumeration, *Theor. Chim. Acta* **82** (1992) 473–498.

Appendix A. Source code 1 (SubDh6h6-X.gap) for concordant preparation of a standard mark table and a standard USCI table of $\boldsymbol{D}_{6h}$ by starting from a benzene skeleton, as well as formation of PCI-CFs for the benzene skeleton

The following source code SubDh6h6-X.gap aims at concordant generations of a standard mark table MarkTableD6h and a standard USCI-CF table USCITableD6h for the point group $\boldsymbol{D}_{6h}$, where the combined-permutation representation (CPR) D6h_benz for a benzene skeleton is used as a typical example. A set of USCI-CFs for characterizing a benzene (l_PCICF_benz) is calculated.

The file SubD6h6X.gap is loaded by Read as shown in the first line (commented by #). The results are output into a log file named SubD6h6Xlog.txt by means of the GAP function LogTo. The file USCICF.gapfunc (cf. Appendix A in [24]) is loaded to use the devised GAP functions MarkTableforUSCI and constructUSCITable.

Source Code 1 (SubDh6h6-X.gap)

```
#Read("c:/fujita00/fujita2020/subductionD6h/gap/SubD6h6X.gap");
LogTo("c:/fujita00/fujita2020/subductionD6h/gap/SubD6h6Xlog.txt");

Read("c:/fujita00/fujita2020/subductionD6h/gap/USCICF.gapfunc");

#generators for D6h_benz
gen_benz := [(1,2,3,4,5,6), (1,4)(2,3)(5,6), (7,8)];;
D6h_benz := Group(gen_benz); #benzene skeleton
Display(Size(D6h_benz));

#generators for D6_benz
gen_benzx := [(1,2,3,4,5,6), (1,4)(2,3)(5,6)];;
D6_benz := Group(gen_benzx); #benzene skeleton
Display(Size(D6_benz));

tom_D6h_benz := TableOfMarks(D6h_benz);;
Display(tom_D6h_benz);

#Subgroups of D6h given
gen := [];;

gen[1] := [ ];; #----1
gen[3] := [ (2,6)(3,5) ];; #----2
gen[7] := [ (7,8) ];; #----3
gen[2] := [ (1,4)(2,5)(3,6) ];; #----4
gen[5] := [ (2,6)(3,5)(7,8) ];; #----5
gen[4] := [ (1,2)(3,6)(4,5) ];; #----6
gen[8] := [ (1,4)(2,5)(3,6)(7,8) ];; #----7
gen[6] := [ (1,2)(3,6)(4,5)(7,8) ];; #----8
gen[9] := [ (1,3,5)(2,4,6) ];; #----9
gen[14] := [ (7,8), (1,4)(2,5)(3,6) ];; #----10
gen[10] := [ (2,6)(3,5), (1,4)(2,5)(3,6) ];; #----11
gen[12] := [ (7,8), (2,6)(3,5) ];; #----12
gen[11] := [ (2,6)(3,5)(7,8), (1,4)(2,5)(3,6) ];; #----13
gen[13] := [ (7,8), (1,2)(3,6)(4,5) ];; #----14
gen[15] := [ (1,4)(2,5)(3,6)(7,8), (2,6)(3,5) ];; #----15
gen[16] := [ (1,3)(4,6)(7,8), (1,6)(2,5)(3,4) ];; #----16
```

```
gen[22] := [ (1,3,5)(2,4,6), (7,8) ];; #----17
gen[18] := [ (1,3,5)(2,4,6), (2,6)(3,5) ];; #----18
gen[20] := [ (1,3,5)(2,4,6), (2,6)(3,5)(7,8) ];; #----19
gen[17] := [ (1,3,5)(2,4,6), (1,2,3,4,5,6) ];; #----20
gen[23] := [ (1,3,5)(2,4,6), (1,2,3,4,5,6)(7,8) ];; #----21
gen[19] := [ (1,3,5)(2,4,6), (1,2)(3,6)(4,5) ];; #----22
gen[21] := [ (1,3,5)(2,4,6), (1,2)(3,6)(4,5)(7,8) ];; #----23
gen[24] := [ (7,8), (2,6)(3,5), (1,4)(2,5)(3,6) ];; #----24
gen[27] := [ (1,3,5)(2,4,6), (7,8), (1,2,3,4,5,6) ];; #----25
gen[25] := [ (1,3,5)(2,4,6), (2,6)(3,5), (1,2,3,4,5,6) ];; #----26
gen[28] := [ (1,3,5)(2,4,6), (7,8), (2,6)(3,5) ];; #----27
gen[26] := [ (1,3,5)(2,4,6), (2,6)(3,5)(7,8), (1,2,3,4,5,6) ];; #----28
gen[29] := [ (1,3,5)(2,4,6), (7,8), (1,2)(3,6)(4,5) ];; #----29
gen[30] := [ (1,3,5)(2,4,6), (2,6)(3,5), (1,2,3,4,5,6)(7,8) ];; #----30
gen[31] := [ (1,3,5)(2,4,6), (2,6)(3,5)(7,8), (1,2,3,4,5,6)(7,8) ];;
#----31
gen[32] := [ (1,2,3,4,5,6), (1,4)(2,3)(5,6), (7,8) ];; #----32

#mark table sorted for USCI table
MarkTableD6h := MarkTableforUSCI(D6h_benz,D6_benz,32,gen,6,8);;
Display(MarkTableD6h);

USCITableD6h := constructUSCITable(D6h_benz,D6_benz,32,gen,6,8);
Display("##USCI-CF␣table␣(USCITableD6h)␣:");
Display(USCITableD6h);


#Matrix form of mark table
Matrix_tomD6h_benz := MatTom(MarkTableD6h);
Display(Matrix_tomD6h_benz);

Display("#Fixed␣point␣vector␣for␣benzene");
FPVbenz := calculateFPvector(D6h_benz,D6_benz,32,gen,6,8);;
Display(FPVbenz);

Display("#Orbits␣for␣benzene");
Orbit_benz := FPVbenz*Inverse(MatTom(MarkTableD6h));;
Display(Orbit_benz);

Display("#SCI-CF␣for␣benzene");
l_SCICF_benz :=
constructSCICF(D6h_benz,D6_benz,Matrix_tomD6h_benz,USCITableD6h,FPVbenz);;
Display(l_SCICF_benz);

Display("#list␣of␣PCI-CFs␣for␣benzene");
l_PCICF_benz := l_SCICF_benz * Inverse(Matrix_tomD6h_benz);
Display(l_PCICF_benz);

Display("#PCI-CFs␣for␣subgroups");
for i in [1..32] do
Print("PCI-CF[", i, "]␣:=␣", l_PCICF_benz[i], "\n");
od;



LogTo();
```